Pacific Gas and Electric Company®

Paula Gerfen
Site Vice President

Diablo Canyon Power Plant
Mail code 104/5/502
P.O. Box 56
Avila Beach, CA 93424

805.545.4596
Internal: 691.4596
Fax: 805.545.4234

April 30, 2020

PG&E Letter DCL-20-031

U.S. Nuclear Regulatory Commission
ATTN: Document Control Desk
Washington, DC 20555-0001

10 CFR 50.54(f)

Docket No. 50-275, OL-DPR-80
Docket No. 50-323, OL-DPR-82
Diablo Canyon Units 1 and 2
Final Supplemental Response to Generic Letter 2004-02

Reference:
1. PG&E Letter DCL-13-052, "Proposed Path to Closure of Generic Safety Issue-191, 'Assessment of Debris Accumulation on Pressurized-Water Reactor Sump Performance,'" dated May 14, 2013 [ML13135A070]
2. NRC Commissioners Staff Requirements Memorandum (SRM) SECY-12-0093, "Closure Options for Generic Safety Issue-191, Assessment of Debris Accumulation on Pressurized-Water Reactor Sump Performance," dated December 14, 2012
3. WCAP-17788-P, Revision 1, "Comprehensive Analysis and Test Program for GSI-191 Closure (PA-SEE-1090)," dated December 2019
4. NRC Letter "Diablo Canyon Power Plant, Unit Nos. 1 and 2 - Request for Additional Information (RAI) Regarding Supplemental Response to Generic Letter 2004-02, 'Potential Impact of Debris Blockage on Emergency Recirculation During Design Basis Accidents at Pressurized Water Reactors' (TAC Nos. MD4682 and MD4683)," dated October 15, 2009 [ML092310763]

Dear Commissioners and Staff:

The purpose of this submittal is to provide the Pacific Gas and Electric Company (PG&E) final supplemental response for Diablo Canyon Units 1 and 2 (DCPP) to Generic Letter (GL) 2004-02, dated September 13, 2004, "Potential Impact of Debris Blockage on Emergency Recirculation During Design Basis Accidents at Pressurized-Water Reactors."

In Reference 1, PG&E submitted a letter of intent per Reference 2 to pursue Closure Option 2 (Mitigative Measures and Alternative Methods Approach) “Risk Informed” approach using risk information for the strainer and in-vessel evaluations (referred to as Option 2b). PG&E has completed additional strainer evaluation, including testing, and in-vessel downstream effects evaluation using Reference 3. Based on these additional evaluations, PG&E has decided to address closure of GL 2004-02 using the Reference 2, Option 2, “Deterministic” approach (referred to as Option 2a), without the need for a License Amendment Request.

The strainer and in-vessel downstream effects evaluation, and response to the Reference 4 NRC request for additional information, is contained in Enclosure 1 to this letter. The Updated Final Safety Analysis Report (UFSAR) changes, made in accordance with10 CFR 50.59, are contained in Enclosure 2 to this letter.

This letter does not include a new regulatory commitment (as defined by NEI 99-04). Because of the PG&E decision to address closure of GL 2004-02 using a deterministic approach, the previous Commitments 1, and 3 through 8 associated with the previous risk-informed approach contained in the Attachment to the Enclosure of Reference 1 are no longer applicable and therefore are withdrawn. Commitment 2, to complete measurements for insulation remediation (double jacket calcium silicate piping and installation of additional cable tray cover), has been completed as documented in Enclosure 1 to this letter.

If you have any questions or require additional information, please contact Mr. Hossein Hamzehee, Regulatory Services Manager, at (805) 545-4720.

I state under penalty of perjury that the foregoing is true and correct.

Executed on April 30, 2020.

Sincerely,

Paula Gerfen
Site Vice President

kjse/50525804
Enclosures
cc: Diablo Distribution
cc/enc: Scott A. Morris, NRC Region IV Administrator
Christopher W. Newport, NRC Senior Resident Inspector
Gonzalo L. Perez, Branch Chief, California Department of Public Health
Balwant K. Singal, NRR Senior Project Manager

Final Supplemental Response to NRC Generic Letter 2004-02

(164 pages, page E1-1 to E1-164)

Enclosure 1 Final Responses to NRC Generic Letter 2004-02

Table of Contents

List of Acronyms

3D	Three-Dimensional
AEC	Atomic Energy Commission
AECL	Atomic Energy of Canada Limited
AFP	Alternate Flow Path
AlOOH	Aluminum Oxyhydroxide
ANL	Argonne National Laboratory
ANS	American Nuclear Society
ANSI	American National Standards Institute
ATS	Applied Technology Services
BEP	Best Efficiency Point
CAD	Computer Aided Design
Cal-Sil	Calcium Silicate
CCP	Centrifugal Charging Pump
CFD	Computational Fluid Dynamics
CFR	Code of Federal Regulations
CLB	Cold Leg Break
CS	Containment Spray
CSHL	Clean Strainer Head Loss
CSS	Containment Spray System
CVCS	Chemical Volume Control System
DCPP	Diablo Canyon Power Plant
DDE	Double Design Earthquake
DEGB	Double-Ended Guillotine Break
DT	Deposition Thickness
ECCS	Emergency Core Cooling System
FA	Fuel Assembly
GDC	General Design Criteria
GL	Generic Letter
GSI	Generic Safety Issue
HE	Hosgri Earthquake
HLB	Hot Leg Break
IMB	Inside Missile Barrier
IOZ	Inorganic Zinc
ISI	In-Service Inspection
LAR	License Amendment Request
LBLOCA	Large Break Loss-of-Coolant Accident
LOCA	Loss-of-Coolant Accident
LOCADM	LOCA Deposition Model
LTCC	Long-Term Core Cooling
NaOH	Sodium Hydroxide
NEI	Nuclear Energy Institute
NPSH	Net Positive Suction Head
NPSHr	Net Positive Suction Head Required

NRC	Nuclear Regulatory Commission
OEM	Original Equipment Manufacturer
OMB	Outside Missile Barrier
PCT	Peak Cladding Temperature
PG&E	Pacific Gas and Electric
PTO	Pool Turnover
PWR	Pressurized Water Reactor
PWROG	Pressurized Water Reactor Owners Group
RAI	Request for Additional Information
RCS	Reactor Cooling System
RG	Regulatory Guide
RHR	Residual Heat Removal
RMI	Reflective Metallic Insulation
RNG	Renormalized Group Theory
RPV	Reactor Pressure Vessel
RWST	Refueling Water Storage Tank
SAS	Sodium Aluminum Silicate
SBLOCA	Small Break Loss-of-Coolant Accident
SE	Safety Evaluation
SG	Steam Generator
SI	Safety Injection
SIP	Safety Injection Pump
SSC	Structure, System, or Component
TIW	Thermal Insulating Wool
TKE	Turbulent Kinetic Energy
TS	Technical Specification
UFSAR	Updated Final Safety Analysis Report
ZOI	Zone of Influence

This enclosure provides Pacific Gas and Electric's (PG&E's) final response to Generic Letter (GL) 2004-02 (Reference 1) and Generic Safety Issue (GSI) 191 in the form of a stand-alone document that supersedes all previous GL 2004-02 submittals for Diablo Canyon Power Plant (DCPP) Unit 1 and Unit 2. Previous Requests for Additional Information (RAIs) are addressed in this submittal document in Section 4. This enclosure follows the format and guidance provided by the Nuclear Regulatory Commission (NRC) (Reference 2; 3; 4; 5) and addresses all topical areas in those documents. The text from the NRC guidance is presented in italic script.

NRC Request, Summary-Level Description

The GL supplemental response should begin with a summary-level description of the approach chosen. This summary should identify key aspects of design modifications, process changes, and supporting analyses that the licensee believes are relevant or important to the NRC staff's verification that corrective actions to address the GL are adequate. The summary should address significant conservatisms and margins that are used to provide high confidence the issue has been addressed even with uncertainties remaining. Licensees should address commitments and/or descriptions of plant programs that support conclusions.

Summary-Level Description for DCPP

The key aspects of the approach chosen by PG&E to resolve the concerns identified in GL 2004-02 are stated below for clarity:

- Design modifications to significantly reduce the potential effects of post-accident debris and latent material on the functions of the emergency core cooling system (ECCS) and containment spray system (CSS) during the recirculation phase of accident mitigation.
- Testing and analysis to determine break locations, identify and quantify debris sources, quantify debris transport, determine upstream and downstream effects, and confirm the recirculation function.
- Changes to the DCPP Unit 1 and Unit 2 licensing basis, including Technical Specification (TS) and updated final safety analysis report (UFSAR) changes, to reflect plant modifications, and the change to a mechanistic sump strainer blockage evaluation.
- Changes to plant programs, processes, and procedures to limit the introduction of materials into containment that could adversely impact the recirculation function and establish monitoring programs to ensure containment conditions will continue to support the recirculation function.
- Application of conservative measures to assure adequate margins throughout the actions taken to address the GL 2004-02 concerns.

More details are provided for the plant-specific analyses, changes to the licensing basis, improvements in processes and programs, and conservatisms and margins.

Analyses

A debris generation analysis has been performed for DCPP Units 1 and 2, which determined the debris generated for all break sizes from 0.5 inches up to the largest double-ended guillotine breaks (DEGBs) at all Class I in-service inspection (ISI) welds at locations inside the first isolation valve where reactor coolant system (RCS) pressure is expected to be present. These locations were analyzed as DEGBs and as partial breaks at 45-degree intervals around the circumference of the pipe. This debris generation analysis was an automated evaluation based on a detailed computer-aided design (CAD) model of containment. Additional discussion of the debris generation analysis is provided in the Responses in Sections 3.a and 3.b.

DCPP has performed testing for strainer head loss and fiber debris bypass. The testing used prototypical test strainer hardware, debris loads and flow velocities and followed the NRC guidance for head loss testing (Reference 3) and the NRC reviewed protocols for fibrous debris bypass testing (Reference 6). Formation of chemical precipitates and their impact on strainer head loss were accounted for in the testing and analysis. Additional discussion is provided in the Responses in Sections 3.f, 3.n, and 3.o.

The strainer head loss results were used to analyze pump Net Positive Suction Head (NPSH) margin, void fraction due to degasification, flashing, vortexing and strainer structural qualification, as detailed in the Responses in Sections 3.f and 3.g. The fiber bypass testing results informed the core debris deposition and core blockage analyses using the methodology in WCAP-16793 (Reference 7) and WCAP-17788 (Reference 8; 9; 10), as summarized in the Response in Section 3.n.

Changes to the Licensing Basis

The Response in Section 3.p includes a markup to the DCPP Unit 1 and Unit 2 UFSAR to summarize the modifications, testing and evaluations performed to resolve GL 2004-02 and demonstrate that the sump recirculation strainer will serve its safety function during the post-LOCA recirculation phase.

DCPP has incorporated NRC-approved TS changes for increased water level in the refueling water storage tank (RWST) at DCPP Unit 1 and Unit 2 to ensure a sufficient quantity of water is available to enable the containment recirculation function to operate as required in the post-loss of coolant accident (LOCA) environment.

Improvements in Procedures, Processes and Programs

PG&E has completed a review of plant procedures, processes, and programs and has updated those procedures, processes, and programs that will ensure the analysis inputs and assumptions can be maintained. This is discussed in the Response in Section 3.i. The changes to those procedures, programs and processes determined to be necessary to support the transition to the mechanistic evaluation methodology licensing basis were in place prior to, or at the time of the change to the licensing basis.

Conservatisms and Margins

PG&E applied conservative measures in the testing programs and analyses required to address the GL 2004-02 concerns. The key areas in which these conservative measures were applied are discussed in Section 3 of the submittal.

1. Overall Compliance

Provide information requested in GL 2004-02 Requested Information Item 2(a) regarding compliance with regulations.

> *GL 2004-02 Requested Information Item 2(a)*
> *Confirmation that the ECCS and CSS recirculation functions under debris loading conditions are or will be in compliance with regulatory requirements listed in the Applicable Regulatory Requirements section of this GL. This submittal should address the configuration of the plant that will exist once all modifications required for regulatory compliance have been made and this licensing basis has been updated to reflect the results of the analysis described above.*

Response to 1:

This submittal by PG&E uses a deterministic approach to address the effects of LOCA-generated debris on ECCS and CSS recirculation functions per the requirements of the NRC GL 2004-02 for DCPP. As demonstrated in Section 3 of this submittal, DCPP has implemented plant modifications and completed testing and analyses to address the GL 2004-02 concerns. PG&E has updated the DCPP licensing basis to reflect that the ECCS and CSS recirculation functions under debris loading conditions are in compliance with the requirements identified in the Applicable Regulatory Requirements section of GL 2004-02.

Applicable Regulatory Requirements

The applicable regulatory requirements identified in GL 2004-02 (Reference 1 pp. 8-9) are:

10 CFR 50.46 Acceptance Criteria for Emergency Core Cooling Systems for Light-Water Nuclear Power Reactors

10 CFR 50 Appendix A General Design Criteria (GDC)
- GDC 35 (1971) - Emergency Core Cooling
- GDC 38 (1971) - Containment Heat Removal
- GDC 41 (1971) - Containment Atmosphere Cleanup

Note that DCPP Unit 1 and Unit 2 were designed to comply with the Atomic Energy Commission (AEC) (now the NRC) GDCs for Nuclear Power Plant Construction Permits, published in July 1967. The DCPP UFSAR (Appendix 3.1A) provides a summary discussion for each criterion of how the DCPP principal design features (the 1967 GDCs plus additional design features) conform to the intent of the 1971 GDCs.

Table 1-1: DCPP Unit 1 and Unit 2 GL 2004-02 Regulatory Compliance

Regulatory Statute	Applicable Requirement	DCPP Unit 1 and Unit 2 Basis for Compliance with GL 2004-02
10 CFR 50.46 (b)(5)	Long-term cooling. After any calculated successful initial operation of the ECCS, the calculated core temperature shall be maintained at an acceptably low value and decay heat shall be removed for the extended period of time required by the long-lived radioactivity remaining in the core.	1. New sump strainer assembly to ensure adequate NPSH during recirculation. 2. Modification of the access/maintenance hatch to allow water to flow from the reactor cavity/instrumentation tunnel to the sump for reactor cavity breaks ensures adequate NPSH during recirculation. 3. Modification of the reactor cavity door to allow more debris to flow into the reactor cavity inactive sump reduces the potential strainer overall debris loading. 4. Addition of three debris interceptors to capture reflective metal insulation (RMI) and unqualified coating paint chips reduces the potential strainer overall debris loading. 5. Removal of cable tray fire stops to reduce the potential strainer fiber loading. 6. Installation of additional banding to calcium silicate (Cal-Sil) piping insulation to reduce the potential strainer particulate loading. 7. Installation of stainless-steel jacketing on Temp-Mat piping insulation to reduce the potential strainer fiber loading. 8. Installation of tray covers to protect the pressurizer heater cable insulation in cable trays below the pressurizer and reduce the potential strainer fiber loading. 9. Installation of stainless-steel jacketed Temp-Mat insulation on the inlet to the pressurizer safety valves to reduce the potential strainer fiber loading. 10. Replacement of Cal-Sil and mineral wool insulation on all four steam generators (SGs) with RMI and stainless-steel jacketed Temp-Mat insulation to reduce the potential strainer particulate and fiber loading. 11. Increase in the minimum TS RWST volume from 400,000 gallons to 455,300 gallons to ensure design basis sump water supply will be available. 12. Downstream fuel and in-vessel evaluations to demonstrate that long term post-LOCA core cooling will be maintained. 13. Pump NPSH analysis to show that the ECCS pumps will have positive NPSH margins when operating in the recirculation mode. 14. Strainer degasification, flashing and vortexing analyses to show that air-entrainment will not impact safety functions of the ECCS pumps during recirculation.
10 CFR 50, Appendix A, GDC 35 (1971)	As shown in Appendix 3.1A of the DCPP UFSAR, GDC 35 (1971) is associated with 1967 GDCs 37 and 44, and the DCPP Unit 1 and Unit 2 designs conform to the intent of this GDC.	The assurance of long-term cooling capability during recirculation (as discussed above) ensures that the design basis emergency core cooling function is maintained.

Regulatory Statute	Applicable Requirement	DCPP Unit 1 and Unit 2 Basis for Compliance with GL 2004-02
10 CFR 50, Appendix A, GDC 38 (1971)	As shown in Appendix 3.1A of the DCPP UFSAR, GDC 38 (1971) is associated with 1967 GDCs 49 and 52, and the DCPP Unit 1 and Unit 2 designs conform to the intent of this GDC.	The assurance of long-term cooling capability during recirculation (as discussed above) ensures that the design basis containment heat removal function is maintained.
10 CFR 50, Appendix A, GDC 41 (1971)	As shown in Appendix 3.1A of the DCPP UFSAR, GDC 41 (1971) is associated with 1967 GDC 37, and the DCPP Unit 1 and Unit 2 designs conform to the intent of this GDC.	The assurance of long-term cooling capability during recirculation (as discussed above) ensures that CS capability and therefore the containment atmosphere cleanup capability are maintained.

2. General Description of and Schedule for Correction Actions

Provide a general description of actions taken or planned, and dates for each. For actions planned beyond December 31, 2007, reference approved extension requests or explain how regulatory requirements will be met as per Requested Information Item 2(b). (Note: All requests for extension should be submitted to the NRC as soon as the need becomes clear, preferably no later than October 1, 2007.)

> *GL 2004-02 Requested Information Item 2(b)*
> *A general description and implementation schedule for all corrective actions, including any plant modifications that you identify while responding to this GL. Efforts to implement the identified actions should be initiated no later than the first refueling outage starting after April 1, 2006. All actions should be completed by December 31, 2007. Provide justification for not implementing the identified actions during the first refueling outage starting after April 1, 2006. If corrective actions will not be completed by December 31, 2007, describe how the regulatory requirements discussed in the Applicable Regulatory Requirements section will be met until the corrective actions are completed.*

Response to 2:

The corrective actions to address the concerns identified in GL 2004-02 at DCPP consisted of plant modifications, testing and analysis, changes to plant programs and processes, and changes to the licensing basis. These actions have been completed in accordance with PG&E regulatory commitments and NRC-approved extensions. The completion dates for these actions are provided below.

Plant Modifications (Unit 1 and Unit 2)

1. PG&E installed a larger sump strainer assembly (with approximately five times the surface area of the strainer upgraded in the tenth refueling outages, and approximately 40 times the area of the original screens) that has passed plant-specific head loss testing for post-LOCA debris loads. This modification was completed during the fourteenth refueling outage for each unit (Spring 2007 and Spring 2008 for Unit 1 and 2, respectively).
2. PG&E modified the access/maintenance hatch to allow water to flow from the reactor cavity/instrumentation tunnel to the sump for a break in the reactor cavity. This modification was completed during the sixteenth refueling outage for each unit (Fall 2010 and Spring 2011 for Unit 1 and 2, respectively).
3. PG&E modified the reactor cavity door (Door 278 in Unit 1 and Door 278-2 in Unit 2) to allow more debris to flow into the reactor cavity inactive sump. These modifications were completed during the fourteenth refueling outage for each unit (Spring 2007 and Spring 2008 for Unit 1 and 2, respectively).
4. PG&E installed perforated plate debris interceptors on Doors 275, 276, 277 (Unit 1) and Doors 275-2, 276-2, and 277-2 (Unit 2) in the crane wall to capture RMI and unqualified coatings chips. This modification was completed during the fourteenth refueling outage for each unit (Spring 2007 and Spring 2008 for Unit 1 and 2, respectively).

5. PG&E removed cable tray fire stops inside the crane wall that had the potential to become debris during a LOCA. This modification was completed during the fourteenth refueling outage for each unit (Spring 2007 and Spring 2008 for Unit 1 and 2, respectively).
6. PG&E installed additional banding to Cal-Sil piping insulation that had the potential to become debris during a LOCA. This modification was completed during the fourteenth refueling outage for each unit (Spring 2007 and Spring 2008 for Unit 1 and 2, respectively).
7. PG&E installed stainless-steel jacketing on Temp-Mat piping insulation that had the potential to become debris during a LOCA. This modification was completed during the fourteenth refueling outage for each unit (Spring 2007 and Spring 2008 for Unit 1 and 2, respectively).
8. PG&E installed tray covers to protect the pressurizer heater cable insulation in cable trays below the pressurizer. This modification was completed during the fourteenth refueling outage for each unit (Spring 2007 and Spring 2008 for Unit 1 and 2, respectively).
9. PG&E installed stainless-steel jacketed Temp-Mat insulation on the inlet to Pressurizer Safety Valves 8010A, 8010B, and 8010C (in both units). This modification was completed for all valves except Valve 8010A in Unit 1 during the fourteenth refueling outage for each unit (Spring 2007 and Spring 2008 for Unit 1 and 2, respectively). The modification for Valve 8010A in Unit 1 was completed during the fifteenth refueling outage for Unit 1 (Spring 2009).
10. PG&E installed RMI and stainless-steel jacketed Temp-Mat on the replacement SGs. This modification was completed for Unit 2 during the fourteenth refueling outage for Unit 2 (Spring 2008) and the fifteenth refueling outage for Unit 1 (Spring 2009).
11. At DCPP Unit 1 and Unit 2, the TS minimum RWST water volume has been increased from 400,000 gallons to 455,300 gallons. The NRC issued Amendment No. 199 to Facility Operating License DPR-80 and Amendment No. 200 to Facility Operating License DPR-82, for Units 1 and 2, respectively, approving the change in the RWST level on March 26, 2008 (Reference 11).

Testing and Analyses

The testing and analyses needed to address GL 2004-02 concerns were completed in December 2018.

Plant Programs and Processes

Significant program and process changes necessary to address the GL 2004-02 concerns have been implemented, as summarized below.

Procedural controls are in place to control the amount of loose debris (paper, rags, trash, clothing, insulation, plastics, etc.) in containment. Procedures require inspection of all accessible areas to verify that no loose debris is present prior to setting containment integrity. Steps are taken to ensure that all equipment, tools, and materials brought into the containment are accounted for and any debris found during the inspections are removed.

A containment clean-up procedure is in place that provides the guidelines for containment cleanliness coming out of a refueling outage. This procedure requires inspection of all accessible areas to ensure that delaminated coatings are reported, all areas are wiped down/vacuumed if determined to be excessively dirty, and loose tags, signs, or markers are removed from containment prior to setting containment integrity.

Insulation installation procedures have been implemented to ensure the installation of insulation in containment meets design requirements for maintaining the inputs considered for GSI-191 resolution.

DCPP has instituted a coatings program which includes procedures to ensure coatings are installed correctly and inspections are performed to ensure the installed coatings continue to meet the assumptions considered for input to the debris generation analysis.

Foreign material exclusion programmatic controls are in place, which ensure that proper work control is specified for debris-generating activities within the containment building. This assists in preventing introduction of foreign material into containment, which could potentially challenge the containment recirculation function. The program has strict controls in place to ensure that foreign materials brought into containment are logged, tracked, and subsequently removed after the completion of tasks.

DCPP engineering change process and procedure ensure that modifications that may affect the ECCS, including sump performance, are evaluated for impact on the inputs and assumptions used for the response to GL 2004-02. During engineering change preparation, the process requires that coordination occurs between the lead discipline engineer and engineering to determine changes that may affect the ECCS or CSS, or may affect the accident analysis (UFSAR Chapter 6). Specific critical attributes are listed, evaluated, and documented when affected in the required Independent Evaluation Form completed by engineering. This includes the introduction of materials into containment that could affect sump performance or lead to equipment degradation. It also includes repair, replacement, or installation of coatings inside of primary containment including installing coated equipment.

DCPP’s standard change process requires activities that affect UFSAR described structure, system, or component (SSC) design functions to be evaluated as a design change in accordance with PG&E’s 10 CFR 50 Appendix B program. This includes modifications that would impact the containment sump. Design changes require an assessment in accordance with 10 CFR 50.59. A failure modes and effects analysis is required if the design change introduces any new failure modes or changes failure modes for the affected SSCs.

The containment inspection procedure was updated to include all of the strainer system components in the final containment closeout inspection. The effect of these changes is to ensure that all components (strainer modules, piping, and pipe connections) are inspected, and that there are no signs of structural distress such as visible signs of corrosion, damaged coatings, damaged perforated plates and wire mesh overlay, unacceptable gaps, bent racks, broken or missing fasteners, or any component showing signs of wear to the point of possibly breaking in any strainer system component.

Temporary configuration changes are controlled by plant procedure, which maintain configuration control for non-permanent changes to plant structures, systems, and components while ensuring the applicable technical reviews and administrative reviews and approvals are obtained.

In accordance with 10 CFR. 50.65 “Maintenance Rule”, DCPP assesses the increase in risk that may result from proposed maintenance activities on structures and systems shown to be significant to public health and safety. The risk assessment ensures that the maintenance activity will not adversely impact the intended safety functions of the structure or system.

Licensing Basis

DCPP Unit 1 and Unit 2 UFSAR was updated to reflect the plant modifications that were implemented to address the GL 2004-02 concerns. A license amendment was also implemented for the change in the minimum required RWST water level (Reference 11). A markup to the UFSAR is attached to this submittal to summarize the evaluation of the effect of post-accident debris on the ECCS and CSS recirculation functions.

3. Specific Information Regarding Methodology for Demonstrating Compliance

3.a. Break Selection

The objective of the break selection process is to identify the break size and location that present the greatest challenge to post-accident sump performance.

1. *Describe and provide the basis for the break selection criteria used in the evaluation.*

Response to 3.a.1:

Nuclear Energy Institute (NEI) 04-07 and the associated NRC Safety Evaluation (SE) on NEI 04-07 (Reference 12 pp. 3-5 - 3-26, 4-1 - 4-5; 13 pp. 12-35, 85-91) provide guidance on how the break selection process should be conducted. The objective of the break selection process is to identify the break conditions that present the greatest challenge to post-accident sump performance. The DCPP debris generation calculation followed the methodology outlined in the above documents. Note that DCPP analyzed a range of breaks, instead of just the worst-case breaks as suggested by NEI 04-07.

DCPP evaluated debris generation quantities for breaks at all of the ISI weld locations of the Class 1 lines inside the crane wall, including breaks at the reactor nozzles. Debris generated by the breaks inside the annulus were not quantified. This is reasonable because the largest lines in containment are those of the primary loop and the majority of insulation lies inside the crane wall. Note that the Class 1 lines inside the containment vary in size from 1.5 to 31 inches while the largest line in the outer annulus is 8 inches. Therefore, the quantity of debris generated from a primary loop break would be bounding in comparison to the much smaller rupture of an 8-inch line.

NEI 04-07 suggests evaluating potential breaks at equal increments along the pipe (Reference 12 pp. 3-9). However, per the NRC’s SE on NEI 04-07, evaluating breaks at equal increments is “only a reminder to be systematic and thorough” (Reference 13 Section 3.3.5.2). The DCPP’s approach of using ISI welds on every Class 1 pipe as break locations is both systematic and thorough because there are multiple ISI welds on every pipe in the RCS and the welds cover the full range of possible break locations. In addition, a weld is generally closer to equipment that has a large quantity of insulation, compared to a span of straight pipe (e.g., a break on the hot leg weld at the base of the SG will typically generate more debris than a break halfway between the SG and reactor vessel), as can be seen in Figure 3.a.1-1 and Figure 3.a.1-2. Also, welds are almost universally recognized as likely failure locations because they can have relatively high residual stress, are preferentially-attacked by many degradation mechanisms, and are most likely to have preexisting fabrication defects (Reference 14 p. xviii).

Non-pipe LOCAs (e.g., breaks at non-piping components or equipment) were not explicitly evaluated. This is reasonable because the debris loads for the breaks at non-piping components would be bounded by already-analyzed breaks at pipe weld locations.

The following types of LOCA breaks were considered for debris generation analysis. Figure 3.a.1-1 and Figure 3.a.1-2 show the graphical representation of the weld locations for Unit 1 and Unit 2, respectively.

- DEGBs at all ISI welds of Class 1 lines including the largest break of the 31-inch crossover leg.
- Partial breaks at all ISI welds of Class 1 lines. For each weld, partial breaks at 8 different angles oriented 45 degrees apart along its circumference was postulated. Partial break sizes included 0.5, 2, 4, 6, 8, 10, 12, 14, 17, 20, 23, and 26 inches, as applicable.

The extensive break locations and break sizes considered in the DCPP debris generation analysis ensured that the breaks with the maximum debris loads and worst debris composition (e.g., with the most problematic debris) were captured. As discussed in the Response to 3.b.4, the insulation types at DCPP Unit 1 and Unit 2 that have major contribution to the debris loads include Cal-Sil, Thermal Insulating Wool (TIW), Fiberglass Overbraid, Flexicone Sleeving, Mica Tape, Temp-Mat, RMI, and Foamglas. As RMI tends to be a non-problematic debris source for non-pit type strainers (Reference 3, Appendix A p. 4-5), maximizing the generation of Cal-Sil and fibrous insulation was the focus of the break selection process. The combination of Cal-Sil and fiber can form tight debris beds with limited porosity, which can cause high head losses even at low approach velocities (Reference 3, Appendix A p. 4-5). The breaks presented in the Response to 3.a.3 maximize the quantities of these problematic debris types.

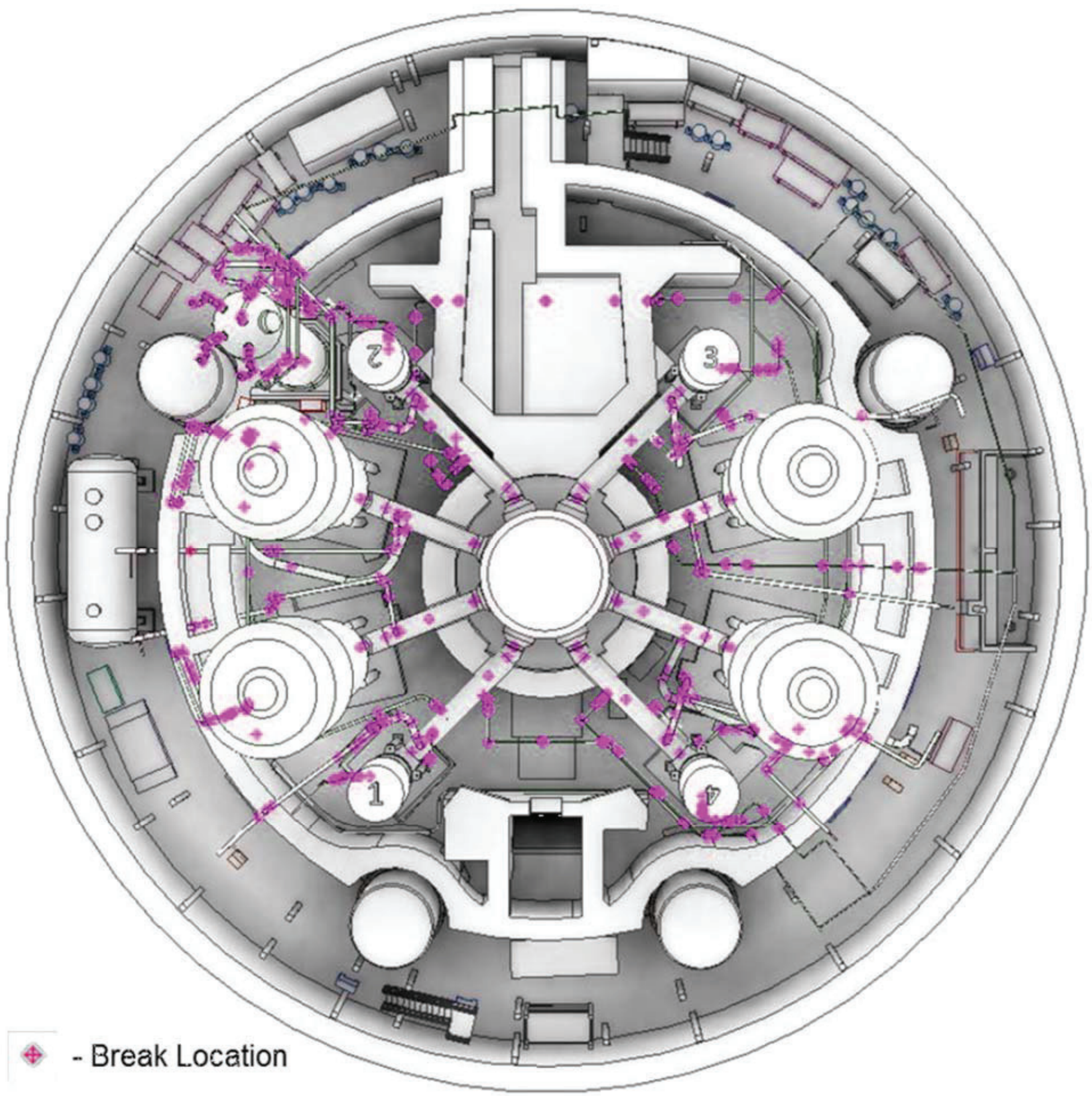

Figure 3.a.1-1: Unit 1 Weld Locations Where Postulated LOCAs Occur

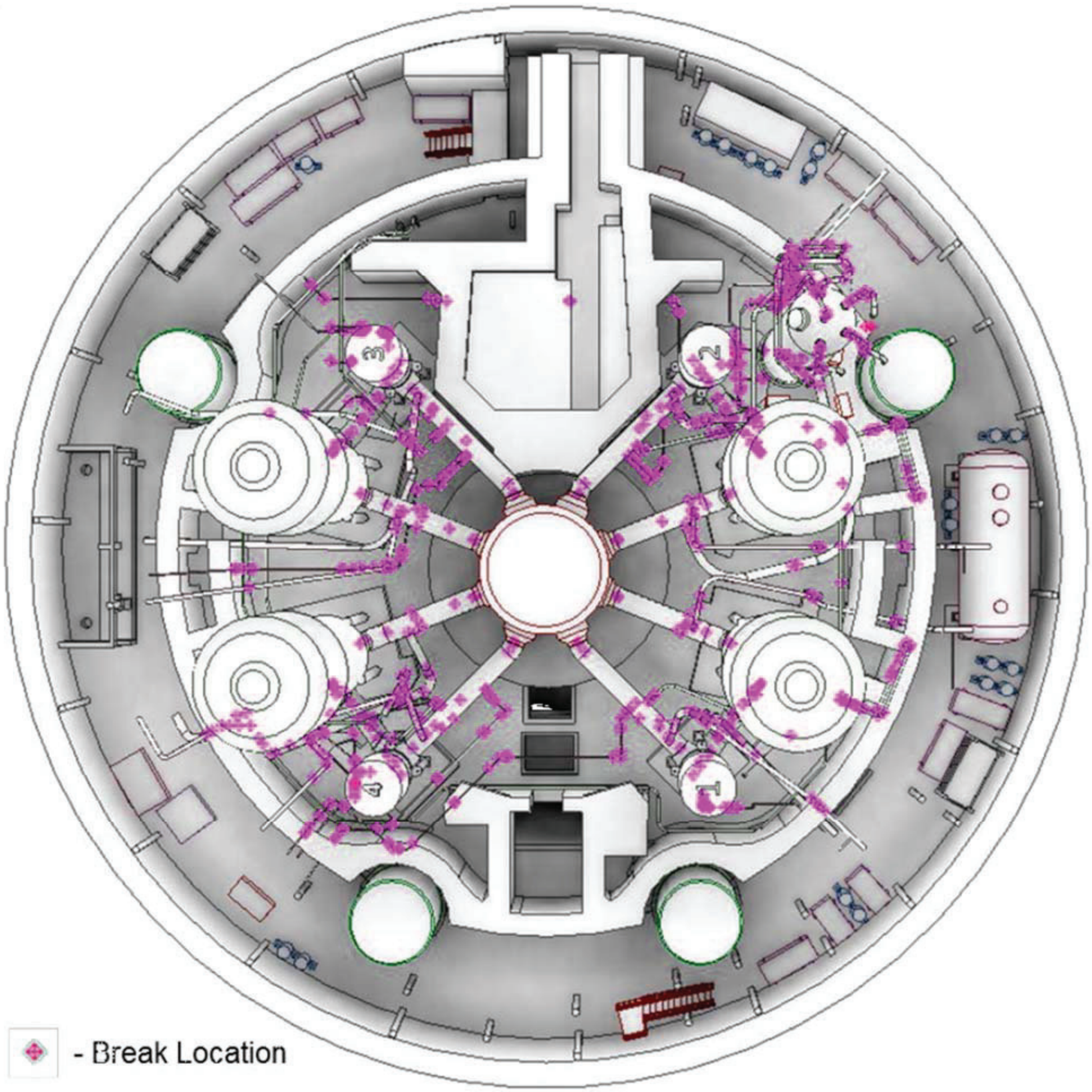

Figure 3.a.1-2: Unit 2 Weld Locations Where Postulated LOCAs Occur

2. *State whether secondary line breaks were considered in the evaluation (e.g., main steam and feedwater lines) and briefly explain why or why not.*

Response to 3.a.2:

Secondary system line breaks (e.g., feedwater or main steam line breaks) are not considered in this evaluation. Recirculation is not a concern for a secondary system line break because the RCS remains intact. With the RCS intact, the RWST drain down is slower and containment spray will be available as long as required to mitigate the increase in containment pressure with water supplied from the RWST. PG&E submitted a license amendment request (Reference 15) to clarify the limiting condition for operation of the CSS. The NRC SE that supports the license amendment (Reference 16) stated that "the recirculation mode of emergency core cooling is only used following a LOCA." Therefore, secondary system line breaks were not considered in this evaluation.

3. *Discuss the basis for reaching the conclusion that the break size(s) and locations chosen present the greatest challenge to post-accident sump performance.*

Response to 3.a.3:

The debris generation calculation for DCPP takes into account a spectrum of break sizes on every ISI weld within the Class 1 piping inside the crane wall. This extensive selection of break locations and sizes ensured that the widest possible set of potential break scenarios were evaluated. This set includes the debris generated by the worst-case scenario LOCAs: DEGBs on the main loop piping.

Given that most large breaks generate similar quantities of debris from latent dirt/dust, miscellaneous debris (stickers, tags, labels, tape), qualified and unqualified coatings, those breaks that generate limiting amounts of Cal-Sil and fibrous debris are more likely to challenge post-accident sump performance (as discussed in the Response to 3.a.1).

Debris would only impact sump performance when it transports to the sump strainers. Therefore, when identifying the worst breaks, debris transport was also considered, as detailed in the Response to 3.e. The breaks with the highest transported fiber, Cal-Sil or total particulate debris were identified for each unit, as summarized in Table 3.a.3-1. The generated and transported debris loads for these breaks are shown in the Responses to 3.b.4 and 3.e.6, respectively. The generated coatings debris loads for these breaks are shown in the Response to 3.h.5.

Table 3.a.3-1: DCPP Worst-Case Breaks

Unit	Loop	Limiting Debris Type	Weld Location	Location Description
1	2	Fiber	WIB-RC-2-1 (SE)	Loop 2 Hot Leg at RPV[1] (largest transported fiber of all breaks)
1	2	Fiber	WIB-RC-2-10	Loop 2 Crossover Leg (largest transported fiber from SG compartments 1-4)
1	3	Cal-Sil/ Particulate	WIB-RC-3-7	Loop 3 Crossover Leg (largest transported Cal-Sil and total particulate of all breaks)
1	1	Cal-Sil/ Particulate	WIB-RC-1-12	Loop 1 Crossover Leg (largest transported Cal-Sil and total particulate from SG compartments 1-2)
2	2	Fiber	WIB-RC-2-6 SE	Loop 2 Crossover Leg (largest transported fiber of all breaks)
2	2	Fiber	WIB-RC-2-16 (SE)	Loop 2 Cold Leg @ RPV[1] (largest transported fiber from reactor cavity breaks)
2	4	Cal-Sil/ Particulate	WIB-RC-4-7	Loop 4 Crossover Leg (largest transported Cal-Sil and total particulate of all breaks)
2	1	Cal-Sil/ Particulate	WIB-RC-1-11	Loop 1 Crossover Leg (largest transported Cal-Sil and total particulate from SG compartments 1-2)

[1] This break is at the reactor pressure vessel (RPV) nozzle.

3.b. Debris Generation/Zone of Influence (excluding coatings)

The objective of the debris generation/ZOI process is to determine, for each postulated break location: (1) the zone within which the break jet forces would be sufficient to damage materials and create debris; and (2) the amount of debris generated by the break jet forces.

1. *Describe the methodology used to determine the ZOIs for generating debris. Identify which debris analyses used approved methodology default values. For debris with ZOIs not defined in the guidance report/SE, or if using other than default values, discuss method(s) used to determine ZOI and the basis for each.*

   Response to 3.b.1:

   In a pressurized water reactor (PWR) reactor containment building, the worst-case pipe break would typically be a DEGB. In a DEGB, jets of water and steam would blow in opposite directions from the severed pipe. One or both jets could hit obstacles and be reflected in different directions. To take into account the double jets and potential jet reflections, NEI 04-07 Volume 1 (Reference 12 p. 1-3; 13 p. vii) proposes using a spherical break zone of influence (ZOI) centered at the break location to determine the quantity of debris that could be generated by a given line break. This guidance was used in the DCPP debris generation analysis. For DEGBs, the ZOI for a given type of material is defined as a spherical volume, in which the jet pressure is higher than its destruction/damage pressure. The ZOI is centered at the break location.

   For any break smaller than a DEGB (i.e., a partial break), the NRC SE on NEI 04-07 accepts the use of a hemispherical ZOI centered at the edge of the pipe (Reference 13 p. 117). Because these types of breaks could occur anywhere along the circumference of the pipe, the partial breaks were analyzed using hemispheres at eight different angles that are 45 degrees apart from each other around the pipe.

   In some cases, if the ZOI for a particular material is very large (i.e., it has a low destruction pressure or is located on a large pipe); the radius of the sphere may extend beyond robust barriers located near the break. Robust barriers consist of structures, such as concrete walls that are impervious to jet flow and prevent further expansion of the jet. Insulation in the shadow of large robust barriers can be assumed to remain intact to a certain extent (Reference 12 pp. 3-14 through 3-15). All ZOIs were truncated to account for robust barriers per the NRC SE on NEI 04-07 (Reference 13 p. vii).

   Materials enveloped by a break ZOI are considered to be debris generated by the break. Volumetric debris quantities were determined by measuring the overlap between a ZOI and corresponding debris sources. This was done within the CAD model environment.

Because different materials have different destruction pressures, material-specific ZOIs were determined. Table 3.b.1-1 shows the primary side break equivalent ZOI radii divided by the diameter of the broken pipe (L/D) for each representative material in the DCPP containment buildings. As indicated in the last column of the table, the ZOI sizes were taken from the NRC SE on NEI 04-07 for most of the materials. For the other debris types, their ZOI sizes were justified and documented in the debris generation analysis, as summarized later in this section.

Table 3.b.1-1: ZOI Radii for DCPP Insulation Types

Material Type	ZOI Radius/ Break Diameter (L/D)	Reference
Cal-Sil	5.45	NRC SE on NEI 04-07 (Reference 13 pp. 30 and II-20)
Transco RMI	2.0	
Johns Manville RMI with standard bands	28.6	
Foamglas	28.6	
Miscellaneous Debris*	28.6	
Temp-Mat with stainless-steel wire retainer	11.7	
Temp-Mat with stainless-steel wire mesh, encapsulated in 0.003-inch thick stainless-steel cladding	3.7	WCAP-17561 (Reference 17, p. 1-3)
TIW	17.0	See discussion below
Pressurizer Heater Cables – Fiberglass overbraid, Mica Tape and Flexicone Sleeving (fiberglass and silicone rubber)	17.0	
Min-K in pressurizer cubicle	11.7	See discussion below

* For the purpose of GSI-191 analyses, miscellaneous debris referred to items that will not disintegrate in the sump pool and can be transported to the strainer, blocking perforated strainer surfaces. See the Response to 3.b.5 for details.

WCAP-17561-P (Reference 17) showed that Temp-Mat encapsulated in stainless-steel foil passed the jet blast test with only small tears. The test data concluded a break ZOI of 3.7D, which was used in the DCPP debris generation analysis when quantifying the encapsulated Temp-Mat debris. It should be noted that the actual encapsulated Temp-Mat debris loads used for DCPP head loss and fiber penetration testing, and analyses of ex-vessel and in-vessel downstream effects and chemical effects exceeded the debris quantities that would result from a larger 11.7D ZOI.

TIW is used on the elbows of Cal-Sil insulated small-bore lines of 2” and smaller at DCPP. The ZOI size for Nukon given in the NRC SE of NEI 04-07 (17.0D) was assumed to be applicable for TIW. Note that, although the as-fabricated density of TIW (1.08 lbm/ft^3) is lower than that of Nukon (2.4 lbm/ft^3), the applied TIW insulation was wrapped and compressed around the pipe fitting so that the density of applied insulation is several times greater than the as-fabricated density. Additionally, the TIW insulation is jacketed with a multibanded stainless steel jacketing system.

The ZOI size for Nukon (17.0D) was also assumed to be applicable for the pressurizer heater cable insulation (e.g., Fiberglass overbraid, Mica Tape and Flexicone Sleeving). This assumption is reasonable because the densities of the fiberglass overbraid and flexicone sleeving (133 lbm/ft^3), and mica tape (74.9 lbm/ft^3) are much higher than that of Nukon (2.4 lbm/ft^3), and NEI 04-07 shows that higher density fiber insulation types typically have smaller ZOI sizes.

It was assumed that the ZOI size (11.7D) for Temp-Mat was applicable for Min-K. At DCPP, Min-K was only used in a floor penetration of the pressurizer cubicle at an Elevation of 140 ft. Temp-Mat was also used in this penetration and was placed below the Min-K. Due to this arrangement, the Min-K would not fail from breaks below the penetration unless the Temp-Mat fails first. Above this penetration, there only exist small bore pipes. If these pipes break, the ZOIs do not extend to the penetration even if the 28.6D ZOI is used for Min-K, as directed in the SE on NEI 04-07 (Reference 13 p. 30). Therefore, applying the Temp-Mat ZOI size is acceptable.

No ZOI size is required for the vapor barrier material. Vapor barrier was bonded to the stainless-steel jacketing used on the Cal-Sil insulation. The surface area of vapor barrier debris was therefore equal to the surface area of the destroyed Cal-Sil and was derived from the Cal-Sil debris quantities.

No ZOI size is required for Kaowool. Kaowool damming board and Kaowool blanket material are used outside the crane wall as fire stops. Based on the guidance provided in NEI 04-07 (Reference 12 Section 3.4.3.3.4), the debris generated from all uncovered fire stops outside of the ZOI but subject to CS and washdown was calculated and added as a source term. Walkdowns of the Unit 1 and Unit 2 annulus identified the number of fire stops outside the crane wall which are subject to erosion from CS. The quantity of Kaowool which would be eroded was determined and applied to all break scenarios where sprays are actuated. It was determined through testing that the Marinite and RTV foam used in the cable trays would not erode.

Temp-Mat is in the primary shield penetrations around the circumference of each hot leg and cold leg. The computation of ZOIs for Temp-Mat insulation in the region of restrained reactor pressure vessel (RPV) nozzle pipe breaks at DCPP was developed using the ANSI/ANS-58.2 methodology. Using a 61-inch length on the hot leg or 60-inch length on the cold leg (corresponding to Temp-Mat destruction pressure of 10.2 psig), only Temp-Mat in the penetration shared by the same leg on which the break was postulated would be destroyed as shown in Figure 3.b.1-1. The Temp-Mat in adjacent penetrations was assumed to be blown out of the penetrations as intact pieces (i.e, the quantity of Temp-Mat blown out for a Loop 1-1 Cold Leg break is from Loop 1-1 Hot Leg and Loop 1-4 Cold Leg). The Temp-Mat quantities for reactor nozzle breaks were computed manually.

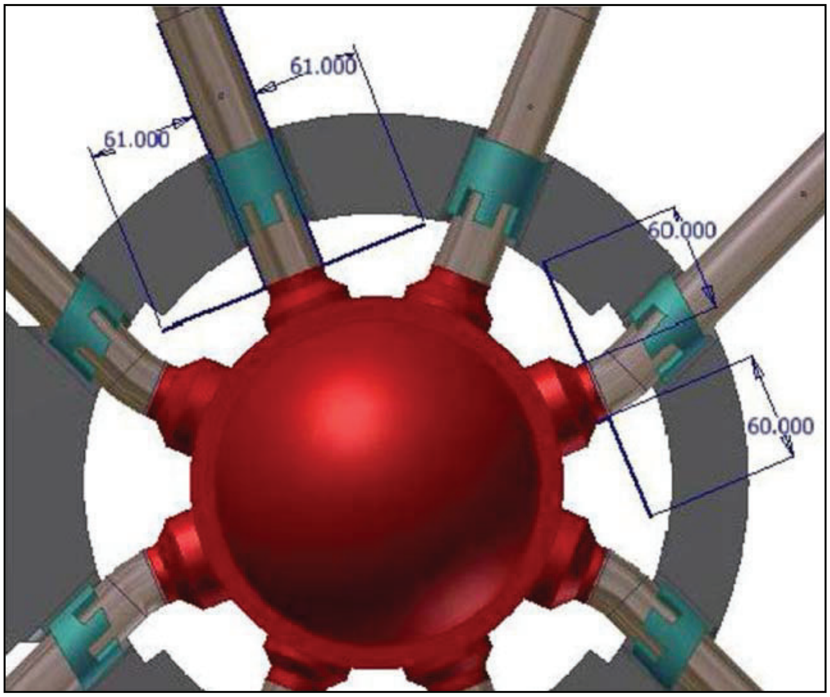

Figure 3.b.1-1: Length of 10.2 psi (Temp-Mat destruction pressure) Jet

2. *Provide destruction ZOIs and the basis for the ZOIs for each applicable debris constituent.*

   Response to 3.b.2:

   See the Response to 3.b.1.

3. *Identify if destruction testing was conducted to determine ZOIs. If such testing has not been previously submitted to the NRC for review or information, describe the test procedure and results with reference to the test report(s).*

   Response to 3.b.3:

   The Response to 3.b.1 shows the ZOI sizes used for different materials in the DCPP debris generation analysis. The ZOI size of encapsulated Temp-Mat differs from that listed in NEI 04-07 and the NRC SE. DCPP has performed additional jet impingement tests to determine the appropriate spherical-equivalent ZOI size for the encapsulated Temp-Mat, as documented in WCAP-17561-P (Reference 17), which was previously submitted to the NRC for information (Reference 18). The new tests addressed lessons learned from the previous tests, including those identified in the NRC RAIs on WCAP-16720-P.

4. *Provide the quantity of each debris type generated for each break location evaluated. If more than four break locations were evaluated, provide data only for the four most limiting locations.*

Response to 3.b.4:

Quantities of debris generated for each break case (a total of 19,849 combined partial breaks and DEGBs for Unit 1 and 17,282 combined partial breaks and DEGBs for Unit 2) were calculated for each type of material. Table 3.b.4-1 shows the quantities of insulation debris generated for the most limiting DEGBs for Unit 1. Note that the Breaks at WIB-RC-2-1(SE) and WIB-RC-2-10 have the highest transported fibrous debris loads, while the other two breaks are bounding with respect to transported Cal-Sil and total transported particulate debris loads (see Table 3.a.3-1). The transported debris loads for these bounding breaks are shown in the Response to 3.e.6. The generated quantities of coatings debris, latent debris and miscellaneous debris for these breaks are shown in the Responses to 3.h.5, 3.d.3 and 3.b.5, respectively.

Table 3.b.4-1: Limiting Debris Generation Quantities for Unit 1

Weld		**WIB-RC-2-1 (SE)**	**WIB-RC-2-10**	**WIB-RC-3-7**	**WIB-RC-1-12**
Location		Loop 2 HL @ RPV	Loop 2 Crossover	Loop 3 Crossover	Loop 1 Crossover
Limiting Debris		Transported Fiber		Transported Cal-Sil and Total Particulate	
Break Size (in)		Nozzle	31	31	31
Temp-Mat (lbm)	Fines	90.48	1.37	1.29	0.00
	Intact	124.80	0.00	0.00	0.00
TIW (lbm)	Fines	0.00	1.65	2.16	1.15
Fiberglass Overbraid and Flexicone Sleeves (lbm)	Fines	0.00	73.08	0.00	0.00
Kaowool (lbm)	Fines	7.38	7.38	7.38	7.38
RMI (ft^2)	Small and Large	0	53,823	36,623	55,391
Cal-Sil (ft^3)	Particulate	0.00	4.00	22.96	11.69
Min-K (ft^3)	Particulate	0.00	0.00	0.00	0.00
Foamglas (ft^3)	Particulate	0.00	0.08	0.00	0.08
Mica Tape (ft^3)	Particulate	0.00	0.72	0.00	0.00

Similar to Unit 1, Table 3.b.4-2 shows the quantities of insulation debris generated for the most limiting DEGBs for Unit 2. Note that the Breaks at WIB-RC-2-6(SE) and WIB-RC-2-16 have the highest transported fibrous debris loads, while the other two breaks are bounding with respect to transported Cal-Sil and total transported particulate debris loads (see Table 3.a.3-1). The transported debris loads for these bounding breaks are shown in the Response to 3.e.6. The generated quantities of coatings debris, latent debris and miscellaneous debris for these breaks are shown in the Responses to 3.h.5, 3.d.3 and 3.b.5, respectively.

Table 3.b.4-2: Limiting Debris Generation Quantities for Unit 2

Weld		**WIB-RC-2-6SE**	**WIB-RC-2-16 (SE)**	**WIB-RC-4-7**	**WIB-RC-1-11**
Location		Loop 2 Crossover	Loop 2 CL @ RPV	Loop 4 Crossover	Loop 1 Crossover
Limiting Debris		Transported Fiber		Transported Cal-Sil and Total Particulate	
Break Size (in)		31	Nozzle	31	31
Temp-Mat (lbm)	Fines	0.19	53.52	5.11	0.00
	Intact	0.00	72.72	0.00	0.00
TIW (lbm)	Fines	1.27	0.00	1.25	0.63
Fiberglass Overbraid and Flexicone Sleeves (lbm)	Fines	91.31	0.00	0.00	0.00
Kaowool (lbm)	Fines	7.38	7.38	7.38	7.38
RMI (ft^2)	Small and Large	52,978	0.0	35,771	53,160
Cal-Sil (ft^3)	Particulate	5.97	0.00	19.70	11.81
Min-K (ft^3)	Particulate	0.00	0.00	0.00	0.00
Foamglas (ft^3)	Particulate	0.09	0.00	0.00	0.09
Mica Tape (ft^3)	Particulate	0.92	0.00	0.00	0.00

5. *Provide total surface area of all signs, placards, tags, tape, and similar miscellaneous materials in containment.*

Response to 3.b.5:

Miscellaneous debris types and quantities were determined via 3 methods:

- Walkdowns for
  - Miscellaneous debris inside crane wall
  - Miscellaneous debris outside crane wall
  - Aluminum Tape
  - Conduit Sheathing

- Plant Drawings for
  - Light Bulbs
- CAD model for break specific types
  - Vapor Barrier
  - Silicone Rubber

Non-Break Specific Miscellaneous Debris

Table 3.b.5-1 summarizes the generated quantities of the non-break specific miscellaneous debris.

Table 3.b.5-1: Generated Quantities of non-Break Specific Miscellaneous Debris

Debris Type	Location	Source Term	Unit 1 (ft^2)	Unit 2 (ft^2)
Unqualified Miscellaneous Debris (Applicable for All Breaks)	Inside Crane Wall	Valve ID Tags (metal tag with paper sticker)	9.56	9.56
		Paper Stickers	1.5	1.5
		Snubber Stickers	9.24	9.24
		Aluminum Tape	20.0	59.8
	Outside Crane Wall	Cable Trays Stickers	0.875	0.875
		Snubber Stickers	3.13	3.13
		Valve ID Tags Stickers	7.54	7.54
		Miscellaneous Stickers	3.14	3.14
		Cabinet Labeling	0.135	0.135
		Masking Tape	0.208	0.208
Qualified Miscellaneous Debris (Applicable for non-Reactor Cavity Breaks Only)	Inside Crane Wall	Reflective Tape	58.04	58.04
		Conduit Tape	10.65	10.65
		Lamacoids	3.61	3.61
		Black Electrical Tape	5.37	5.37
		Tie-wraps	2.39	2.39
		Paper Radiation Survey Tags	2.75	2.75
		Light Bulbs	170.8	170.8
		Conduit Sheathing	105.0	105.0

After applying the transport fractions shown in the Response to 3.e.6, the total transported quantities of non-break specific miscellaneous debris are shown in Table 3.b.5-2 below.

Table 3.b.5-2: Transport Quantities of non-Break Specific Miscellaneous Debris

Break Type	Unit 1 (ft^2)	Unit 2 (ft^2)
Reactor Cavity Breaks	7.72	8.51
Non-Reactor Cavity Breaks	11.61	12.41

Break Specific Miscellaneous Debris

For break-specific miscellaneous debris (vapor barrier and silicon rubber), their generated quantities were determined using the CAD model for the postulated breaks. Table 3.b.5-3 summarizes the maximum generated and transported quantities for these debris types of each unit. Note that, for conservatism, the debris quantities of each unit are not from the same break. The transport fractions used for these debris types are given in the Response to 3.e.6.

Table 3.b.5-3: Maximum Quantities of Break-Specific Miscellaneous Debris

Debris Type	Unit	Generated Quantities (ft^2)	Transported Quantities (ft^2)
Silicon Rubber	Unit 1	79.3	0
	Unit 2	94.2	0
Vapor Barrier	Unit 1	241.7	161.94
	Unit 2	218.0	146.06

To summarize the above results, Unit 1 has a maximum of 173.55 ft^2 (161.94 ft^2 + 11.61 ft^2) of total miscellaneous debris transported to the strainer, which bounds the maximum quantity of Unit 2. This maximum total miscellaneous debris surface area was rounded up to add margin, resulting in a sacrificial strainer surface area of 205.16 ft^2, which was used during head loss testing (see the Response to 3.f.4).

3.c. Debris Characteristics

The objective of the debris characteristics determination process is to establish a conservative debris characteristics profile for use in determining the transportability of debris and its contribution to head loss.

1. *Provide the assumed size distribution for each type of debris.*

   Response to 3.c.1:

   The size distribution for each debris type (except for coatings and non-break specific miscellaneous debris) considered in the DCPP debris generation analysis is shown in Table 3.c.1-1. The table also shows a summary of the debris material properties, as requested by 3.c.2. The information for coatings is presented in the Response to 3.h.6. The non-break specific miscellaneous debris (except for aluminum tape) was assumed to fail as small pieces with dimensions ranging between 1/8 and ½ inches, large enough to block the strainer perforation. The characteristic size of the aluminum tapes was assumed to be ¼ to 4 inches.

   Temp-Mat inside the primary bio-shield wall penetrations could become debris for the reactor cavity breaks. The Temp-Mat in the penetration for the hot or cold leg on which the break was postulated was assumed to be destroyed into fines while the Temp-Mat in adjacent penetrations was assumed to be blown out of the penetration as intact pieces (e.g., for a Loop 1-1 Cold Leg break, the Temp-Mat inside the Loop 1-1 Hot Leg and Loop 1-4 Cold Leg penetrations were assumed to be blown out). See additional discussion in the Response to 3.b.2.

Table 3.c.1-1: DCPP Unit 1 and Unit 2 Debris Material Properties

<table>
<tr><th>Debris</th><th>Distribution</th><th>Density (lbm/ft^3)</th><th>Characteristic Size</th></tr>
<tr><td>Temp-Mat</td><td>100% Fines</td><td rowspan="3">11.8 (bulk)
162 (fiber)</td><td rowspan="2">9 µm</td></tr>
<tr><td rowspan="2">Temp-Mat from Reactor Cavity Breaks</td><td>100% Fines (for postulated nozzle break)</td></tr>
<tr><td>Intact Blanket (for adjacent penetrations)</td><td>Intact Blanket[1]</td></tr>
<tr><td>TIW</td><td>100% Fines</td><td>1.08 (bulk)
159 (particulate)</td><td>6.75 µm</td></tr>
<tr><td>Fiberglass (Overbraid)</td><td>100% Fines</td><td>133 (bulk)</td><td>7 µm</td></tr>
<tr><td>Fiberglass (Flexicone Sleeving)</td><td>100% Fines</td><td>127 (bulk)</td><td>7 µm</td></tr>
<tr><td>Kaowool Blanket</td><td>100% Fines</td><td>161 (particulate)</td><td>2.7-3 µm</td></tr>
<tr><td>Johns Manville/ Transco RMI</td><td>75% Small Pieces
25% Large Pieces</td><td>-</td><td><4 inches
≥4 inches</td></tr>
<tr><td>Cal-Sil</td><td>100% Particulate</td><td>14.5 (bulk)
144 (particulate)</td><td>5 µm</td></tr>
<tr><td>Min-K</td><td>100% Particulate</td><td>16 (bulk)
161 (particulate)</td><td>2.5-20 µm</td></tr>
<tr><td>Foamglas</td><td>100% Particulate</td><td>9.8 (bulk)
156 (particulate)</td><td>10 µm</td></tr>
<tr><td>Mica Tape</td><td>100% Particulate</td><td>74.9 (bulk)</td><td>22 µm</td></tr>
<tr><td>Vapor Barrier</td><td>100% Small Pieces</td><td>57.4 (bulk)</td><td>1/8 to ½ inches</td></tr>
<tr><td>Silicone Rubber (Flexicone Sleeving)</td><td>100% Small Pieces</td><td>58.0 (bulk)</td><td>1/8 to ½ inches</td></tr>
</table>

2. *Provide bulk densities (i.e., including voids between the fibers/particles) and material densities (i.e., the density of the microscopic fibers/particles themselves) for fibrous and particulate debris.*

Response to 3.c.2:

See the Response to 3.c.1 for the material and bulk densities of debris used in the GSI-191 analyses.

[1] In the Response to 3.l.1, assumed dimensions were used to demonstrate that the intact pieces of Temp-Mat debris generated by a reactor cavity break will not clog the trash racks. Note that those dimensions were conservatively small for the purpose of that analysis.

3. *Provide assumed specific surface areas for fibrous and particulate debris.*

   Response to 3.c.3:

   This question is not applicable for DCPP because head loss testing data (instead of analytical methods) was used to determine strainer head losses (see the Response to 3.f). Therefore, specific surface areas were not used or calculated for the head loss evaluation.

4. *Provide the technical basis for any debris characterization assumptions that deviate from NRC-approved guidance.*

   Response to 3.c.4:

   The debris characterizations for all debris types followed NRC-approved guidance.

3.d. Latent Debris

The objective of the latent debris evaluation process is to provide a reasonable approximation of the amount and types of latent debris existing within the containment and its potential impact on sump-screen head loss.

1. *Provide the methodology used to estimate the quantity and composition of latent debris.*

   Response to 3.d.1:

   Walkdowns have been completed for DCPP Unit 1 specifically for the purpose of characterizing latent debris. These walkdowns utilized the guidance in NEI 02-01 and the NRC SE on NEI 04-07. Samples were collected from eight surface types including floors, the containment liner, ventilation ducts, cable trays, walls, equipment, piping, and grating.

   Samples were taken to determine the latent debris mass distribution per unit area, referred to as latent debris density (e.g. g/1,000 ft^2) of representative surfaces throughout containment including vertical surfaces such as the liner and walls. These debris densities were then applied to all of the representative surface areas inside containment to calculate the total amount of latent debris inside containment. The total latent debris was calculated using the sum of the latent debris for each surface type. A total of twenty-nine samples were taken for Unit 1.

   The estimated latent debris inside the Unit 1 containment building is 59.2 lbm. This value was assumed to be applicable to Unit 2 (see the Response to 3.d.2). To provide operating margin, this total was increased to 100 lbm in each containment building.

   Per the SE on NEI 04-07 (Reference 13 p. 50), latent debris was treated as 15% latent fiber and 85% latent particulate by mass.

2. *Provide the basis for assumptions used in the evaluation.*

   Response to 3.d.2:

   A latent debris survey was performed for DCPP Unit 1 during refueling outage 1R13 in 2005 and for DCPP Unit 2 during 2R14 in 2008. The results of the Unit 1 1R13 latent debris survey bounded the Unit 2 2R14 survey results. The results of the Unit 1 1R13 latent debris survey were considered applicable to Unit 2 due to similar configurations and similar cleaning methods and acceptance criteria. The estimated latent debris inside the Unit 1 containment building is 59.2 lbm, and was assumed to be applicable to Unit 2. To provide operating margin, this total was increased to 100 lbm.

3. *Provide results of the latent debris evaluation, including amount of latent debris types and physical data for latent debris as requested for other debris under c. above.*

Response to 3.d.3:

The results of the latent debris calculation conservatively determined the debris loading to be 59.2 lbm in each containment building. DCPP elected to use a conservative bounding value of 100 lbm for the latent debris source term in containment building. This assumed value has proven to be appropriately conservative with regards to any latent debris surveys subsequently performed after the 1R13/2R14 surveys.

The properties and generated quantities of latent fiber and particulate debris are summarized in Table 3.d.3-1. The characteristic size and density of latent particulate debris were from the SE on NEI 04-07 (Reference 13 pp. 50-52 and VII-4). The bulk density, microscopic density and characteristic size of latent fiber were set to be the same as fiberglass insulation, in accordance with the SE on NEI 04-07, which recommends that fiberglass insulation properties can be utilized for latent fiber (Reference 13 pp. VII-3).

Table 3.d.3-1: Properties and Generated Quantities of Latent Debris

	Latent Debris (lbm)	Bulk Density (lbm/ft^3)	Microscopic Density (lbm/ft^3)	Characteristic Size (μm)
Particulate (85%)	85	-	169	17.3
Fiber (15%)	15	2.4	94	7
Total	100	-		

4. *Provide amount of sacrificial strainer surface area allotted to miscellaneous latent debris.*

Response to 3.d.4:

In the Response to 3.b.5, a sacrificial strainer area is specified to account for blockage of strainer surfaces by miscellaneous debris (e.g., tape, tags and labels). No additional sacrificial strainer area was allotted for latent fiber or latent particulate debris.

3.e. Debris Transport

The objective of the debris transport evaluation process is to estimate the fraction of debris that would be transported from debris sources within containment to the sump suction strainers.

1. *Describe the methodology used to analyze debris transport during the blowdown, washdown, pool-fill-up, and recirculation phases of an accident.*

   Response to 3.e.1:

   The methodology used in the transport analysis is based on the NEI 04-07 guidance and the associated NRC SE (Reference 13) for refined analyses, as well as the refined methodologies suggested by the SE in Appendices III, IV, and VI (Reference 13). The overall transport process was divided into four "phases" which were analyzed individually first in the debris transport calculation. These phases of transport are:

   - Blowdown Transport – the vertical and horizontal transport of debris to all areas of containment by the break jet
   - Washdown Transport – the vertical (downward) transport of debris by the CS and break flow, and condensation
   - Pool Fill-Up Transport – the transport of debris by break and CS flows from the RWST to regions that may be active or inactive during recirculation
   - Recirculation Transport – the transport of debris from the active portions of the recirculation pool to the sump strainer by the flow through the pool

   The transport fractions of individual transport phases were then fed into logic trees to evaluate the overall transport fraction of each type of debris determined from the debris generation calculation. Figure 3.e.1-1 shows an example logic tree for the insulation fiber debris. Note that the logic tree shown in the figure is slightly different from the baseline guidance from NEI 04-07. This departure was made to account for certain non-conservative assumptions identified by the NRC SE (Reference 13) including the transport of large pieces of insulation fiber debris, erosion of small and large pieces of insulation fiber debris, the potential for washdown debris to enter the pool after inactive areas have been filled, and the direct transport of debris to the sump strainer during pool fill-up.

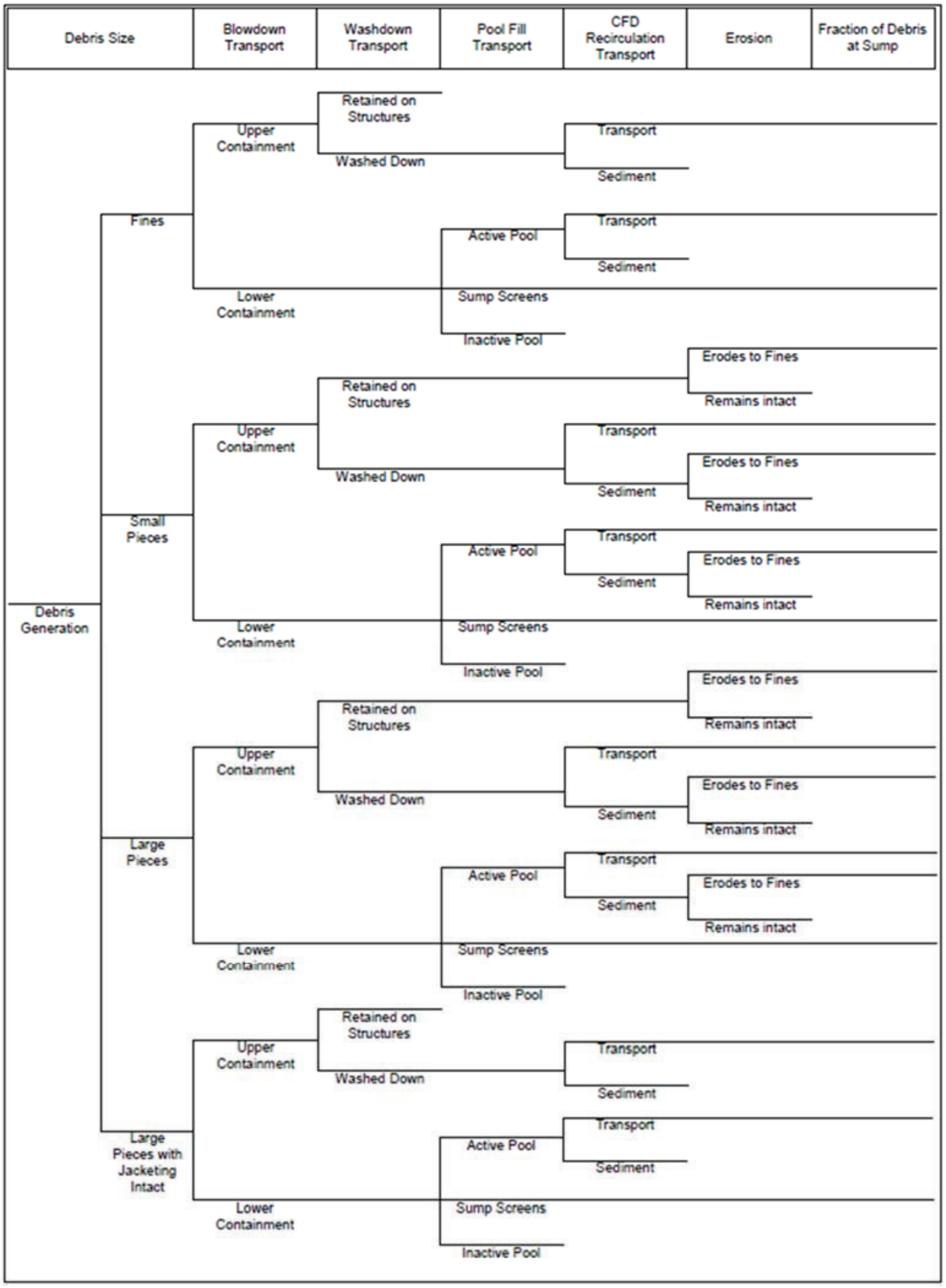

Figure 3.e.1-1: Generic Debris Transport Logic Tree

The basic methodology for the DCPP transport analysis is summarized as follows. Note that the DCPP containment buildings are mirror images of one another, and thus a single transport evaluation was performed.

1. The CAD model was provided as input to determine break locations and sizes.
2. The debris generation calculation was provided as input into the calculation for debris types and sizes.
3. Potential upstream blockage points were addressed.
4. The fraction of debris blown into upper containment and lower containment for breaks in each compartment was determined based on the volumes of upper and lower containment and sizes of the debris. The potential for debris to be trapped by structures and gratings was considered.
5. The fraction of debris washed down by CS flow from the upper containment was determined, along with the locations where the debris would be washed to. It was conservatively assumed that all of the debris blown to the upper containment was washed back to lower containment with the exception of the small pieces of debris that is trapped by the gratings at higher elevations.
6. The quantity of debris transported to inactive areas or directly to the sump strainers was calculated based on the volume of the inactive and sump cavities proportional to the water volume at the time these cavities are filled.
7. The location of each type/size of debris at the beginning of recirculation was determined/assumed based on the break location.
8. A computational fluid dynamics (CFD) model was developed to simulate the flow patterns inside the recirculation pool during the recirculation phase.
9. A graphical determination of the transport fraction of each type of debris was made using the velocity and turbulent kinetic energy (TKE) profiles from the CFD model output, along with the initial distribution of debris.
10. The overall transport fraction for each type/size of debris was determined by combining each of the previous steps into logic trees.
11. The quantity of debris that could experience erosion due to the break flow or spray flow was determined.

Potential upstream blockage points were addressed in the debris transport calculation. It was determined that there are not any upstream blockage points in the DCPP containment building. Upstream effects are discussed in the Response to 3.l.

<u>CFD Model of Containment Recirculation Pool</u>

The CFD model of the recirculation pool was developed using the software package of Flow-3D. A diagram showing the significant parts of the CFD model is shown in Figure 3.e.1-2. The sump mass sink, which was used to model the recirculation sumps, and the various direct and runoff spray regions are highlighted in the figure.

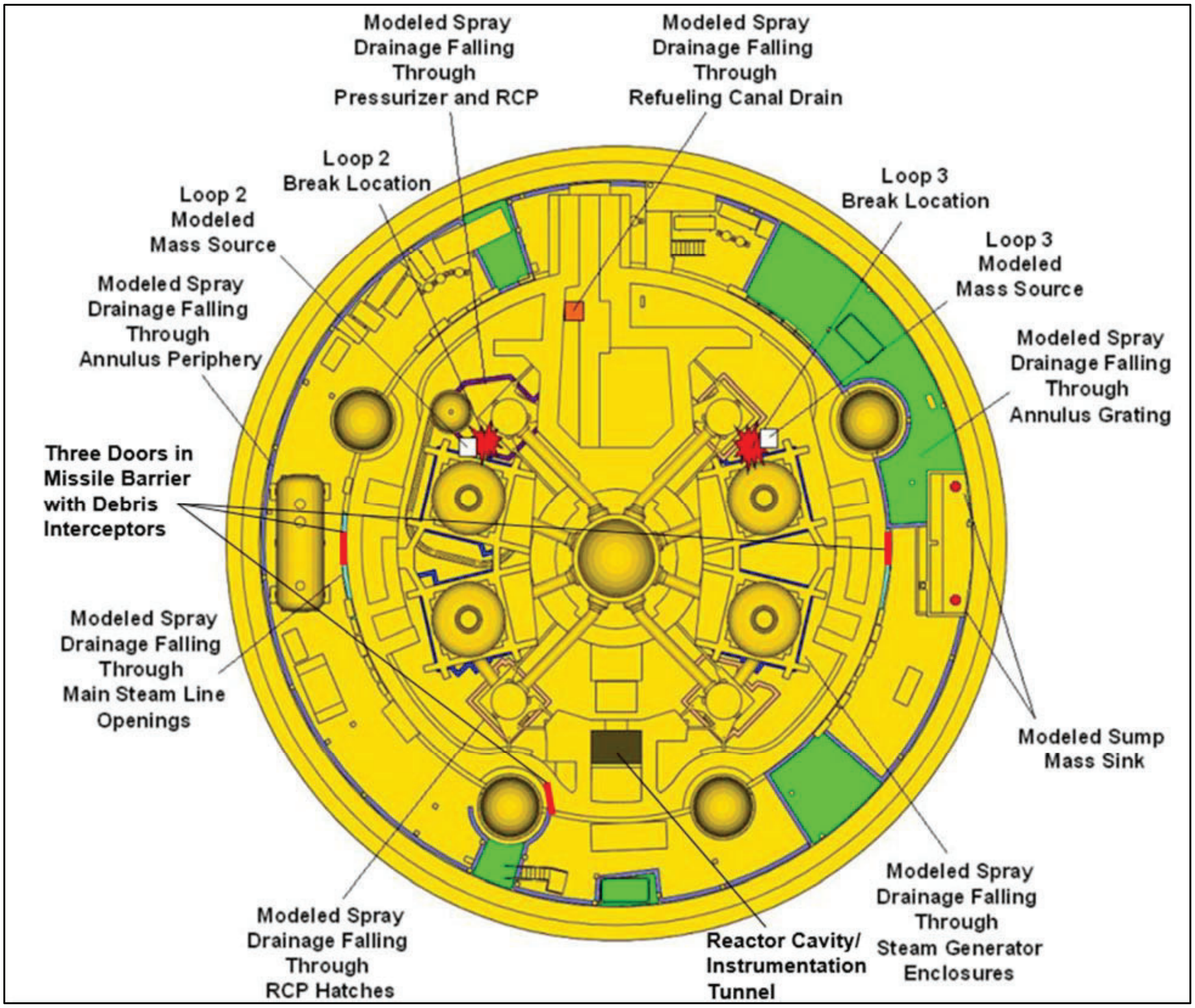

Figure 3.e.1-2: Significant Features in CFD Model

The key CFD modeling attributes/considerations included the following:

Computational Mesh

A rectangular mesh was defined in the CFD model that was fine enough to resolve important features, but not so fine that the simulation would take excessively long to run. A 6-inch cell length was chosen as the largest cell size that could reasonably resolve the concrete structures that compose the containment floor. For the cells right above the containment floor, the mesh was set to 3 inches tall in order to closely resolve the vicinity (area right above the floor where tumbling velocities are analyzed) of settled debris. To further define specific objects, node planes were placed at the edges of key structures including the top of the sump curb, and the edges of the break and spray mass source obstacles. The total cell count in the model was 720,000.

Modeling of CS Flows

Various plan and section drawings, as well as the containment building CAD model, were considered when determining the spray flow path to the pool. Spray water would drain to the pool through many pathways. Some of these pathways include the SG compartments through the open area above the SGs, the SG compartments through the grating above the reactor coolant pumps and the pressurizer, the 8-inch drain line from the refueling canal, the annulus through various open sections of grating, and the annulus through the periphery. Assuming that spray flow is uniform across containment, the fraction of spray landing on any given area can be calculated using the ratio of that area to the overall area. Also, for sprays landing on a solid surface, such as the operating deck, the runoff flow split to different regions, such as the annulus, can be reasonably approximated using the ratios of open perimeters where water could drain off. The regions, where CS was determined to reach the recirculation pool, were populated with discreet mass source particles, which introduced fluid at assigned flow rates for different regions.

Modeling of Break Flow

When modeling flow inside the recirculation pool during the recirculation phase, the water falling from the postulated break would introduce momentum into the containment pool that influences the flow dynamics. This break stream momentum was accounted for by introducing the break flow to the pool at the velocity a freefalling object would have if it fell the vertical distance from the location of the break to the surface of the pool.

Modeling of Recirculation Sump

The containment recirculation sump at DCPP includes front and rear strainers and is located in the containment annulus. The strainer assembly consists of vertically oriented perforated plates, water collection plenums, and a vortex suppressor. A trash rack with an integral debris curb is positioned in front of the strainers. The sump has two suction pipes, which feed the two RHR trains. The mass sink used to pull flow from the CFD model was defined above the two pipes. A negative flow rate was set for the sump mass sink, which tells the CFD model to draw the specified amount of water from the pool over the entire exposed surface area of the mass sink obstacle.

Turbulence Modeling

Flow-3D provides several different turbulence-modeling options, as listed below (ranging from least to most sophisticated).

- Prandtl mixing length
- Turbulent energy model
- Two-equation k-ε model
- Renormalized group theory (RNG) model
- Large eddy simulation model

The RNG turbulence model was determined to be the most appropriate for this CFD analysis. The RNG model has a large spectrum of length scales that would likely exist in the turbulent flow of the pool during recirculation. The RNG approach applies statistical methods in a derivation of the averaged equations for turbulence quantities (such as TKE and its dissipation rate). RNG-based turbulence schemes rely less on empirical constants while setting a framework for the derivation of a range of models at different scales.

Steady-State Metrics

The CFD model was started from a stagnant state at a defined pool depth (minimum pool depth at the start of recirculation) and run long enough for steady-state conditions to develop. A plot of mean kinetic energy was used to determine when steady-state conditions were reached. Checks were also made of the velocity and turbulent energy patterns in the pool to verify that steady-state conditions were reached.

Debris Transport Metrics

The metrics for predicting debris transport during recirculation were the TKE necessary to keep debris suspended, and the flow velocity necessary to tumble sunken debris along the floor or lift it over a curb. Debris transport metrics have been derived or adopted from data. The metrics utilized in the DCPP transport analysis originated from the sources below.

- NUREG/CR-6772 Tables 3.4 and 3.5 (Reference 19 pp. 21, 22)
- NUREG/CR-6808 Figure 5-2 (Reference 20 p. 5-14)
- NUREG/CR-6916 Tables 3-2 and 4-3 (Reference 21 pp. 18, 22)
- DCPP Specific Transport Testing

DCPP Specific Transport Testing

DCPP performed plant specific transport testing to determine the settling and tumbling velocities for various types of miscellaneous debris (Aluminum Tape, silicone rubber, light bulbs, various types of tape, stickers/labels, and tags) and unqualified coatings paint chips. Plant specific testing was also performed to determine the capture efficiency of the debris interceptors for unqualified paint chip debris.

For the tumbling velocity tests, the debris was evenly distributed on the floor of the test section with plenty of space between each particle. Testing began with the water flow at a standstill and then slowly and incrementally increased until a specific particle motion (incipient or bulk motion) was observed. For the settling velocity tests, individual particles were allowed to fall through a column of still (non-moving), room-temperature water. The time required for the particles to descend were recorded. Results were averaged for each debris type over the tests. Note that performing settling test at room temperature is slightly conservative because the particles settle more slowly in cooler water and stay in suspension for a longer period of time.

The debris interceptor testing is discussed in the Response to 3.e.4.

Graphical Determination of Debris Transport Fractions for Recirculation

The following steps were taken to determine the recirculation transport fraction for a particular type of debris. An example implementation of these steps is presented later in this section.

1. Colored contour velocity and TKE maps were generated from the Flow-3D results in the form of bitmap files indicating regions of the pool that have sufficiently high TKE to suspend the debris and/or sufficiently high velocity just above the floor to tumble the sunken debris.
2. The bitmap images from the previous step were overlaid on the initial debris distribution plots and imported into AutoCAD with the appropriate scaling factor to convert the length scale of the color maps to feet.
3. Closed polylines were drawn over transportable zones for the given debris type/size. A detailed discussion on how the transportable zones are identified can be found later in this section.
4. The areas within the closed polylines were determined using an AutoCAD querying feature.
5. The ratio between the combined area within the polylines and the initial debris distribution area is taken to be its transport fraction.

As discussed above, the initial debris distribution at the start of recirculation is needed in order to determine its recirculation transport fraction, as summarized below.

1. All of the latent debris in containment was conservatively assumed to be uniformly distributed on the floor at the beginning of recirculation.
2. The unqualified coatings and miscellaneous debris in upper containment were assumed to be distributed in the washdown locations at the start of recirculation. The unqualified coatings and miscellaneous debris in lower containment were assumed to be uniformly distributed either inside or outside the crane wall based on the locations where they fail.
3. The fine debris in lower containment was assumed to be uniformly distributed in the pool at the beginning of recirculation. The fine debris washed down from upper containment was assumed to be distributed in the vicinity of the location where it is washed down.
4. Small and large pieces of insulation debris in lower containment were conservatively assumed to be distributed uniformly inside the crane wall. The small piece debris blown to upper containment was assumed to wash down in the same locations as the fine debris.

The following figures and discussion are presented as an example of how the transport analysis was performed for small pieces of debris blown into the lower containment by a Loop 2 break. Note that some of the small pieces are blown into upper containment by the break before being washed down into the lower containment. Such debris may have a different distribution in the lower containment at the start of recirculation, compared with that shown in Figure 3.e.1-3. However, its recirculation transport was analyzed using the same approach as outlined in the example. This approach was also applied to various other debris types analyzed at DCPP.

As shown in Figure 3.e.1-3, the small debris blown into the lower containment by the break (depicted by green shading) was assumed to be uniformly distributed inside the missile barrier at the start of recirculation. The debris interceptors installed in the three crane wall doors were assumed to stop all sunken debris (small or large pieces) inside the crane wall from entering the annulus. Thus, the only way that small or large debris could get past an interceptor is if the TKE is high enough to suspend it at the interceptor location. Paint chips were evaluated separately from other types of debris at the debris interceptors. Paint chips have a specific interceptor bypass fraction which is discussed in the Response to 3.e.4.

Figure 3.e.1-3: Distribution of Small Debris Blown into Lower Containment at Start of Recirculation

Figure 3.e.1-4 shows the TKE and velocity magnitude in the pool, generated from the CFD modeling. The yellow areas in the figure represent regions where TKE is sufficiently high to keep the small debris in suspension. Note that the yellow areas represent three-dimensional zones that have sufficiently high TKE. Therefore, any debris inside the yellow areas is in suspension, regardless of its elevation. The red areas in Figure 3.e.1-4 represent regions where the velocity just above the floor (1.5 inches) is sufficiently high to tumble the sunken small debris along the floor. Unit flow vectors are shown in the plots to indicate flow directions.

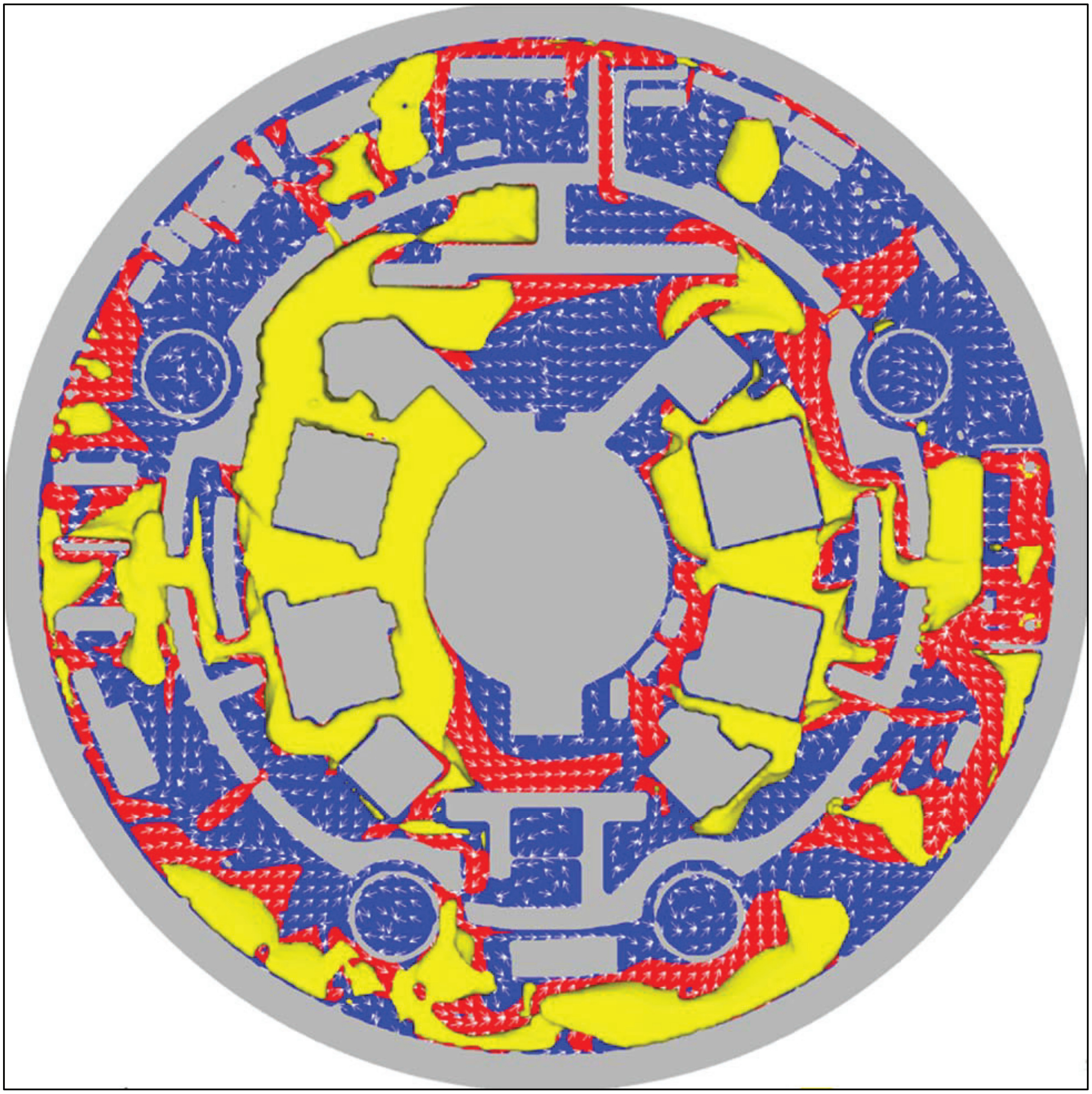

Figure 3.e.1-4: TKE and Velocity in the Recirculation Pool with Limits Set at Suspension/ Tumbling of Small Debris

Figure 3.e.1-4 is overlaid on the initial distribution of small debris (as shown in Figure 3.e.1-3) to determine small debris in which areas of the pool can be transported to the sump strainer. The transportable zones are represented by the hatched areas in Figure 3.e.1-5. Debris in a yellow area would be transportable if the area overlaps with the initial debris distribution and has a continuous flow path to the strainer. Similarly, debris in a red area would be transportable if the area overlaps with the initial debris distribution and the flow travels towards the strainer. The total area of the transportable zones (hatched areas) is then determined and is divided by the

total initial distribution area of the debris (Figure 3.e.1-3), resulting in the recirculation transport fraction of the small debris.

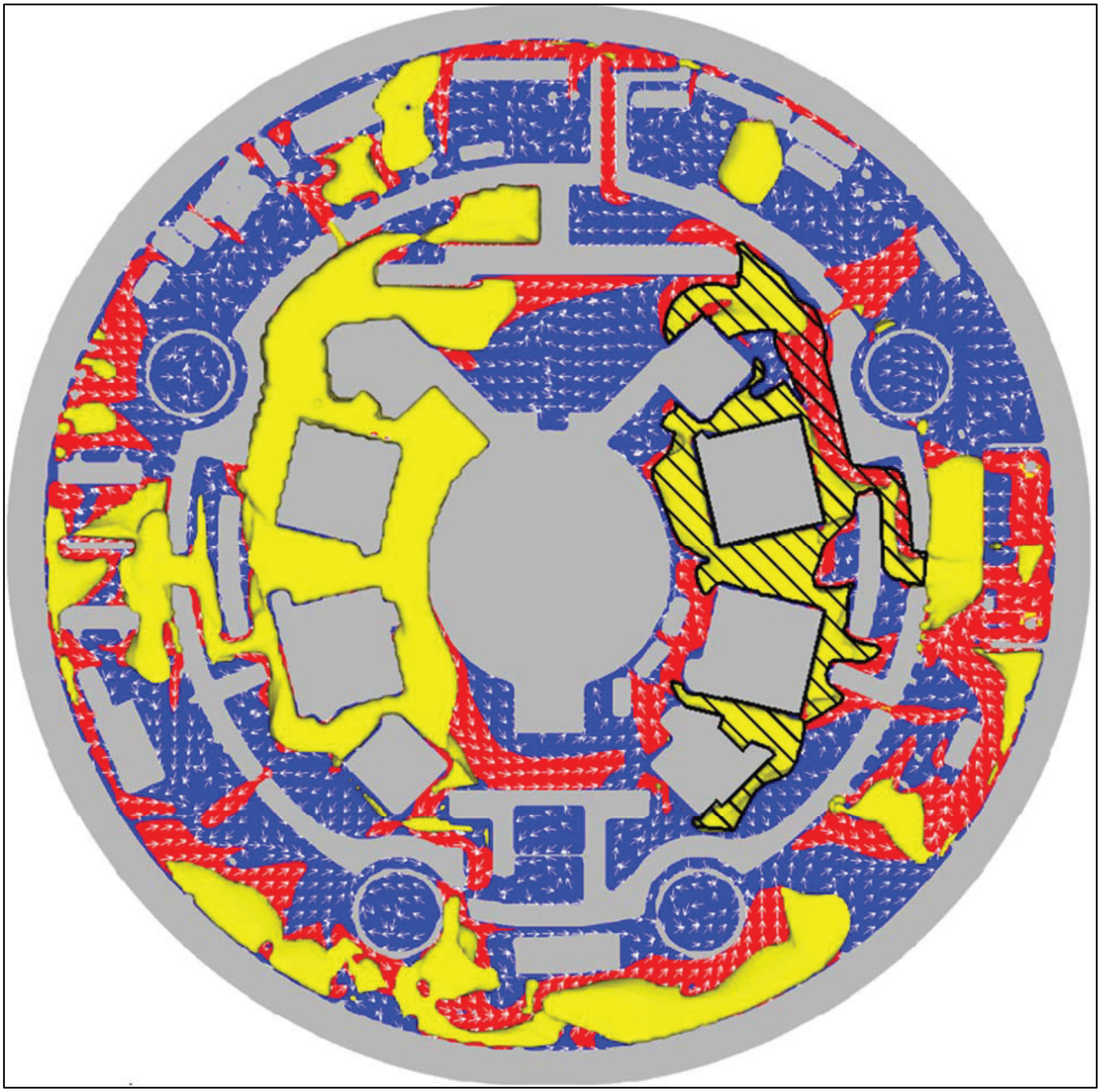

Figure 3.e.1-5: Floor Area where Small Debris Would Transport to the Sump Strainers (hatched area) during Recirculation

This same analysis was applied for each type of debris and break location. Recirculation pool transport fractions were identified for each debris type associated with its initial location. This includes a recirculation transport fraction for debris blown to lower containment, debris washed down inside the missile barrier, and debris washed down into the annulus.

Erosion Discussion

Due to the turbulence in the recirculation pool and the force of break and spray flow, Temp-Mat debris may erode into smaller pieces, making transport of this debris to the strainer more likely. An erosion fraction of 10% is used for the small and large pieces of Temp-Mat in the pool based on 30-day erosion testing. This fraction was applied to both transportable debris and sediment debris present in the pool to maximize the amount of erosion. For pieces of Temp-Mat debris held up on grating above the pool, an erosion fraction of 1% was used for small and large pieces of Temp-Mat, consistent with the NRC's SE on NEI 04-07 (Reference 13 pp. VI-30).

2. *Provide the technical basis for assumptions and methods used in the analysis that deviate from the approved guidance.*

Response to 3.e.2:

The assumptions and methodology used in the DCPP transport analysis are based on and do not deviate from the NEI 04-07 guidance and the associated NRC SE, as well as the refined methodologies suggested by the SE in Appendices III, IV, and VI (Reference 13).

3. *Identify any computational fluid dynamics codes used to compute debris transport fractions during recirculation and summarize the methodology, modeling assumptions, and results.*

Response to 3.e.3:

As discussed above, to determine recirculation transport fractions, CFD simulations were performed using Flow-3D. Two breaks were analyzed in the transport calculation to determine the recirculation transport fractions – one break close to the sump (near break), and one break far from the sump (far break). All cases were run with maximum ECCS flow rates (total 2 train RHR and CS flow rate of 7,769 gpm) and with the minimum water level right above the strainer (2.9 ft). Using the maximum flow rates and minimum water level maximize the turbulence and velocity in the pool.

In general, a break close to the sump tends to transport a larger fraction of small and large debris than a break farther from the sump. The simulation results include a series of contour plots of velocity and TKE. These results have been combined with settling and tumbling velocities from the GSI-191 literature and test results to determine the recirculation transport fractions for all debris types present in the DCPP containment building. See the Response to 3.e.1 for additional discussion of the CFD modeling. The resulting recirculation transport fractions are shown in the Response to 3.e.6.

4. *Provide a summary of, and supporting basis for, any credit taken for debris interceptors.*

   Response to 3.e.4:

   As part of DCPP's debris reduction modifications, debris interceptors were installed in all three crane wall doors. These debris interceptors are vertically mounted perforated stainless-steel plates (18-inches tall, 11 gauge, with 1/8-inch diameter holes) with a horizontal lip (10 inches, also stainless-steel plate) that projects into the flow.

   DCPP performed testing to demonstrate the performance of the debris interceptors at the PG&E Applied Technology Services (ATS) testing facilities in San Ramon, California. This testing was performed under the ATS quality program. As was shown in testing, debris which transports to the debris interceptor by tumbling along the floor will be stopped by the interceptor. Debris which is suspended near the debris interceptor is assumed to transport over the interceptor, with the exception of paint chips.

   DCPP performed specific debris interceptor testing to quantify the capture of suspended paint chips. The flume velocity of the tests performed ranged between 0.630 and 0.647 ft/s, and the water level ranged between 33.13 and 42 inches, which is within the bounds of the expected velocity and water level through each debris interceptor (maximum flow rate and minimum water level at the beginning of recirculation). Paint chips were measured upstream and downstream of the interceptor to determine the bypass fraction of this debris. This testing replicated an RMI debris bed with a thickness of 5 inches in front of the interceptor, and suspended 9-mil unqualified coatings chips and 2-mil high heat aluminum chips (in separate tests) uniformly throughout the flow stream. The test showed that the debris interceptor is effective in capturing 65% of 9-mil coatings chips and 23% of 2-mil coatings chips, even with sufficient TKE to suspend them at the interceptor.

   In the debris transport analysis, it was assumed that the interceptors stop all sunken debris (small or large pieces). With this assumption, the only way that small or large debris can get past an interceptor is if the TKE is high enough to suspend it at the interceptor location. As discussed above, a portion of the coatings chips debris was assumed to be captured by the interceptors.

5. *State whether fine debris was assumed to settle and provide basis for any settling credited.*

   Response to 3.e.5:

   No credit was taken for settling of fine debris.

6. *Provide the calculated debris transport fractions and the total quantities of each type of debris transported to the strainers.*

Response to 3.e.6:

As discussed in the Response to 3.e.1, the overall debris transport process was evaluated in four separate phases: blowdown, washdown, pool fill-up and recirculation. The debris transport fractions for each of these phases are shown in Table 3.e.6-1 through Table 3.e.6-8. The transport fractions of the four phases were used as inputs to build logic trees and to determine the overall transport fractions for different debris types and sizes. The resulting overall transport fractions are summarized in Table 3.e.6-9 for different debris types. Finally, the overall transport fractions were multiplied by the generated debris quantities to determine the transport debris quantities for each break. The transport debris loads for the worst fiber, Cal-Sil and particulate debris breaks (as identified in the Response to 3.a.3) are summarized in Table 3.e.6-10 and Table 3.e.6-11 for Units 1 and 2, respectively.

Note that these fractions shown in this section result in the bounding quantity of debris transported to the strainer. Cells with a "-" in the tables of this section represent values that are not applicable (i.e., debris type not generated for a specific location, debris type not available for washdown/pool fill-up, etc.).

<u>*Blowdown Transport*</u>

Table 3.e.6-1 shows the blowdown transport fractions for each type/size of debris to upper containment due to the blowdown forces for breaks inside the missile barrier. All debris not blown to upper containment was assumed to be blown to the recirculation pool.

Since the blowdown would relieve to all areas in the containment building, the blowdown flow to various regions of the containment was estimated based on their relative volumes. Fine debris within the break ZOI (including fiber fines and particulate) can be easily suspended and carried by the blowdown flow. Therefore, the fraction of fine debris inside the break ZOI that is blown into the upper containment was determined to be 80%, which is equal to the fraction of the upper containment volume with respect to the overall containment volume.

The approach discussed above was also used to evaluate blowdown of small pieces of debris (including RMI and various types of miscellaneous debris inside the missile barrier). Different from the fine debris, a fraction of the small pieces will be trapped by gratings as they are blown into upper containment. Such impact was accounted for in the analysis which resulted in a blowdown fraction of 28% to the upper containment for the small pieces of debris, as shown in Table 3.e.6-1.

Note that debris outside the ZOI (including latent particulate and fiber debris) is not affected by the break jet. Therefore, the transport fraction to upper containment due to blowdown for this debris would be 0%.

For breaks in the reactor cavity, the intact pieces of Temp-Mat that are in the primary shield penetrations would be blown out of the penetrations to lower containment. Therefore, 100% of the intact pieces of Temp-Mat that are in the primary shield penetrations would be blown to lower containment.

Table 3.e.6-1: Blowdown Transport Fractions of Debris to Upper Containment

Debris Type	Fines	Small Pieces	Unjacketed Large Pieces (Large Pieces)	Jacketed Large Pieces (Intact Pieces)
Stainless-Steel RMI, Aluminum Tape	-	28%	0%	-
Temp-Mat	80%	-	-	-
Temp-Mat (Intact from primary shield penetrations)[2]	-	-	-	0%
Vapor Barrier Material	-	28%	-	-
Silicone Rubber (Flexicone Sleeving)	-	28%	-	-
Fiberglass Braid (Flexicone Sleeving)	80%	-	-	-
Conduit Sheathing	-	28%	-	-
Light Bulbs	-	28%	-	-
Fiberglass Inside ZOI[3]	80%	-	-	-
Fiberglass Outside ZOI[3]	0%	-	-	-
Cal-Sil, Min-K, Foamglas, Mica Tape	80%	-	-	-
Coatings Inside ZOI[4]	80%	-	-	-
Coatings Outside ZOI[5]	0%	0%	-	-
Latent Particulate	0%	-	-	-
Latent Fiber	0%	-	-	-
Miscellaneous Debris IMB[6]	-	28%	-	-
Miscellaneous Debris OMB[7]	-	0%	-	-

[2] Intact Temp-Mat from the primary shield penetrations are only generated by reactor cavity breaks.
[3] Includes TIW fiberglass, Kaowool, and fiberglass overbraid (Pressurizer heater cables)
[4] Includes qualified inorganic zinc (IOZ) and epoxy coatings
[5] Includes unqualified T-50 Coatings Systems, OEM coatings, miscellaneous modifications and defective coatings, and IOZ primer only coatings
[6] Includes miscellaneous debris inside missile barrier (IMB): reflective tape, valve ID tags, conduit tape, lamacoids, black electrical tape, tie-wraps, paper RP survey tags, and stickers/labels
[7] Includes miscellaneous debris outside missile barrier (OMB): stickers/labels and masking tapes

Washdown Transport

Debris blown into upper containment can be washed down by containment sprays. Three washdown flow paths were considered in the analysis: into the annulus, inside missile barrier and through the refueling canal drain. Since the debris blown to upper containment was fines and small pieces, it was conservatively assumed that all debris in upper containment is washed back down to lower containment except for the small pieces of RMI held up by the gratings in the annulus and inside the missile barrier during washdown.

The majority of debris blown to upper containment lands on the operating deck or in the refueling canal. Therefore, the fractions of fine and small pieces of debris (except for RMI) washed to specific locations (inside annulus, inside missile barrier and through the refueling canal drain) were determined based on the spray flow split to these areas. The analysis resulted in 66% of debris washed into the annulus, 23% inside the missile barrier, and 11% through the refueling canal drains. For small pieces of RMI, its washdown fractions inside the annulus and missile barrier were reduced due to holdup by the gratings. The washdown fractions are summarized in Table 3.e.6-2, Table 3.e.6-3, and Table 3.e.6-4.

Table 3.e.6-2: Washdown Transport Fractions of Debris from Upper Containment to Annulus

Debris Type	Fines	Small Pieces	Unjacketed Large Pieces (Large Pieces)	Jacketed Large Pieces (Intact Pieces)
Stainless-Steel RMI, Aluminum Tape	-	60%	-	-
Temp-Mat	66%	-	-	-
Temp-Mat (Intact from primary shield penetrations)	-	-	-	0%
Vapor Barrier Material	-	66%	-	-
Silicone Rubber (Flexicone Sleeving)	-	66%	-	-
Fiberglass Braid (Flexicone Sleeving)	66%	-	-	-
Conduit Sheathing	-	66%	-	-
Light Bulbs	-	66%	-	-
Fiberglass Inside ZOI	66%	-	-	-
Fiberglass Outside ZOI	-	-	-	-
Cal-Sil, Min-K, Foamglas, Mica Tape	66%	-	-	-
Coatings Inside ZOI	66%	-	-	-
Coatings Outside ZOI	-	66%	-	-
Latent Particulate	-	-	-	-
Latent Fiber	-	-	-	-
Miscellaneous Debris IMB	-	66%	-	-
Miscellaneous Debris OMB	-	-	-	-

Table 3.e.6-3: Washdown Transport Fractions of Debris from Upper Containment to Inside Missile Barrier

Debris Type	Fines	Small Pieces	Unjacketed Large Pieces (Large Pieces)	Jacketed Large Pieces (Intact Pieces)
Stainless-Steel RMI, Aluminum Tape	-	20%	-	-
Temp-Mat	23%	-	-	-
Temp-Mat (Intact from primary shield penetrations)	-	-	-	0%
Vapor Barrier Material	-	23%	-	-
Silicone Rubber (Flexicone Sleeving)	-	23%	-	-
Fiberglass Braid (Flexicone Sleeving)	23%	-	-	-
Conduit Sheathing	-	23%	-	-
Light Bulbs	-	23%	-	-
Fiberglass Inside ZOI	23%	-	-	-
Fiberglass Outside ZOI	-	-	-	-
Cal-Sil, Min-K, Foamglas, Mica Tape	23%	-	-	-
Coatings Inside ZOI	23%	-	-	-
Coatings Outside ZOI	-	23%	-	-
Latent Particulate	-	-	-	-
Latent Fiber	-	-	-	-
Miscellaneous Debris IMB	-	23%	-	-
Miscellaneous Debris OMB	-	-	-	-

Table 3.e.6-4: Washdown Transport Fractions of Debris from Upper Containment to Refueling Canal Drain Discharge

Debris Type	Fines	Small Pieces	Unjacketed Large Pieces (Large Pieces)	Jacketed Large Pieces (Intact Pieces)
Stainless-Steel RMI, Aluminum Tape	-	11%	-	-
Temp-Mat	11%	-	-	-
Temp-Mat (Intact from primary shield penetrations)	-	-	-	0%
Vapor Barrier Material	-	11%	-	-
Silicone Rubber (Flexicone Sleeving)	-	11%	-	-
Fiberglass Braid (Flexicone Sleeving)	11%	-	-	-
Conduit Sheathing	-	11%	-	-
Light Bulbs	-	11%	-	-
Fiberglass Inside ZOI	11%	-	-	-
Fiberglass Outside ZOI	-	-	-	-
Cal-Sil, Min-K, Foamglas, Mica Tape	11%	-	-	-
Coatings Inside ZOI	11%	-	-	-
Coatings Outside ZOI	-	11%	-	-
Latent Particulate	-	-	-	-
Latent Fiber	-	-	-	-
Miscellaneous Debris IMB	-	11%	-	-
Miscellaneous Debris OMB	-	-	-	-

Pool-Fill Transport

A portion of debris could be washed into inactive cavities in the lower containment during sump pool fill-up. The fraction of debris washed to inactive cavities during pool fill-up was determined using the following equation.

$$F_{fill-up} = 1 - e^{-\left(\frac{V_{cavity}}{V_{pool}}\right)}$$

Where:

$F_{fill\text{-}up}$ = Amount of debris transported to cavity during pool fill-up
V_{cavity} = Cavity volume
V_{pool} = Pool volume

The primary cavities below the floor elevation at DCPP are the sump cavity, the incore instrumentation tunnel, and reactor cavity, which have a 6-inch curb around them. The volume of the sump cavity up to the top of the 6-inch sump curb is 662 ft^3, and the free volume of the incore instrumentation tunnel and reactor cavity up to the 6-inch curb was calculated to be 10,493 ft^3. The pool volume at a 6-inch depth not including the cavities was calculated to be 5,129 ft^3. Since the sump and the reactor cavities are not in close proximity to each other, and flow into one cavity will not be significantly impacted by flow to the other, the sump cavity will fill first.

Inserting these values into the equation above yields a pool fill-up transport of 12% to the sump cavity. The remaining debris is available for transport to the reactor cavity during pool-fill. Using the volumes and equation shown above, the calculated pool-fill fraction for the reactor cavity was higher than 15%. In accordance to Section 3.6.3 of the NRC SE on NEI 04-07 (Reference 13 pp. 79-80), the pool-fill transport fraction to the reactor cavity was set to 15%. Table 3.e.6-5 shows the fraction of debris that would transport to inactive areas, and Table 3.e.6-6 shows the fraction of debris that would transport directly to the sump during pool fill-up.

Note that the pool-fill transport fractions described above depend primarily on the volumes of cavities and are applicable for all debris types except for unqualified coatings and miscellaneous debris outside of the ZOI. This was done because unqualified coatings and the miscellaneous debris outside of the ZOI were assumed to fail after pool fill-up has occurred, resulting in a 0% pool-fill transport fraction for these debris types. Since the intact pieces of Temp-Mat debris are assumed to float in the pool, this debris will not transport to the inactive cavity during pool fill.

Table 3.e.6-5: Pool fill Transport Fractions of Debris to Reactor Cavity

Debris Type	Fines	Small Pieces	Unjacketed Large Pieces (Large Pieces)	Jacketed Large Pieces (Intact Pieces)
Stainless-Steel RMI, Aluminum Tape	-	0%	0%	-
Temp-Mat	15%	-	-	-
Temp-Mat (Intact from primary shield penetrations)	-	-	-	0%
Vapor Barrier Material	-	15%	-	-
Silicone Rubber (Flexicone Sleeving)	-	0%	-	-
Fiberglass Braid (Flexicone Sleeving)	15%	-	-	-
Conduit Sheathing	-	0%	-	-
Light Bulbs	-	0%	-	-
Fiberglass Inside ZOI	15%	-	-	-
Fiberglass Outside ZOI	0%	-	-	-
Cal-Sil, Min-K, Foamglas, Mica Tape	15%	-	-	-
Coatings Inside ZOI	15%	-	-	-
Coatings Outside ZOI	0%	0%	-	-
Latent Particulate	15%	-	-	-
Latent Fiber	15%	-	-	-
Miscellaneous Debris IMB	-	0%	-	-
Miscellaneous Debris OMB	-	0%	-	-

Table 3.e.6-6: Pool fill Transport Fractions of Debris to Sump

Debris Type	Fines	Small Pieces	Unjacketed Large Pieces (Large Pieces)	Jacketed Large Pieces (Intact Pieces)
Stainless-Steel RMI, Aluminum Tape	-	0%	0%	-
Temp-Mat	12%	-	-	-
Temp-Mat (Intact from primary shield penetrations)	-	-	-	0%
Vapor Barrier Material	-	12%	-	-
Silicone Rubber (Flexicone Sleeving)	-	0%	-	-
Fiberglass Braid (Flexicone Sleeving)	12%	-	-	-
Conduit Sheathing	-	0%	-	-
Light Bulbs	-	0%	-	-
Fiberglass Inside ZOI	12%	-	-	-
Fiberglass Outside ZOI	0%	-	-	-
Cal-Sil, Min-K, Foamglas, Mica Tape	12%	-	-	-
Coatings Inside ZOI	12%	-	-	-
Coatings Outside ZOI	0%	0%	-	-
Latent Particulate	12%	-	-	-
Latent Fiber	12%	-	-	-
Miscellaneous Debris IMB	-	0%	-	-
Miscellaneous Debris OMB	-	0%	-	-

Recirculation Transport

For the recirculation transport fractions, two different cases form the basis for the transport analysis, and were evaluated in the debris transport calculation. These cases are listed below:

- Loop 2 Break: Large Break LOCA (LBLOCA) in Crossover Leg of Loop 2
- Loop 3 Break: LBLOCA in Crossover Leg of Loop 3

See the Response to 3.e.1 for the methodology used for recirculation transport.

Fine fiber debris (e.g., Temp-Mat, TIW, Kaowool, Fiberglass Overbraid, latent fiber) and particulate debris (e.g., Cal-Sil, Foamglas, Min-K, Qualified and Unqualified Coatings, Mica Tape and latent particulate) were assumed or shown not to settle in the recirculation pool. Therefore, the recirculation transport fraction for these debris types is 100% for all break locations analyzed. Note that Aluminum Coatings on the pressurizer would be subject to failure only for breaks that result in the removal of the RMI insulation which it lies under. Therefore, the Aluminum Coatings would only be exposed for Loop 1 and 2 breaks. It was conservatively assumed that Aluminum Coatings on the pressurizer would be generated for all Loop 1 and 2 breaks.

The intact pieces of Temp-Mat from the primary shield penetrations generated by the reactor cavity breaks were assumed not to transport to the sump during recirculation. This is reasonable because the intact pieces are likely to get caught on miscellaneous structures, equipment, or the trash racks, given the size of these pieces (vary in length from 10 inches to 65 inches, in width from 3 inches to 14.5 inches, and in thickness from 4 inches to 5 inches). Note that the trash rack comprises grids of 4-inch by 4-inch openings on the sides and 1-inch by 3.94-inch on the top. Therefore, the recirculation transport fraction for the intact pieces of Temp-Mat debris is 0%.

For both break locations analyzed, RMI small debris was shown not to transport during recirculation for debris initially distributed inside the missile barrier (IMB), washed down IMB, and washed down the refueling canal (RFC) drain. Small RMI debris was shown to have a recirculation transport fraction of 8% for debris washed down into the annulus.

For both break locations analyzed, RMI large debris was shown not to transport during recirculation for debris initially distributed IMB. Since no RMI large pieces are blown into the upper containment during blowdown, no large pieces of RMI are washed down into the annulus. This results in a 0% recirculation transport fraction for the RMI large pieces.

The Unqualified 9-mil Triangle T-50 Coating Systems Chips (T-50 Alkyd Primer and Phenoline 305F Epoxy) was shown to transport as shown in Table 3.e.6-7. See the Response to 3.h for additional information regarding the failure of Triangle T-50 Coatings Systems. Note that the recirculation transport fractions below represent the amount that bypassed the debris interceptors (see the Response to 3.e.4 for discussion of the debris interceptor testing).

Table 3.e.6-7: Recirculation Transport Fractions for Unqualified 9-mil Triangle T-50 Coating Systems Chips

Location	Debris IMB	Debris Washed IMB	Debris OMB	Debris Washed down RFC
Loop 2	0%	0%	5%	0%
Loop 3	8%	8%	5%	0%

The recirculation transport fraction of Vapor Barrier was assumed to be 100%. This is conservative because no credit was taken for retention of this debris in the pool. For all other miscellaneous debris types, their recirculation transport was analyzed using the CFD model results, similar to the example shown in the Response to 3.e.1. Table 3.e.6-8 summarizes the recirculation transport fractions for the miscellaneous debris.

Table 3.e.6-8: Recirculation Transport Fractions for Miscellaneous Debris

Debris Type	Break Location	Debris IMB	Debris Washed IMB	Debris OMB	Debris Washed OMB	Debris Washed RFC
Vapor Barrier	Loop 2	100%	100%	-	100%	100%
	Loop 3	100%	100%	-	100%	100%
Silicone Rubber/ Conduit Sheathing	Loop 2	0%	0%	-	3%	0%
	Loop 3	0%	0%	-	3%	0%
Survey Tags	Loop 2	0%	0%	-	8%	0%
	Loop 3	0%	0%	-	8%	0%
Stickers/ Labels	Loop 2	55%	21%	31%	31%	0%
	Loop 3	53%	32%	31%	31%	0%
Aluminum Tape	Loop 2	0%	0%	-	11%	0%
	Loop 3	0%	0%	-	11%	0%
Masking Tape	Loop 2	-	-	33%	-	-
	Loop 3	-	-	32%	-	-
Reflective Tape	Loop 2	0%	0%	-	10%	0%
	Loop 3	0%	0%	-	10%	0%
Conduit Tape	Loop 2	8%	8%	-	11%	0%
	Loop 3	25%	25%	-	12%	0%
Lamacoids	Loop 2	0%	0%	-	2%	0%
	Loop 3	2%	2%	-	2%	0%
Black Electrical Tape	Loop 2	21%	21%	-	33%	0%
	Loop 3	32%	32%	-	32%	0%
Tie-Wraps	Loop 2	0%	0%	-	5%	0%
	Loop 3	20%	20%	-	6%	0%
Light Bulbs	Loop 2	0%	0%	-	1%	0%
	Loop 3	0%	0%	-	1%	0%

<u>Overall Debris Transport Fractions</u>

The transport fractions of the four phases of debris transport (as shown in Table 3.e.6-1 through Table 3.e.6-8) were used as inputs to build logic trees and to determine the overall transport fractions for different debris types and sizes. The overall transport fractions are provided in Table 3.e.6-9.

Table 3.e.6-9: Overall Transport Fractions

Debris Type	Debris Size	Group A (Loops 1 & 2 Breaks)	Group B (Loops 3 & 4 Breaks)
Insulation Debris			
Temp-Mat	Fines	97%	97%
Temp-Mat (from primary shield penetrations)	Fines	97%	97%
	Intact Pieces	0%	0%
TIW Fiberglass	Fines	97%	97%
Fiberglass Overbraid (Heater Cables)	Fines	97%	97%
Fiberglass Braid (Flexicone Sleeving)	Fines	97%	97%
Kaowool (Cable Tray Fire Stops)	Fines	97%	97%
Stainless-Steel RMI	Small Fines	1%	1%
	Large Pieces	0%	0%
Cal-Sil	Particulate	97%	97%
Min-K	Particulate	97%	97%
Foamglas	Particulate	97%	97%
Mica Tape (Heater Cables)	Particulate	97%	97%
Coatings Debris			
Qualified Epoxy Coatings	Particulate	97%	97%
Qualified Inorganic Zinc (IOZ) Coatings	Particulate	97%	97%
Unqualified Coatings (e.g., T-50 system, Original Equipment Manufacturer (OEM), degraded and high heat aluminum coatings)	Particulate	100%	100%
Unqualified T-50 Systems Coatings	9 mil Chips	4%	5%
Latent Debris			
Latent Fiber	Fines	85%	85%
Latent Particulate	Particulate	85%	85%
Miscellaneous Debris			
Vapor Barrier Material	See the Response to 3.c.1	67%	67%
Silicone Rubber (Flexicone Sleeving)		0%	0%
Valve ID Tags inside Crane Wall		1%	1%
Stickers/Labels inside Crane Wall		35%	35%
Stickers/Labels outside Crane Wall		23%	23%
Aluminum Tape		2%	2%
Masking Tape outside Crane Wall		25%	24%
Reflective Tape inside Crane Wall		1%	1%
Conduit Tape inside Crane Wall		6%	16%
Lamacoids inside Crane Wall		0%	1%
Black Electrical Tape inside Crane Wall		17%	23%
Tie-wraps inside Crane Wall		1%	13%
Paper Radiation Survey Tags		1%	1%
Light Bulbs		0%	0%
Conduit Sheathing		0%	0%

Debris Transport Quantities

The overall transport fractions were multiplied by the generated debris quantities to determine the transport debris quantities for each break. The transported debris quantities for the most limiting break cases, as defined in the Response to 3.a.3 are presented in the following tables. The transported quantities for the miscellaneous debris are in the Response to 3.b.5.

Table 3.e.6-10: Limiting Transported Debris Quantities for Unit 1

Weld		**WIB-RC-2-1 (SE)**	**WIB-RC-2-10**	**WIB-RC-3-7**	**WIB-RC-1-12**
Location		Loop 2 HL @ RPV	Loop 2 X-Over	Loop 3 X-Over	Loop 1 X-Over
Limiting Debris		Transported Fiber		Transported Cal-Sil and Total Particulate	
Break Size (in)		Nozzle	31	31	31
Insulation Debris					
Temp-Mat (lbm)	Fines	87.77	1.33	1.25	0.00
	Intact	0.00	0.00	0.00	0.00
TIW (lbm)	Fines	0.00	1.60	2.10	1.11
Fiberglass Overbraid and Flexicone Sleeves (lbm)	Fines	0.00	70.89	0.00	0.00
Kaowool (lbm)	Fines	7.16	7.16	7.16	7.16
RMI (ft^2)	Small and Large	0.0	403.7	274.7	415.4
Cal-Sil (ft^3)	Particulate	0.00	3.88	22.27	11.34
Min-K (ft^3)	Particulate	0.00	0.00	0.00	0.00
Foamglas (ft^3)	Particulate	0.00	0.08	0.00	0.08
Mica Tape (ft^3)	Particulate	0.00	0.70	0.00	0.00
Coatings Debris					
Qualified Epoxy (ft^3)	Particulate	0.54	3.16	0.63	1.63
Qualified IOZ (ft^3)	Particulate	0.00	0.27	0.39	0.30
Unqualified Coatings (ft^3)	Particulate	13.6	13.2	13.2	13.2
	Chips	1.4	1.4	1.4	1.4
Latent Debris					
Latent Debris (lbm)	Fiber Fines	12.75	12.75	12.75	12.75
	Particulate	72.25	72.25	72.25	72.25

Table 3.e.6-11: Limiting Transported Debris Quantities for Unit 2

Weld		**WIB-RC-2-6SE**	**WIB-RC-2-16 (SE)**	**WIB-RC-4-7**	**WIB-RC-1-11**
Location		Loop 2 X-Over	Loop 2 CL @ RPV	Loop 4 X-Over	Loop 1 X-Over
Limiting Debris		Transported Fiber		Transported Cal-Sil and Total Particulate	
Break Size (in)		31	Nozzle	31	31
Insulation Debris					
Temp-Mat (lbm)	Fines	0.18	51.91	4.96	0.00
	Intact	0.00	0.00	0.00	0.00
TIW (lbm)	Fines	1.23	0.00	1.21	0.61
Fiberglass Overbraid and Flexicone Sleeves (lbm)	Fines	88.57	0.00	0.00	0.00
Kaowool (lbm)	Fines	7.16	7.16	7.16	7.16
RMI (ft^2)	Small and Large	397.3	0.0	268.3	398.7
Cal-Sil (ft^3)	Particulate	5.79	0.00	19.11	11.46
Min-K (ft^3)	Particulate	0.00	0.00	0.00	0.00
Foamglas (ft^3)	Particulate	0.09	0.00	0.00	0.09
Mica Tape (ft^3)	Particulate	0.89	0.00	0.00	0.00
Coatings Debris					
Qualified Epoxy (ft^3)	Particulate	0.78	0.50	0.63	1.63
Qualified IOZ (ft^3)	Particulate	0.49	0.00	0.39	0.30
Unqualified Coatings (ft^3)	Particulate	6.7	7.3	6.7	6.7
	Chips	1.46	1.46	1.46	1.46
Latent Debris					
Latent Debris (lbm)	Fiber Fines	12.75	12.75	12.75	12.75
	Particulate	72.25	72.25	72.25	72.25

3.f. Head Loss and Vortexing

The objectives of the head loss and vortexing evaluations are to calculate head loss across the sump strainer and to evaluate the susceptibility of the strainer to vortex formation.

1. *Provide a schematic diagram of the emergency core cooling system (ECCS) and containment spray systems (CSS).*

   Response to 3.f.1:

   See Figure 3.f.1-1 and Figure 3.f.1-2 for ECCS and CSS schematics during cold leg and hot leg recirculation, respectively.

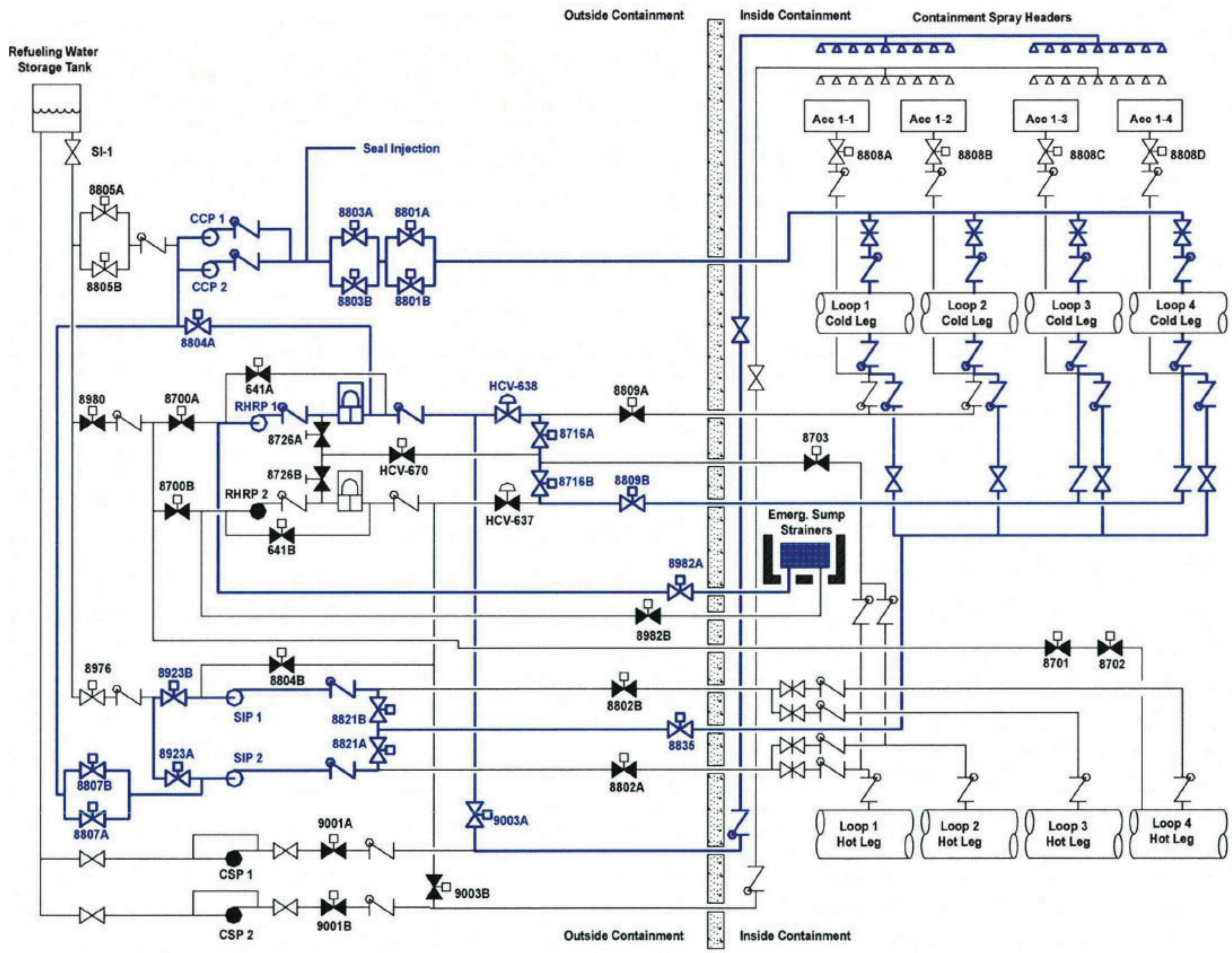

Figure 3.f.1-1 ECCS and CS System Schematics during Cold Leg Recirculation

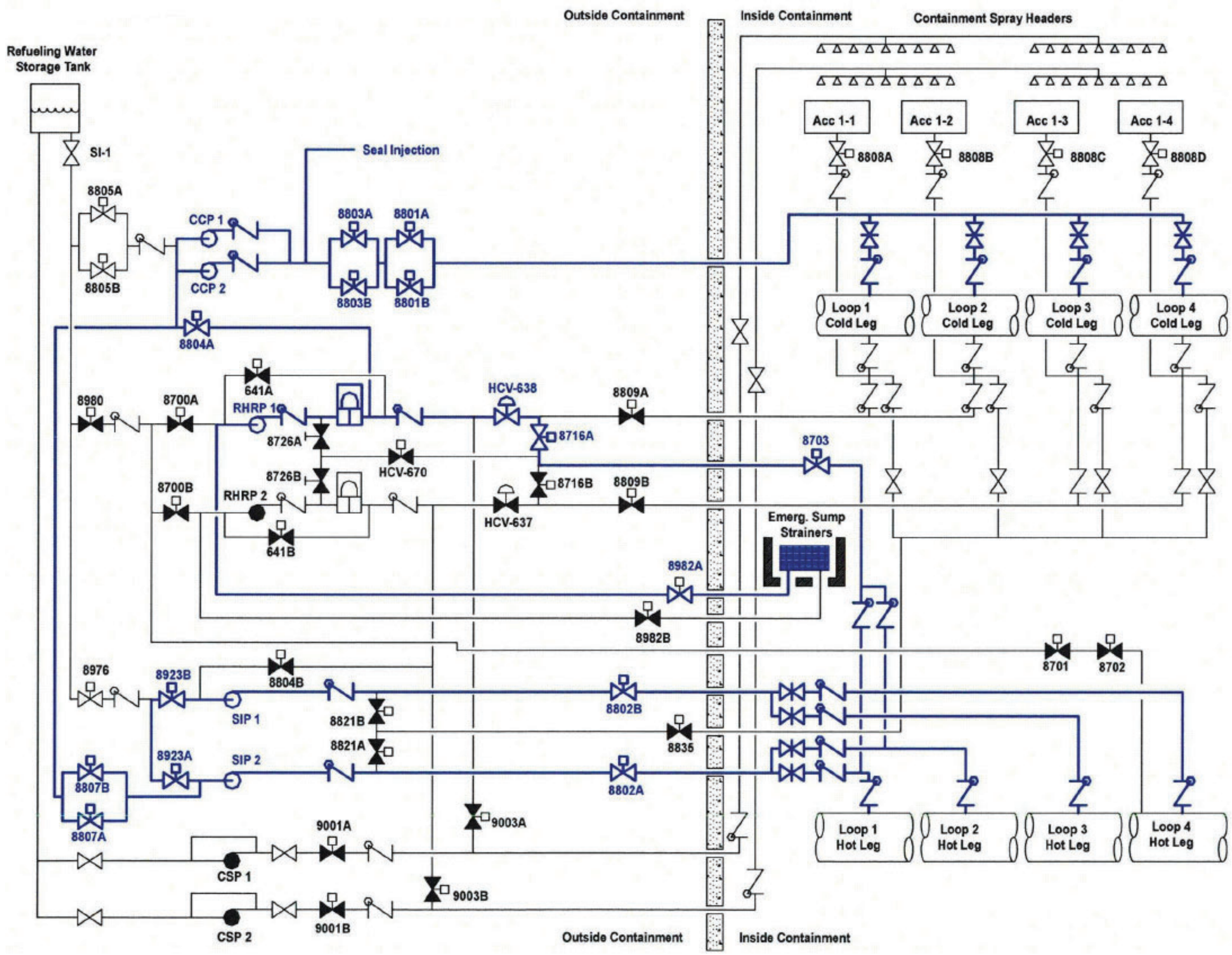

Figure 3.f.1-2 ECCS and CS System Schematics during Hot Leg Recirculation

2. *Provide the minimum submergence of the strainer under small-break loss-of-coolant accident (SBLOCA) and large-break loss-of-coolant (LBLOCA) conditions.*

   Response to 3.f.2:

   As shown in the Response to 3.g.1, the minimum water level results in a strainer submergence of 0.03 ft for breaks greater than 6 inches when the first RHR pump is started at the beginning of the manual cold leg recirculation switchover. The minimum submergence increases to 1.3 ft when the switchover to recirculation is complete with all CS pumps secured and no longer taking suction from the RWST.

   For breaks of 6 inches and smaller, the strainer is partially submerged at the start of recirculation, leaving the top 0.5 ft of the rear disks and 0.27 ft of the front disks unsubmerged.

3. *Provide a summary of the methodology, assumptions, and results of the vortexing evaluation. Provide bases for key assumptions.*

   Response to 3.f.3:

   Vortexing evaluation was performed separately for breaks >6 inches and breaks ≤6 inches. For the breaks ≤6 inches, the vortexing evaluation was done for the front and rear sections of the strainer separately. As discussed in detail below, air-entraining vortices will not form for any postulated breaks at DCPP.

   <u>Breaks Larger than 6 in</u>

   In 2016, vortexing testing was performed during the Alden head loss testing, which is further described in the Response to 3.f.4. The results are applicable for evaluating vortexing for breaks larger than 6 inches for the following reasons.

   - The maximum conventional debris loads for all postulated breaks are well bounded by the tested debris loads of both the confirmatory and thin-bed head loss tests (see the Response to 3.f.7).
   - The addition of chemical debris was terminated after the head loss was observed to continue decreasing after introducing the last two batches. Therefore, the impact of chemical debris on head loss and vortexing was fully captured (see the Response to 3.f.4).
   - The design and arrangement of the test strainer are prototypical to the plant strainer (see the Response to 3.f.4). Therefore, the flow profile approaching the plant strainer was closely modeled during testing.
   - The test flow rate was maintained within -0/+5% of a nominal value, which corresponds to a plant strainer flow rate of 8000 gpm, exceeding the maximum plant strainer flow rate of 7769 gpm with both RHR pumps in operation.

No air entraining vortices were observed on the clean strainer when the water level was decreased to reach the minimum strainer submergence of 0.03 ft at start of recirculation (see the Response to 3.f.2). After conventional and chemical debris addition at the end of the confirmatory head loss test, the flow rate was maintained above 8000 gpm for the plant strainer while the test tank was drained down to the minimum strainer submergence of 0.03 ft. It was observed that small surface dimples formed on the water surface about the strainer but quickly died out. No evidence of air transport from the strainer assembly was observed (i.e., bubbles in the discharge piping) even when the water level was decreased further, leaving the X-Frame/ rear strainer disk support cross-member unsubmerged.

Based on the discussions above, it is concluded that no air entraining vortices would form on the plant strainer during the recirculation phase for breaks larger than 6 inches. Note that the minimum strainer submergence used during the vortexing test (0.03 ft) occurs at the start of recirculation and increases to 1.3 ft by the time when the switchover to recirculation is completed (see the Response to 3.f.2). Additionally, applying the result of the debris laden vortex test is conservative because, at the start of recirculation when the minimum strainer submergence (0.03 ft) is evaluated, the strainer is expected to be clear of debris.

Breaks Less than and Equal to 6 in

For breaks of 6 inches and smaller, the strainer is partially submerged at the start of recirculation (see the Response to 3.f.2). A vortexing evaluation was performed for these smaller breaks based on testing data.

Vortexing of Strainer Front Section

Flow that is filtered through the front strainer disks first collects inside the front plenums before entering the square elbows behind the two plenums at the ends of the strainer. Flow inside each of the two elbows then travels through a vertical downcomer and merges with the flow from the rear strainer disks/plenums. To prevent gas ingestion by vortices that form on the front strainer disks to travel to the pump, four “vortex breaker” plates (3 inches apart) were installed inside the square elbow, and each plate has three 6-inch diameter holes to introduce cross flows and interrupt vortex cores that may form. Additionally, a cruciform was installed inside the downcomer to facilitate breakdown of the vortices.

Vortexing tests were performed on the above arrangement over a variety of flow rates (*Q*) and water depths (*S*). As shown in Table 3.f.3-1, the arrangement is effective at breaking down vortices for a range of testing conditions with different Froude numbers, resulting in minimal (≤0.1%) void fraction observed during testing.

Table 3.f.3-1 Testing Parameters for Front Plenum Connection Vortexing Testing

Q (gpm)	*u* (ft/s)	*S* (in)	Fr	Void Fraction (%)
824	9.35	42.1	0.88	0
685	7.77	38.3	0.77	0
960	10.89	43.1	1.01	0.1
956	10.85	41.1	1.03	0.1
826	9.37	38.1	0.93	0.1
410	4.65	30.6	0.51	0.1
550	6.24	29.6	0.70	0.1

For the plant strainer, the Froude number at the exit of the downcomer was calculated to be 0.57 based on a conservatively low submergence based on the minimum SBLOCA water level and high flow rate through the front section of the strainer. The plant strainer Froude number (0.57) is lower than most of the test cases shown in Table 3.f.3-1. Since vortexing is less likely for flow with a lower Froude number, it is reasonable to conclude that any vortices that could possibly travel through the front disks and plenums will be broken down inside the square elbow and downcomer.

Note that the vortexing testing did not include any strainer disks which are arranged vertically and could serve as vortex suppressors. Additionally, the torturous flow paths at the connections between strainer disks and plenums could also break down the vortices. None of these were credited in the above analysis.

Vortexing of Strainer Rear Section

Vortexing over the rear strainer disks for breaks of 6 inches and smaller is evaluated based on observations made during the previous modular head loss testing[8]. The test data is applicable and conservative for this analysis because of the following.

- The testing configuration accurately models the rear section of the plant strainer. The test strainer used for the modular head loss testing had 15 full-sized disks installed on top of a plenum. This configuration matches the rear section of the plant strainer.
- The test flow rate corresponds to a plant strainer flow rate of 8004 gpm, which exceeds the maximum total strainer flow rate of 7769 gpm with both RHR pumps in operation. The test flow rate is therefore higher than the expected flow rate through the rear section of the plant strainer and is therefore conservative for the purpose of vortexing evaluation.
- During testing, the water level was incrementally reduced to 38.875 inches below the top of the test strainer disks. This water level is lower than the minimum water level expected at the plant for the breaks of 6 inches and

[8] This modular head loss test is different from the latest Alden head loss tests described in the Response to 3.f.4.

smaller, which is 0.5 inches below the top of the rear strainer disks (see the Response to 3.f.2). This testing condition is very conservative for vortexing.

The modular head loss testing showed that no vortexing or air entrainment was observed during testing for the conditions described above. Given that the testing conditions conservatively bound the plant conditions with respect to vortexing, it is concluded that for the rear strainer section, no air entraining vortices will form for breaks of 6 inches and smaller.

4. *Provide a summary of methodology, assumptions, and results of prototypical head loss testing for the strainer, including chemical effects. Provide bases for key assumptions.*

Response to 3.f.4:

Head loss tests were performed to measure the head losses caused by conventional debris (fiber and particulate) and chemical precipitation debris generated by a LOCA and transported to the sump strainers during recirculation. The test program used a test strainer, debris quantities, and approach velocities that were representative of the plant conditions. Two different tests were performed following the thin bed and full debris load protocols, respectively, in accordance with the 2008 NRC Review Guidance (Reference 3). In this submittal, the two tests are referred to as the Full Debris Load Test and Thin-Bed Test, respectively.

The objective of the full debris load test is to measure debris head losses associated with the maximum fiber, particulate and chemical debris quantities calculated to transport to the sump strainer after a LOCA. The objective of the thin-bed test is to measure debris head losses associated with the maximum particulate debris quantities postulated to occur with the minimum amount of fiber on the strainer required to filter particulate out of the water.

Test Setup

The test strainer assembly consisted of the front and rear sections (see Figure 3.f.4-1) and is a full-scale section of the plant strainer. The front disks were mounted to the front side of a plenum (with respect to direction of flow), and the rear disks were mounted on top of another plenum. The front plenum was connected to the rear plenum by a pipe that contained a flow meter to measure the flow rate of the front strainer section. The test strainer was both geometrically and hydraulically similar to the plant strainer and had the following parameters which matched those of the plant strainer at the test flow rate:

- Disk dimensions of the plant large disks, which compose 95% of the plant strainer area
- Key dimensions of the perforated plates (e.g., hole diameter, hole pitch, and thickness)
- Area ratio between the front and rear sections

- Flow split between the front and rear sections
- Gap-to-disk-area ratio for the front strainer section from which flow approaches
- Overall average approach velocity at strainer disks
- Individual disk approach velocity distribution at clean condition

The test strainer assembly was installed in a test tank, where the rear strainer section was located in a pit to match the plant strainer installation. The strainer region was designed such that the spacing between the exterior sides of the test strainer and the surrounding acrylic walls imitated the gaps between the DCPP strainer and the sump pit walls that surround it. An illustration of the test strainer and tank is provided in Figure 3.f.4-1.

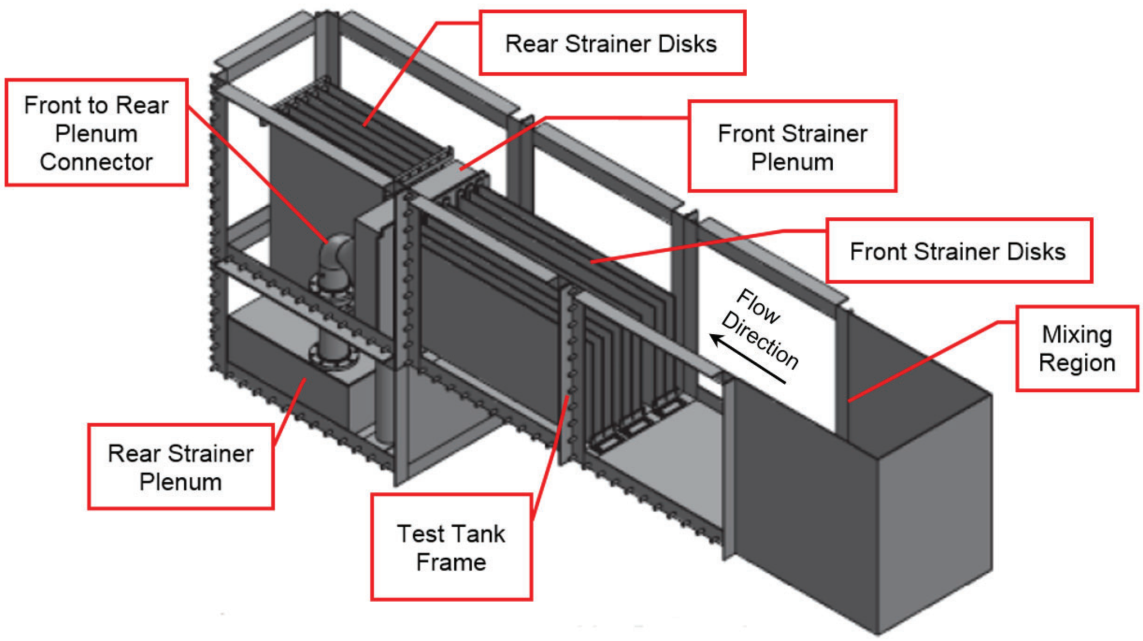

Figure 3.f.4-1: Head Loss Test Strainer Assembly inside Test Tank

A flow diagram of the test loop is provided in Figure 3.f.4-2 below. The test loop had a recirculation pump that took suction from the rear plenum underneath the test strainer (consistent with the plant strainer design) and returned the water back into the test tank through the mixing lines placed at upstream downstream ends of the test tank or through a debris hopper during debris introduction. The placement of the mixing lines was adjusted such that the turbulence from the flow exiting the mixing lines promoted a homogeneous mixture of debris in the tank water but did not affect the debris bed on the test strainer. The flow rate through the loop, head loss across the test strainer and tank water temperature were recorded continuously during each test. Flow control valves, and heating and cooling loops were used to control the test flow rate and water temperature. The test loop also included a continuously mixed transition tank that was brought online during conventional and chemical debris introduction to increase the effective volume of the test loop and decrease the amount of draining operations required during testing. The filter housings with filter bags installed were used to clean up the test loop but were bypassed during head loss testing.

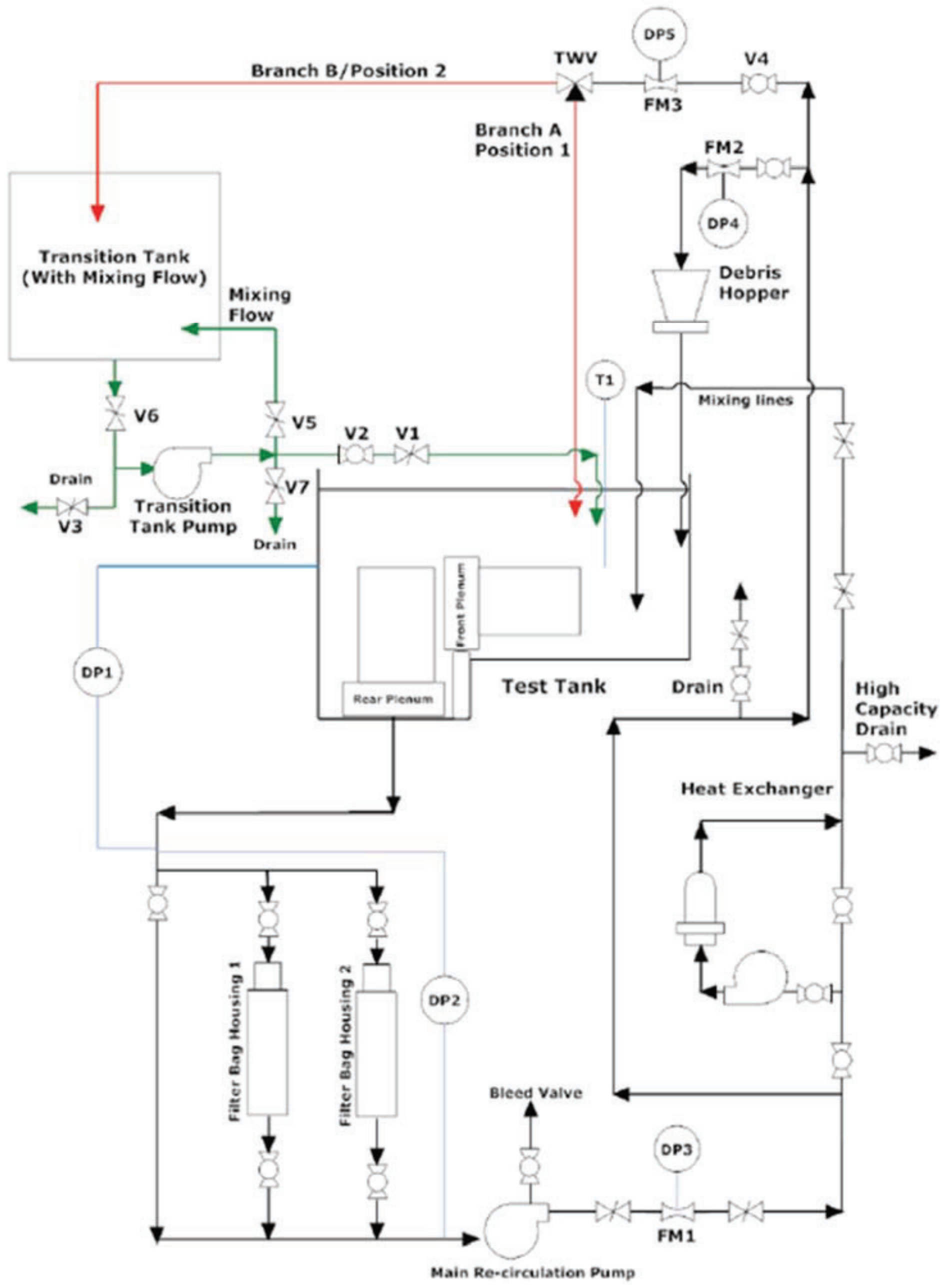

Figure 3.f.4-2: Flow Diagram of Head Loss Test Loop

Test Parameters and Scaling

The debris loads and flow rates used for head loss testing were scaled from the plant debris loads and flow rates using the ratio of the test strainer surface area (340.2 ft^2) to the net surface area (3,073.5 ft^2) of the plant strainer. The net surface area of the plant strainer is equal to the total strainer surface area (3,278.7 ft^2) minus the sacrificial strainer surface area (205.16 ft^2, see the Response to 3.b.5). Since the test flow rate was also scaled using the ratio of the test strainer surface area to the net surface area of the plant strainer, the average approach velocity of the test strainer matched the average approach velocity of the plant strainer. The test flow rate was determined to be 885.5 gpm (8,000 gpm × 340.2 ft^2/ 3,073.5 ft^2) and is equivalent to a plant strainer flow rate of 8,000 gpm. During testing, the flow rate is maintained between -0/+5% of the test flow rate. The nominal test temperature was 120°F.

Flow sweeps were performed during each head loss test for both clean strainer and debris-laden conditions. For each flow sweep, head losses across the strainer at several different flow rates were measured. The flow sweep results on the debris-laden strainer were used to characterize the flow through the debris bed and to scale the debris head loss measured at testing conditions (i.e., flow rate and temperature) to plant conditions of interests. See the response to 3.f.10 for more information.

Debris Materials and Preparation

As shown in the Responses to 3.d.3, 3.e.6 and 3.h.1, DCPP has the following fibrous debris types that needed to be considered during head loss testing: Temp-Mat, TIW, fiberglass overbraid and flexicone sleeves, Kaowool, and latent fiber. The particulate debris types included Cal-Sil, foamglas, mica tape, coating particulate and coating chips. During head loss testing, either the actual debris material or a surrogate was used.

Temp-Mat was used as a surrogate for fiberglass overbraid and flexicone sleeves due to their high macroscopic density and tight packing. Nukon fines were used as a surrogate for latent fiber, as recommended in the NRC SE on NEI 04-07 (Reference 13 pp. VII-3) and for TIW due to their similarities in density and fiber size. Performance Contracting Inc (PCI) “PWR Dirt/Dust” mix was used as surrogate for latent particulate debris. Sil-Co-Sil with a mean size of approximately 10 μm was used as surrogate for coatings, foamglass and mica tape particulate debris. Acrylic paint chips were used as surrogate for coating chip debris. No surrogate materials were used for Temp-Mat, Cal-Sil or Kaowool debris.

Nukon, Temp-Mat, and Kaowool fines were prepared in accordance with the NEI fibrous debris preparation protocol (Reference 6). Nukon insulation sheets were heat treated by the vendor and were baked single-sided on a hot plate until the binder burn gradient ends approximately half-way through the sheets. This results in approximately 50% of Nukon in each sheet that was heat treated. The Nukon sheets were cut into approximately 2-inch x 2-inch cubes and then weighed out into pre-set batches for each test.

Temp-Mat was also procured heat treated, similar to Nukon. However, Temp-Mat sheets were shredded through a mechanical shredder before being weighed out. This was necessary because the raw material will not otherwise break up sufficiently by pressure washing.

The test vendor heat treated Kaowool by replicating the burned-out portion of heat-treated Nukon using an oven rather than a hot plate. A piece of non-heat treated Nukon and multiple pieces of non-heated Kaowool having similar mass were placed in an oven to bake at a nominal temperature of 500°F. The pieces were rotated every ten minutes until the color and texture of the baked Nukon matched that of the burnt portion of purchased Nukon sheets. When weighing out Kaowool for batches, each batch contained a mixture of 50% (by mass) heat treated material, and 50% un-heat treated, for consistency with the heat treatment of Nukon.

After being weighed out according to batch size requirements, batches of Nukon, Kaowool, and Temp-Mat were each pressure washed in accordance to the NEI protocol (Reference 6). This was done in a 50-gallon debris preparation vessel equipped with a slide gate valve at the bottom to control the removal of the debris slurry after preparation. Inside the vessel, a high-pressure nozzle assembly (with three nozzles rated at 1500 psi and 3 gpm) was mounted such that flow exited from the nozzles at a downward angle of approximately 30 degrees, resulting in a fan type flow distribution. The assembly was also oriented to provide tangential momentum to the debris slurry inside the vessel.

Each debris type was prepared separately. Preheated test water was first added to the vessel using a low-pressure water spray until the fiber debris was wetted and the high-pressure nozzles were submerged. The debris was then sprayed with test water pressurized to 1500 psi. The initial amount of test water inside the vessel, the high pressure spray nozzle position and orientation, and the amount of time the high pressure spray was applied were controlled to ensure consistency in characteristics of the prepared debris batches. Fiber fines were acceptable once their composition was predominantly Class 2 fibers as defined in NUREG/CR-6224 (Reference 22 Table B-3), consisting mainly of individual fibers with lesser quantities of fiber shards and small clumps. A sample of each prepared debris batch was photographed in a lighted water column. See Figure 3.f.4-3 for photographs of Nukon, Kaowool, and Temp-Mat fines prepared using this process.

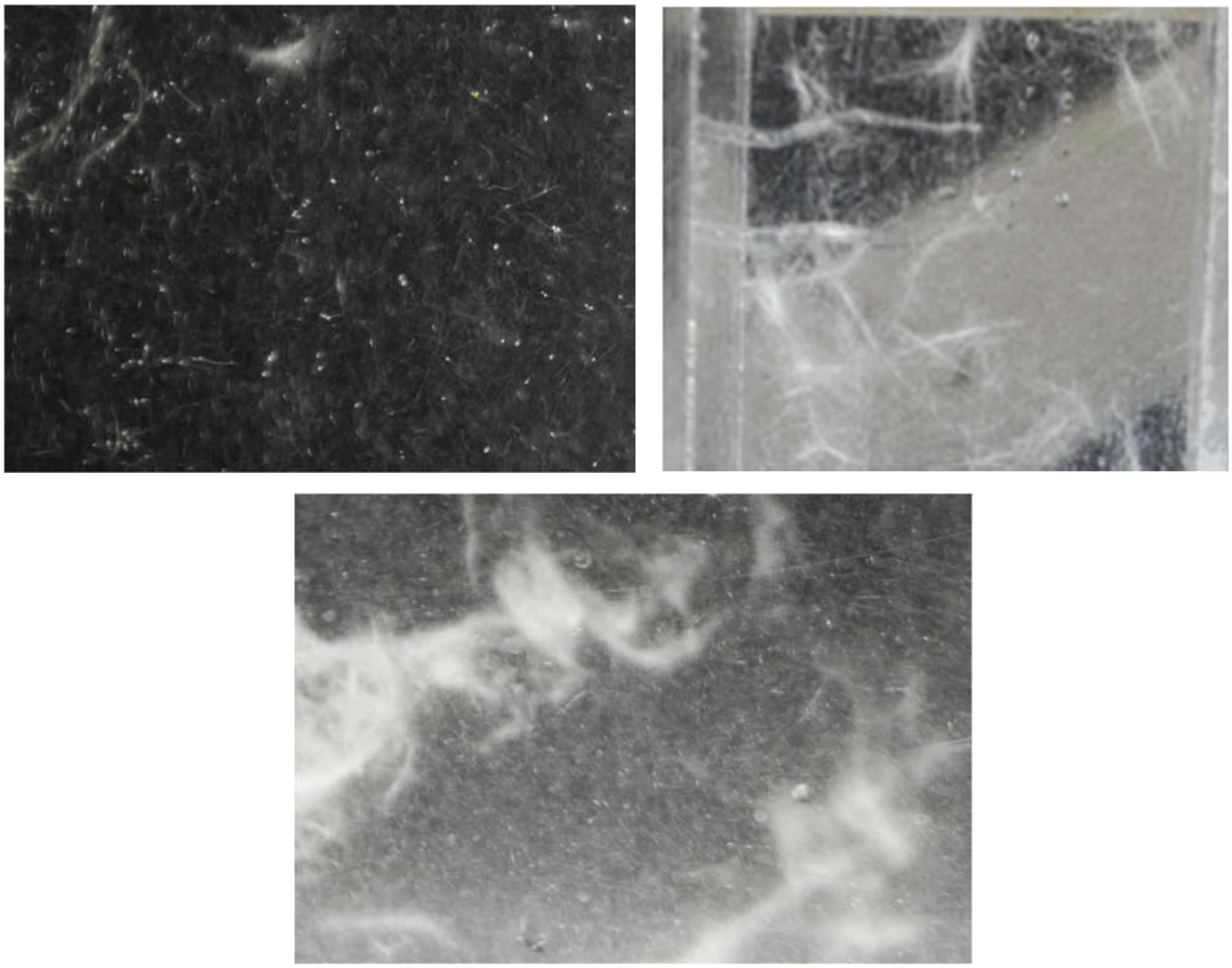

Figure 3.f.4-3: Nukon (left), Temp-Mat (right), and Kaowool (bottom) Fines Prepared for DCPP Head Loss Testing

Sil-Co-Sil was used a surrogate for failed coatings, Foamglas insulation, and Mica Tape particulate debris on an equal volume basis. The Sil-Co-Sil used during testing had a mean size distribution of approximately 10 μm and is therefore appropriate to model the particulate debris with a characteristic size of 10 μm (see the Response to 3.h.1). Sil-Co-Sil has a specific gravity of 2.65, or a density of 165 lbm/ft^3. The required amount of Sil-Co-Sil for a debris batch was weighed out and placed in a bucket. The particulate was then wetted with test water while being gently stirred to avoid the formation of foam.

Acrylic paint chips, with a material density of 1.43 kg/L and nominal sizes ranging from 0.05 to 0.15 inches, were added to the head loss test to model the coating chips debris on an equal volume basis. The coating chips debris at DCPP has characteristic sizes of 1/8 in x1/8 in to ½ in x1 in with a thickness of 9 mil. The surrogate material is therefore finer than the actual debris and is conservative for the purpose of head loss testing because finer debris is less likely to create voids in the debris bed and reduce head loss. Similar to Sil-Co-Sil, paint chips were wetted with test water before introduction to the test loop.

Pulverized Cal-Sil was prepared for test introduction using a similar method as the Sil-Co-Sil.

The PCI "PWR Dirt/Dust" mix used as a surrogate for latent particulate was sprinkled in its dry form directly into the test tank and required no preparation.

Aluminum oxyhydroxide (AlOOH) was used as a chemical debris surrogate for head loss testing. The chemical debris was prepared in accordance with WCAP-16530-NP-A (Reference 23) and met the settling volume acceptance requirements specified in WCAP-16530-NP-A. See the Response to 3.o.2.12 for additional information.

Debris Introduction

For the Full Debris Load head loss test, the particulate debris (Sil-Co-Sil, Cal-Sil, paint chips) were mixed with the fibrous debris (Nukon, Temp-Mat, and Kaowool) to form a homogenous slurry prior to introduction into the test loop. The fiber and particulate slurry was added to the test loop via the debris introduction hopper. The hopper used a portion of recirculating loop flow to provide mixing of the debris slurry to prevent agglomeration as the debris was carried to the front and rear mixing regions of the test tank. To prevent clogging of the hopper, each batch of dirt/dust mix was sprinkled in its dry form directly into the test tank immediately upstream of the leading edge of the front strainer at the same time as the mixed components of the respective debris batch.

For the Thin-Bed Test, all particulate debris, except for the dirt/dust mix, was added to the test tank in succession through the debris hopper prior to the introduction of fibrous debris. Dirt/dust mix was added directly to the test tank's mixing region after the addition of cal-sil and Sil-Co-Sil. All particulate debris was added in succession, and afterwards, a homogenous mixture of fiber fines was added in small batches until a particulate filtering debris bed was formed on the test strainer. The fiber debris batch sizes varied slightly and all batches had LDFG-equivalent theoretical uniform bed thicknesses ranging between 0.027 and 0.049 inches. A particulate-filtering debris bed was observed to form when the test loop water began to clear and when the increase in head loss from a batch of fiber fines was observed to be much smaller than the preceding batches.

Chemical debris was added to the test tank in a similar fashion for both the Full Debris Load and Thin-Bed tests. After conventional debris introduction was completed and the head loss was allowed to stabilize, a flow sweep was performed. Afterwards, chemical precipitate debris was added to the test tank. Prepared AlOOH solution was pumped into the test tank in several batches. After each batch of introduction, the head loss was stabilized before the next batch. Once chemical precipitate debris introduction was completed, another flow sweep was performed, the test loop was cooled to about 100°F, and a final flow sweep was performed.

Test Water Preparation

Test water was prepared by first adding boric acid to deionized water to reach a boron concentration of 2,431 ppm. The water was continuously mixed while the boric acid was added. Afterwards, NaOH was added in small batches to achieve a pH of 7.5. During this process, the solution was continuously mixed with the pH closely monitored.

DCPP Full Debris Load Test

The total conventional debris loads for the DCPP Full Debris Load Test are scaled to equivalent plant debris loads using the ratio in surface area between the test strainer and plant strainer (see Table 3.f.4-1). The peak conventional debris head loss observed for this test is shown in Table 3.f.4-5.

Table 3.f.4-1: Conventional Debris Quantities for DCPP Full Debris Load Test

Nukon Fines (lbm)	Temp-Mat Fines (lbm)	Kaowool Fines (lbm)	Total Fiber Fines (lbm)	Cal-Sil (ft^3)	Sil-Co-Sil (ft^3)	Latent Particulate (lbm)	Coatings Chips (ft^3)
15.42	164.31[9]	7.88	187.61	24.46	14.94	72.67	1.46

After all conventional debris was added, the head loss was allowed to stabilize, and a flow sweep was performed. Afterwards, chemical debris was batched into the test tank. Each batch of prepared AlOOH had a volume of 500 gallons and contained 3.96 kg of AlOOH, which corresponds to 35.8 kg of AlOOH at plant scale (3.96 kg × 3073.5 ft^2/ 340.2 ft^2). The aluminum contained in one batch of AlOOH is calculated to be 16.1 kg based on molecular weight values of the elements. The chemical debris batches for the DCPP Full Debris Load Test are summarized in Table 3.f.4-2 and scaled to equivalent plant debris loads.

Table 3.f.4-2: Chemical Debris Batches for Full Debris Load Test

Batch ID	AlOOH (kg)	Aluminum Precipitated (kg)
A1	35.8	16.1
A2	35.8	16.1
A3	35.8	16.1
A4	35.8	16.1
Total	**143.2**	**64.4**

Head loss increased relatively quickly when the first batch of chemical debris was added to the test tank. The head loss peaked during the addition of the second batch and then decreased and stabilized to a head loss lower than it was before the second batch was introduced. The third batch increased the head loss, but the peak

[9] This quantity of tested Temp-Mat fines is greater than the plant debris load when a 11.7D ZOI is applied for all Temp-Mat insulation, including encapsulated Temp-Mat.

from the third batch was less than the peak from the second batch. The fourth batch had a negligible effect on head loss, and the head loss continued to slowly decrease with time. Chemical debris batches were no longer added because a decreasing head loss was observed and new peaks were not formed. The maximum chemical debris head loss for the DCPP Full Debris Load Test is considered to be the first peak observed after introducing the second batch (Batch A2 in Figure 3.f.4-5). The test results are provided in Table 3.f.4-5.

Figure 3.f.4-4 and Figure 3.f.4-5 show a plot of raw head loss test data for the DCPP Full Debris Load Test with time to identify the key testing activities. Note that the flow rates shown in this figure are at the test scale and the head loss values have not been adjusted to subtract the test strainer’s clean strainer head loss.

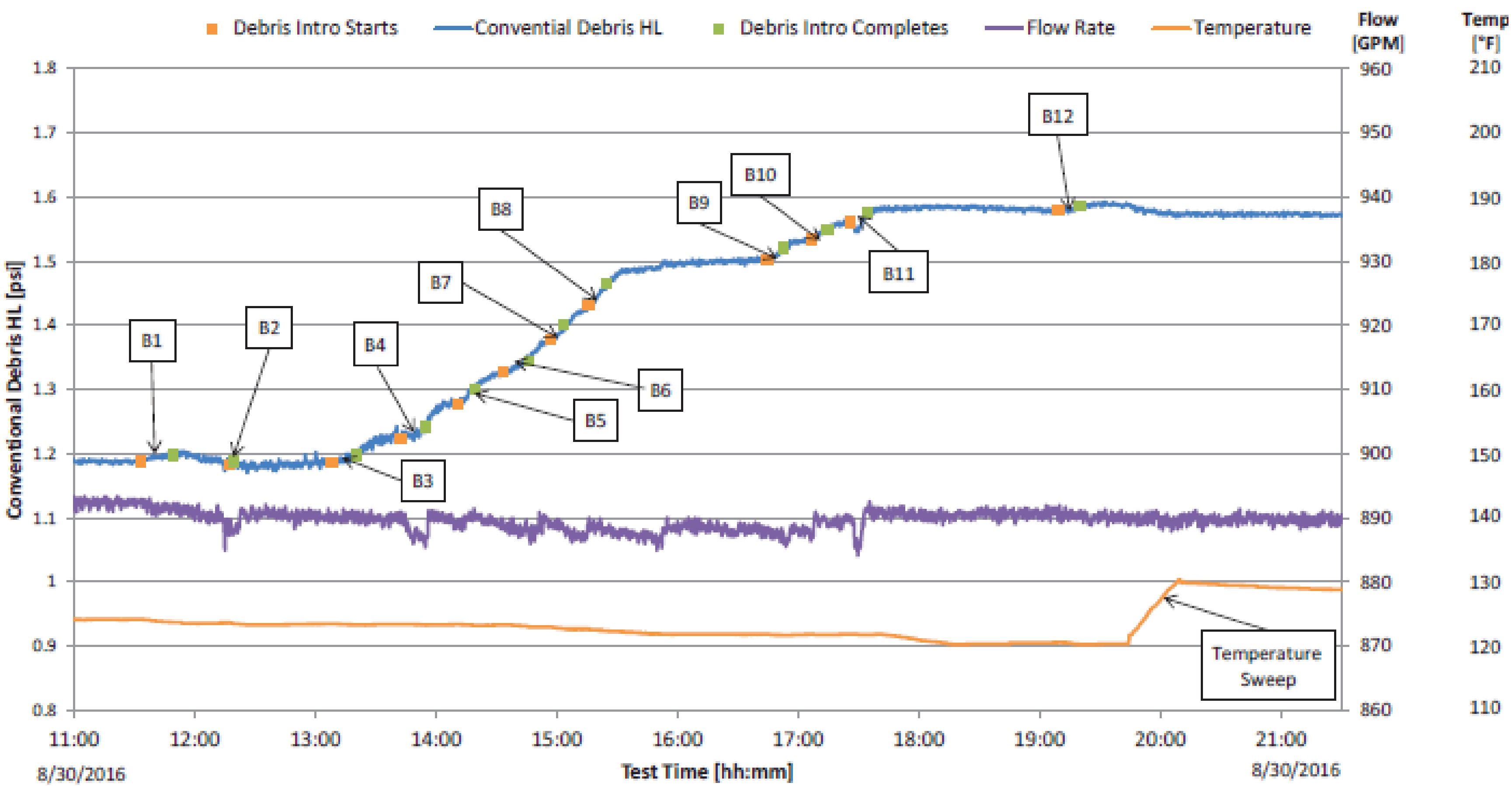

Figure 3.f.4-4: DCPP Full Debris Load Test Conventional Debris Timeline

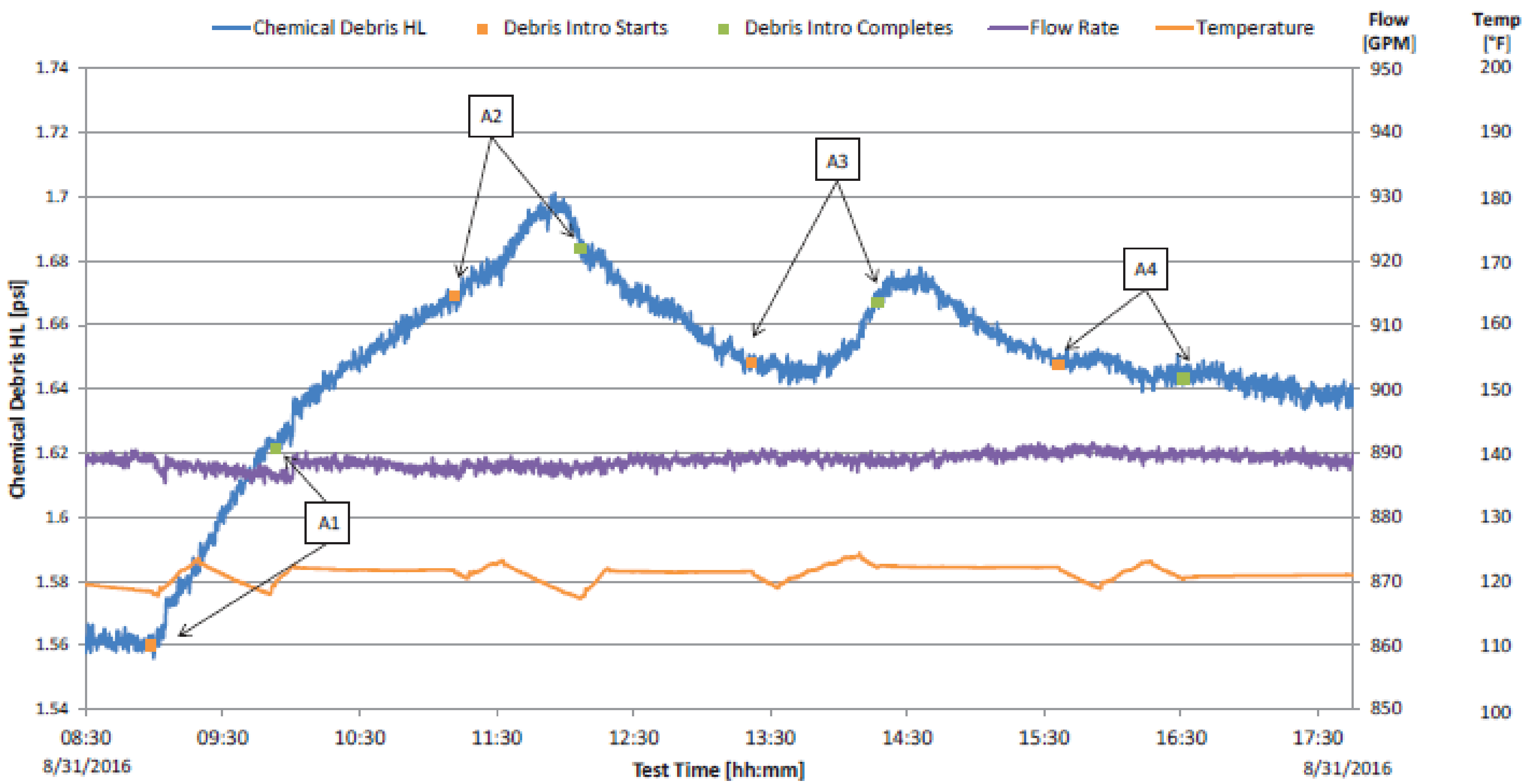

Figure 3.f.4-5: DCPP Full Debris Load Test Chemical Debris Timeline

DCPP Thin-Bed Test

The total conventional debris loads for the DCPP Thin-Bed Test are scaled to equivalent plant debris loads (see Table 3.f.4-3). The peak conventional debris head loss observed for this test is shown in Table 3.f.4-5.

Table 3.f.4-3: Conventional Debris Quantities for the DCPP Thin-Bed Test

Nukon Fines (lbm)	Temp-Mat Fines (lbm)	Kaowool Fines (lbm)	Total Fiber Fines (lbm)	Cal-Sil (ft^3)	Sil-Co-Sil (ft^3)	Latent Particulate (lbm)	Coatings Chips (ft^3)
15.42	164.33[10]	7.88	187.63	24.48	14.94	72.67	1.46

After all conventional debris was added, the head loss had stabilized, and a flow sweep had been performed, chemical precipitate debris was added to the test tank. The first two batches of AlOOH added to the test tank had volumes of 200 and 300 gallons, respectively. As stated previously in this section, every 500 gallons of prepared AlOOH solution contained 35.8 kg of AlOOH at plant scale. Therefore, the first two batches had 14.3 kg (35.8 kg × 200 gallons/500 gallons) and 21.5 kg of AlOOH, respectively. The aluminum contained in each batch of AlOOH is similarly calculated as that discussed earlier based on molecular weight values of the elements. The chemical precipitate debris batches for the DCPP Thin-Bed Test are summarized in Table 3.f.4-4 and scaled to equivalent plant debris loads.

Table 3.f.4-4: Chemical Precipitate Debris Batches for the DCPP Thin-Bed Test

Batch ID	AlOOH (kg)	Aluminum Precipitated (kg)
A1	14.3	6.4
A2	21.5	9.7
A3	35.8	16.1
A4	35.8	16.1
Total	**107.4**	**48.3**

Head loss increased when the first batch of chemical debris was added to the test tank. The head loss decreased with time after the second, third, and fourth chemical debris batches were added to the test. After the fourth batch, chemical debris batches were no longer added because a decreasing head loss was observed and new peaks were not formed. The maximum chemical debris head loss for the Thin-Bed Test is considered to be the first peak observed during introduction of the first batch (or Batch A1 in Figure 3.f.4-7). The test results are provided in Table 3.f.4-5.

Figure 3.f.4-6 and Figure 3.f.4-7 show a plot of raw head loss test data for the DCPP Thin-Bed Test with time to identify the key testing activities. Note that the flow rates

[10] This quantity of tested Temp-Mat fines is greater than the plant debris load when a 11.7D ZOI is applied for all Temp-Mat insulation, including encapsulated Temp-Mat.

shown in this figure are at the test scale and the head loss values have not been adjusted to subtract the test strainer's clean strainer head loss.

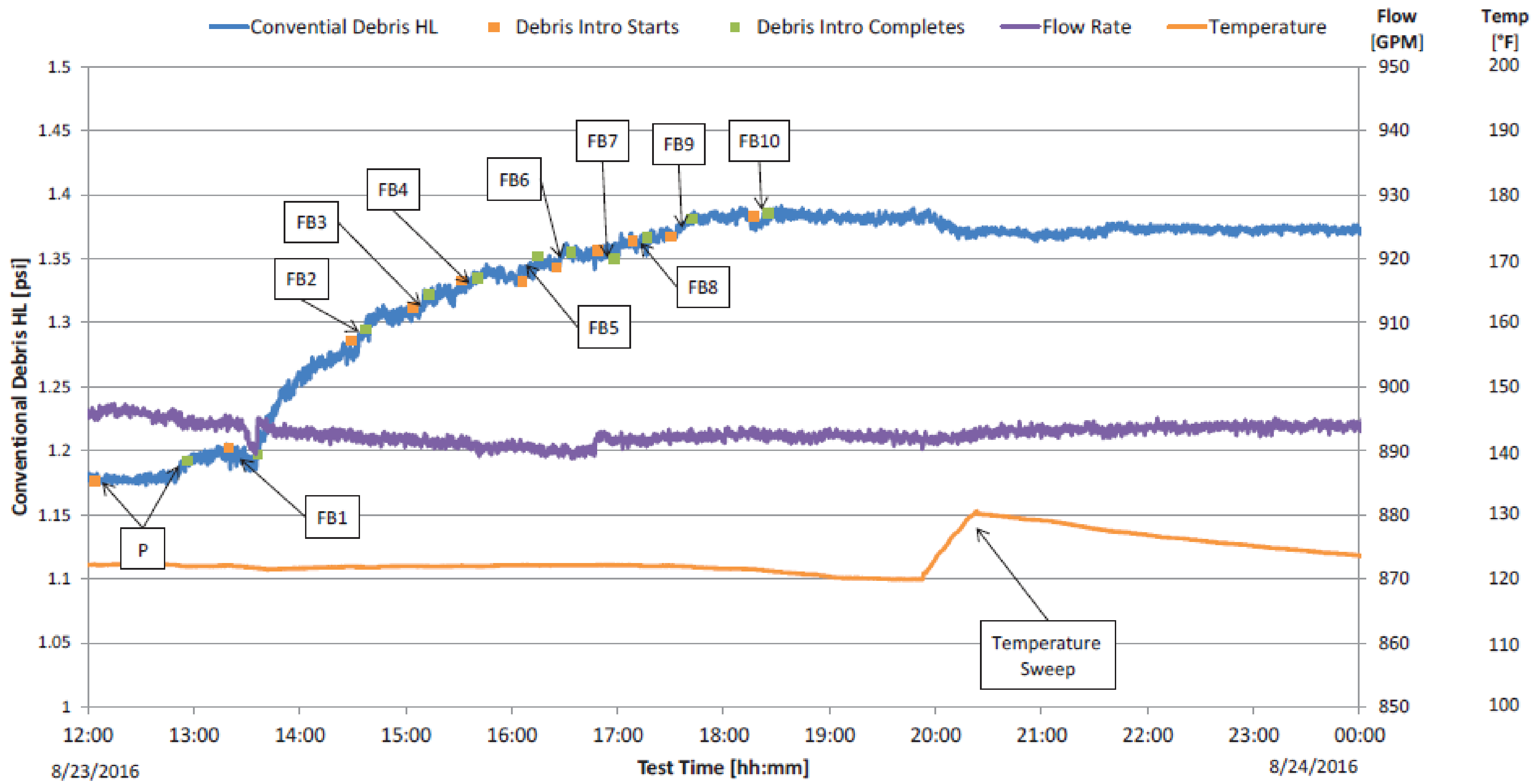

Figure 3.f.4-6: DCPP Thin-Bed Test Conventional Debris Timeline

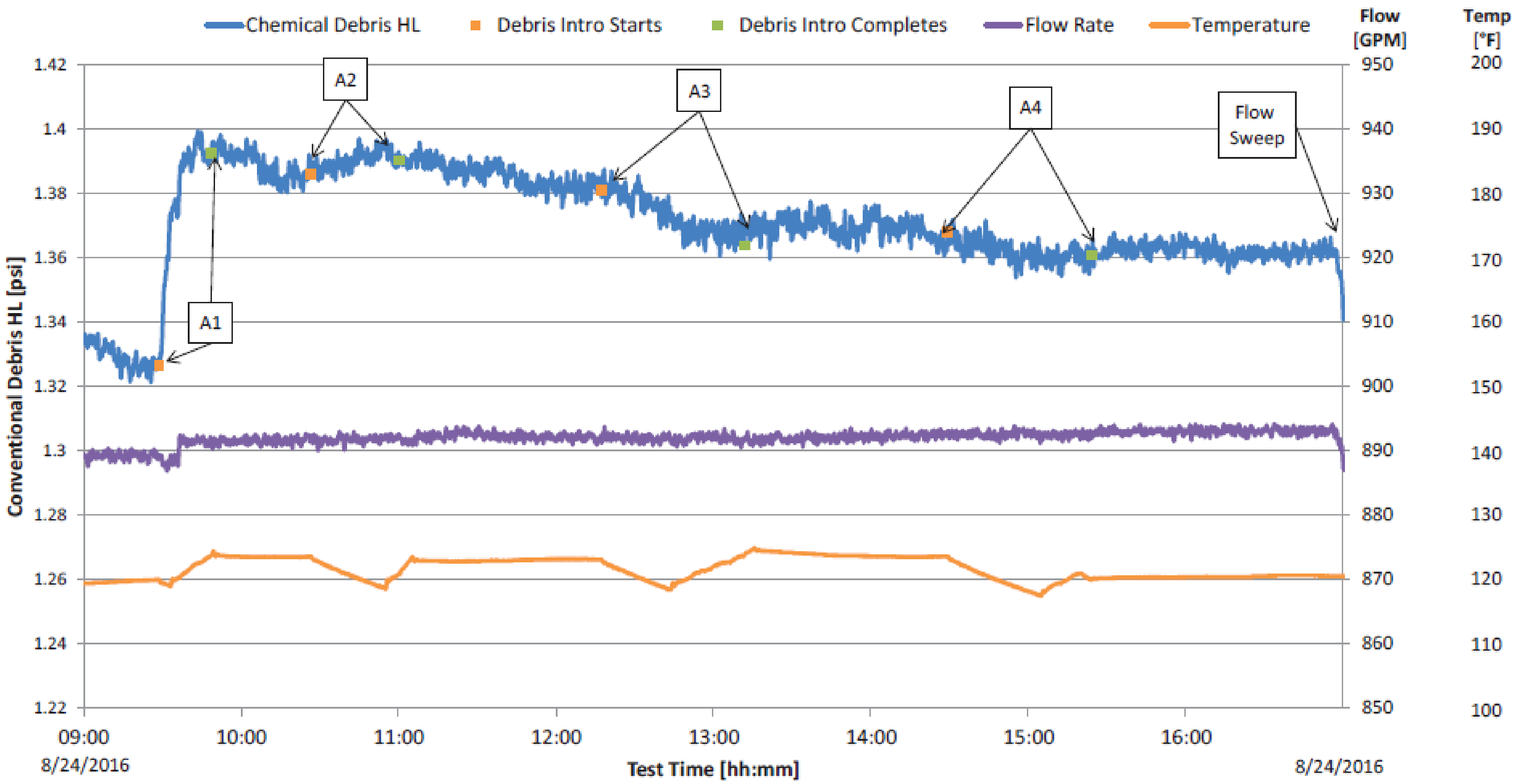

Figure 3.f.4-7: DCPP Thin-Bed Test Chemical Debris Timeline

Summary of DCPP Head Loss Test Results

A summary of the debris head loss results from the DCPP tests are provided in Table 3.f.4-5. The head loss values shown in the table already had the test strainer clean strainer head loss subtracted. The maximum debris head losses observed during conventional and chemical debris introduction (bold-faced in the table) were used to derive the head losses for the plant strainer.

Table 3.f.4-5: Summary of DCPP Head Loss Test Results

Test Point	Debris Head Loss (psi)	Test Flow Rate (at Plant Scale) (gpm)	Temperature (°F)
DCPP Full Debris Load Test			
Conventional Debris Max Head Loss	**0.437**	**888.7 (8,029)**	**120.3**
Conventional Debris Stabilized Head Loss	0.422	890.3 (8,043)	120.4
Aluminum Precipitate Max Head Loss	**0.550**	**888.0 (8,023)**	**120.9**
Aluminum Precipitate Stabilized Head Loss(1)	0.469	887.4 (8,017)	120.8
DCPP Thin-Bed Test			
Conventional Debris Max Head Loss	0.277	892.0 (8,059)	121.9
Conventional Debris Stabilized Head Loss	0.204	892.2 (8,060)	120.0
Aluminum Precipitate Max Head Loss	0.249	883.9 (7,985)	115.0
Aluminum Precipitate Stabilized Head Loss(1)	0.179	887.7 (8,020)	120.5

(1) The stabilized aluminum precipitate head loss was taken at the beginning of the flow sweep. Note that, during each test, the flow sweep was performed after the full load of chemical debris was added to the test tank and head loss was allowed to stabilize.

5. *Address the ability of the design to accommodate the maximum volume of debris that is predicted to arrive at the screen.*

Response to 3.f.5:

As discussed in the Response to 3.f.4, the head loss tests used test strainers that are prototypical to the plant strainer designs. Additionally, the test debris loads were scaled based on the ratio of the test strainer surface area and the plant's net strainer surface area. The arrangement of the test strainer within the test tank modeled the configuration in the arrangement of the plant strainer within the sump. The Full Debris Load Test for DCPP modeled the maximum debris load that could occur at the plant. With these considerations, the impact of the maximum debris volume on the plant strainer were directly determined from the head loss test results.

6. *Address the ability of the screen to resist the formation of a "thin bed" or to accommodate partial thin bed formation.*

Response to 3.f.6:

The "thin-bed effect" is defined as the relatively high head loss across a thin bed of fibrous debris, which can sufficiently filter particulate debris to form a dense debris bed (i.e., with high particulate to fiber ratio). As discussed in the Response to 3.f.4, the DCPP head loss testing included a test to measure head loss for a dense debris bed. During this test, the maximum particulate load was added into the test tank prior to the addition of fiber fines in small batches (with theoretical uniform bed thicknesses less than 1/16 in). This batching schedule allowed the formation of a debris bed with a high particulate to fiber ratio. As a result, any thin-bed effects, should the DCPP strainer be susceptible to them, would be captured by the measured head losses. The Thin-Bed Test resulted in lower conventional and chemical debris head losses than the Full Debris Load Test, and the "thin-bed" effect head loss is bounded by full debris load head loss. Therefore, the "thin-bed" effect on the DCPP sump strainer was properly accounted for during head loss testing and analysis.

7. *Provide the basis for strainer design maximum head loss.*

Response to 3.f.7:

A head loss calculation was performed to evaluate maximum strainer head loss using the head loss test data. The total strainer head loss was evaluated by combining the calculated plant strainer clean strainer head loss (CSHL) and measured debris head loss from testing after scaling the test data to plant conditions. The head loss calculation is only valid for breaks bounded by the head loss test conditions (e.g., approach velocity, conventional debris loads, and chemical debris load). In this section, the test conditions are compared with the plant conditions to ensure the plant conditions are bounded. The calculated total strainer head losses were compared with the strainer's crush pressure (see the Response to 3.f.10) and used for NPSH margin, degasification and vortexing evaluations (see the Response to 3.g).

Comparison of Plant Strainer and Head Loss Test Flow Conditions

As discussed in the Response to 3.g.2, the maximum flow rate through the plant strainer is 7,769 gpm, which corresponds to an approach velocity of 0.0056 ft/s for a total strainer area of 3,073.5 ft^2 (see the Response to 3.f.4). During head loss testing, the flow rate was maintained between 885.5 gpm and 929.8 gpm, which correspond to approach velocities of 0.0058 ft/s and 0.0061 ft/s, respectively for a test strainer surface area of 340.2 ft^2 (see the Response to 3.f.4). The approach velocity used during the head loss tests therefore bounds the plant condition. Note that the measured peak head losses were scaled to actual plant flow rates (see the Response to 3.f.10). Performing head loss testing at a higher approach velocity is conservative because the higher tested approach velocity would result in additional compression of the debris bed than the plant condition.

Comparison of Plant and Head Loss Test Debris Loads

Table 3.f.7-1 compares the bounding conventional debris loads of DCPP with those used in the DCPP head loss tests (see the Response to 3.f.4). As shown in the table, the plant debris loads are bounded by both tests for total fiber (including insulation and latent fiber), Cal-Sil, total non-latent particulate (including Cal-Sil, coating particulate, foamglas and Mica Tape), latent particulate and coating chips. Note that the plant debris quantities shown in Table 3.f.7-1 for each unit represent the maximum quantity of each debris type and are not from one single break at the plant. This approach is conservative for the purpose of this comparison. The Response to 3.f.4 states that the maximum recorded conventional debris head loss from testing was used to derive the plant strainer head loss. Therefore, the resulting conventional debris head losses are bounding and applicable for all breaks analyzed for DCPP.

Table 3.f.7-1: Comparison between Head Loss Test Debris Loads and Plant Debris Loads

Debris Type	Unit	Test Debris Loads		Plant Debris Loads	
		Confirmatory Test	Thin-Bed Test	Unit 1	Unit 2
Total Fiber Fines	**(lbm)**	**187.61(1)**	**187.63(1)**	**107.68(3)**	**109.89(3)**
Cal-Sil	(ft^3)	24.46	24.48	22.27	19.11
Coating, Foamglas and Mica Tape Particulate	(ft^3)	14.94	14.94	-	-
Total Non-Latent Particulate	**(ft^3)**	**39.4(2)**	**39.42(2)**	**36.49(4)**	**26.83(4)**
Latent Particulate	**(lbm)**	**72.67**	**72.67**	**72.25**	**72.25**
Coatings Chips	**(ft^3)**	**1.46**	**1.46**	**1.4**	**1.46**

(1) Calculated by combining the mass of tested Nukon, Temp-Mat, and Kaowool in Table 3.f.4-1 and Table 3.f.4-3, respectively.
(2) Calculated by combining the volumes of tested Cal-Sil and Sil-Co-Sil in Table 3.f.4-1 and Table 3.f.4-3, respectively.
(3) Calculated by combining the mass of Temp-Mat, TIW, Fiberglass Overbraid and Flexicone Sleeves, Kaowool and latent fiber for Break WIB-RC-2-1 (SE) in Table 3.e.6-10 for Unit 1, and for Break WIB-RC-2-6SE in Table 3.e.6-11 for Unit 2.
(4) Calculated by combining the volumes of Cal-Sil, Min-K, Foamglas, mica tape and coatings particulate for Break WIB-RC-3-7 in Table 3.e.6-10 for Unit 1, and for Break WIB-RC-4-7 in Table 3.e.6-11 for Unit 2.

The Response to 3.o.2.7.ii shows that the maximum quantity of aluminum release due to chemical precipitation in the post-LOCA pool is 248.35 lbm. This quantity is higher than those used during head loss tests (see Table 3.f.4-2 and Table 3.f.4-4).

However, as discussed in the Response to 3.f.4, chemical debris addition was terminated only after no head loss increase was observed from the previous introductions. As a result, further addition of chemical debris would not create any new head loss peaks. The Response to 3.f.4 states that the maximum debris head loss observed during chemical debris addition was used to derive the plant strainer chemical debris head loss. Therefore, the resulting chemical debris head losses are bounding and applicable for all breaks analyzed for DCPP.

8. *Describe significant margins and conservatisms used in head loss and vortexing calculations.*

Response to 3.f.8:

Vortex Evaluation

The vortexing testing and analyses have the following conservatisms. More detailed discussion can be found in the Response to 3.f.3.

- For breaks greater than 6 inches, the vortexing testing used conventional debris loads and flow rates higher than those expected at the plant conditions.
- For the breaks of 6 inches and smaller, the vortexing testing of the rear strainer section used a flow rate higher than that expected for the rear strainer section and a water level significantly lower than the minimum water level at the start of recirculation.
- For all breaks, the vortexing analysis was performed and verified by testing using the minimum water level at the start of recirculation, neglecting the water level increase as the switchover to recirculation is completed.

Head Loss Evaluation

The head loss testing and analysis have the following conservatisms. More detailed discussion can be found in the Responses to 3.f.4, 3.f.8, 3.f.9 and 3.f.10.

- The strainer head loss was evaluated at a maximum strainer flow rate of 7,769 gpm with two RHR pumps in operation with CS. This flow rate is higher than the actual strainer flow rate after the RHR pump flow to the cold legs is throttled per the emergency operating procedure.
- When one RHR pump is in operation, the strainer head loss was evaluated at a flow rate of 4,921 gpm with one RHR pump in cold leg recirculation. This flow rate is conservative because it represents a momentary flow rate before the operator throttles down the flow.
- Head loss testing was performed at conservatively higher conventional debris loads and flow rates than plant conditions (see the Response to 3.f.7).

- When evaluating plant strainer debris head losses, the maximum observed debris head losses (instead of the stabilized head losses) from testing were used.
- Clean strainer head loss for a debris-laden strainer is evaluated assuming uniform flow through the strainer, which conservatively lengthens the average flow path through the strainer and increases head loss. While debris accumulation does promote development of uniform flow, it would require a substantial debris coverage and head loss to achieve a perfectly uniform flow distribution on the strainer.
- Though the maximum chemical precipitate temperature was determined to be 173.25°F (see the Response to 3.o.2.7.ii), chemical debris head loss is applied for temperatures at or above 180°F.

9. *Provide a summary of methodology, assumptions, bases for the assumptions, and results for the clean strainer head loss calculation.*

Response to 3.f.9:

The total clean strainer head loss was calculated by adding the strainer disk head loss to the plenum head loss, as shown in Table 3.f.9-1.

The bounding disk head loss was calculated using the highest disk approach velocity corresponding to the worst non-uniform flow distribution across the strainer at clean conditions. The evaluation also considered operating scenarios with either one or two RHR pumps in service. As a result, this disk head loss bounds all possible pump lineups at the plant and flow distribution of the plant strainer. The disk head loss included head losses experienced by the flow when entering the gap between two adjacent disks, through the wire cloth and perforated plate, merging inside the disk, traveling along the length of the disk, and exiting the disk. These head loss components were conservatively modeled as pipe fittings using loss coefficients from widely-accepted industrial handbooks (e.g., Crane Technical Paper No. 410 and the Handbook of Hydraulic Resistances by Idelchik). The bounding strainer disk head loss was conservatively applied to all cases when calculating total clean strainer head loss.

The plenum head loss is due to the hydraulic losses associated with flow through the front and rear plenums and out of the plenums to the RHR suction inlet in both the east and the west directions. The plenum head loss was calculated by combining head losses experienced by flow along the longest flow path between a strainer disk and strainer exit, accounting for head losses of various constrictions, for example, the floating sleeves between front plenums, the narrowing between certain rear plenums, the vortex breakers inside the square elbows, the vortex suppressors inside the downcomer pipes, and flow merging inside RHR suction boxes. Similarly, these head loss components were modeled as pipe fittings using loss coefficients from widely-accepted sources.

The evaluation of plenum head loss conservatively assumed that the flow distribution across the strainer is uniform and all strainer disks have the same approach velocity. This assumption is conservative because the flow distribution will be biased toward the disks closer to the strainer exit(s) for the in-service RHR pump(s). Assuming a uniform distribution forces more flow to the disks further away from the strainer exit(s), resulting in higher overall head loss. Note that debris accumulation does promote development of uniform flow distribution across the strainer. However, it would require a substantial debris coverage and head loss to achieve a perfectly uniform flow distribution as assumed above.

Table 3.f.9-1 summarizes the disk head loss, plenum head losses and CSHL for two different cases. As shown in the table, the plenum head loss for the single-pump operation case is higher than the two-pump case, although the strainer flow rate for the single-pump operation case is lower. This is caused by the conservative assumption of uniform flow distribution across the strainer. Note that for the single-pump case, the assumption forces flow to travel the full length of the strainer before reaching the strainer exit. For the two-pump case, two parallel flow paths exist through the strainer and each involves approximately half of the strainer surface area supplying flow to one pump. As a result, flow only travels through approximately half length of the strainer, resulting in a lower plenum head loss than the single-pump case.

Table 3.f.9-1: Calculated Clean Strainer Head Loss

	Strainer Flow Rate (gpm)	Disk Head Loss (ft)	Plenum Head Loss (ft)	CSHL (ft)
Two pump operation	7,769	0.162	0.751	0.913
Worst single pump operation	4,921	0.162	1.564	1.726

The CSHL was evaluated at a few different strainer flow rates for a sump temperature of 100°F. When using the CSHL to calculate total strainer head loss, no temperature adjustment was applied. Applying this CSHL value to temperatures above 100°F is conservative because the head loss will decrease when corrected to a higher temperature. It is also reasonable to apply this CSHL to lower temperatures (down to 60°F) because the measured CSHL on the test strainer varied little with temperature due to the turbulent nature of the flow inside the strainer.

10. *Provide a summary of methodology, assumptions, bases for the assumptions, and results for the debris head loss analysis.*

Response to 3.f.10:

The total strainer head loss was calculated by combining the calculated plant strainer CSHL (see the Response to 3.f.9) and the measured debris bed head losses (see the Response to 3.f.4) scaled to plant conditions (e.g., temperature and strainer flow rate). The methodology for scaling measured debris head losses from testing conditions to plant conditions is detailed in this section. Note that the Full Debris Load test resulted in higher debris head losses than the Thin-Bed test. Therefore, the test results of the Full Debris Load test, as bold-faced in Table 3.f.4-5, were used to determine the total strainer head loss. At the end of this response, the total strainer head losses calculated for selected plant conditions are presented.

Debris head losses at various sump pool temperatures and plant strainer flow rates are of interest. However, testing was conducted at a few specific temperatures and equivalent plant flow rates. To scale the measured debris head losses to plant conditions, the flow regime (i.e., turbulent vs. laminar) through the debris bed was first characterized using the flow sweep data recorded during the Full Debris Load test.

For conventional debris head loss, the flow sweep data taken after adding the full conventional debris load is plotted in the figure below and was curve fit to a quadratic function of test flow rate.

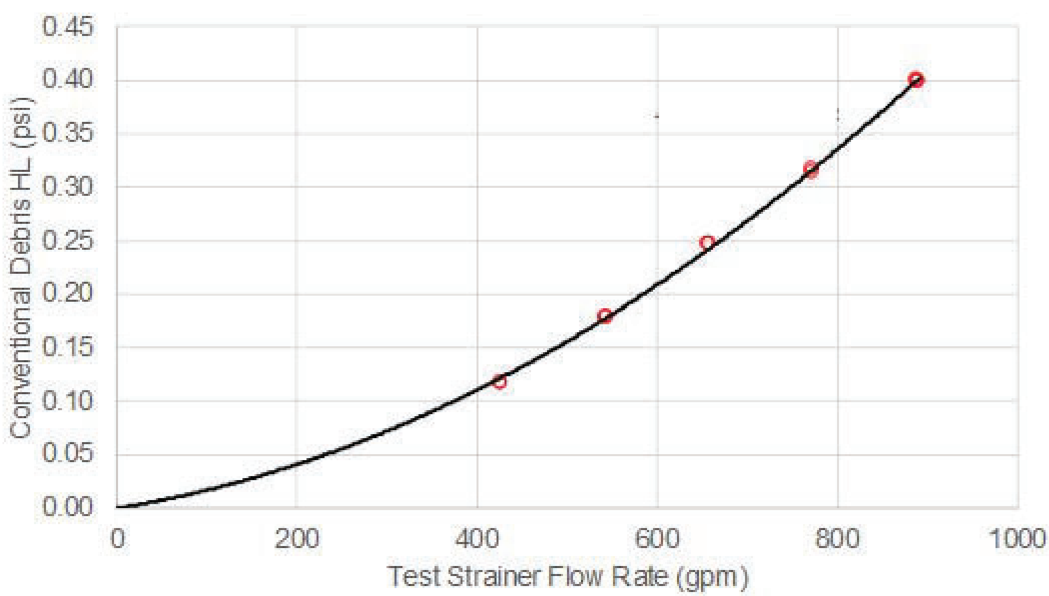

Figure 3.f.10-1: Conventional Debris Head Loss Flow Sweep Curve Fit

Using the curve-fit of the flow sweep data, the laminar and turbulent fractions for the flow through the conventional debris bed were calculated at the target test flow rate. These laminar and turbulent fractions were then used to scale the maximum conventional debris head loss from testing (0.437 psi at 8,029 gpm and 120.3°F, see Table 3.f.4-5) to plant conditions.

The scaling was done using the following equation which relates the head losses through a debris bed (h_L) at two different flow rates and temperatures by a weighted average for the impact of flow (Q), and water density (ρ) and viscosity (μ). The laminar and turbulent fractions (L_{Frac} and T_{Frac}) discussed above were used as weighting factors. In the equation, the variables with the subscript “1” represent testing conditions while those with subscript “2” are for plant conditions of interest. This equation was derived from Equation 6-4 in NUREG/CR-6224 (Reference 22), which showed that head loss through a debris bed can be correlated to flow rate by a quadratic function.

$$h_{L,2} = \left[L_{Frac} \frac{\mu_2}{\mu_1} \frac{Q_2}{Q_1} + T_{Frac} \frac{\rho_2}{\rho_1} \left(\frac{Q_2}{Q_1} \right)^2 \right] h_{L,1}$$

The same methodology was used to scale the maximum chemical debris head loss from testing (0.550 psi at 8,023 gpm and 120.9°F, see Table 3.f.4-5) to plant conditions. Note that the flow sweep data taken after adding the full conventional and chemical debris loads was used.

The scaled debris head losses were then combined with the calculated CSHL to determine the total strainer head losses. Table 3.f.10-1 summarizes the total strainer head loss values at different pool temperatures and strainer flow rates. The maximum total strainer head loss is well bounded by the strainer crush pressure of 4.5 psi (over 10 ft-H_2O), as shown in the Response to 3.k.1.

Table 3.f.10-1: DCPP Maximum Head Loss

Temperature (°F)	Strainer Flow Rate (gpm)	Debris Head Loss (ft-H_2O)	CSHL (ft-H_2O)	Total Head Loss (ft-H_2O)
60	7,769	1.410	0.913	2.32
	4,921	0.658	1.726	2.38
212	7,769	0.823	0.913	1.74
	4,921	0.366	1.726	2.09

11. *State whether the sump is partially submerged or vented (i.e., lacks a complete water seal over its entire surface) for any accident scenarios and describe what failure criteria in addition to loss of net positive suction head (NPSH) margin were applied to address potential inability to pass the required flow through the strainer.*

Response to 3.f.11:

For breaks of 6 inches and smaller, the strainer is partially submerged at the start of sump recirculation (see the Response to 3.f.2). In addition to the NPSH margin acceptance criterion, the head loss effects were evaluated using the acceptance criterion of RG 1.82, which requires the strainer head loss to be less than half the strainer submerged depth.

Using the minimum water level for breaks of 6 inches and smaller, half of the strainer submerged depth was determined to be 1.01 ft for the front strainer disks and 1.79 ft for the rear disks. This is conservative because the pool water level is expected to continue rising until switchover is complete. Since the strainer is free of debris at the start of recirculation, the flow distribution across the strainer is not uniform with disks closer to the in-service pump suctions experiencing higher approach velocities (see the Response to 3.f.9). This non-uniform flow condition was analyzed by balancing the pressure drops of various flow paths between different strainer disks and strainer exits. The analysis resulted in a maximum strainer head loss of 0.758 ft. Since the head loss is less than half of the minimum strainer submerged depth, there will be adequate flow passing through the strainer when it is partially submerged at the start of recirculation.

12. *State whether near-field settling was credited for the head-loss testing, and if so, provide a description of the scaling analysis used to justify near-field credit.*

Response to 3.f.12:

No near-field settling was credited for head loss testing. Sufficient turbulence was provided in the test tank to allow the introduced debris to stay suspended in the water column and transport to the test strainer.

13. *State whether temperature/viscosity was used to scale the results of the head loss test to actual plant conditions. If scaling was used, provide the basis for concluding that boreholes or other differential-pressure induced effects did not affect the morphology of the test debris bed.*

Response to 3.f.13:

As shown in the Response to 3.g.10, the measured debris head losses were scaled for temperature and flow rate from test conditions to plant conditions. The scaling was done using flow regime information derived from DCPP-specific flow sweep data collected during the latest head loss testing, instead of assumed laminar and turbulent fractions. Therefore, any boreholes and other differential-pressure induced effects on bed morphology were captured and properly accounted for when scaling the head loss.

14. *State whether containment accident pressure was credited in evaluating whether flashing would occur across the strainer surface, and if so, summarize the methodology used to determine the available containment pressure.*

Response to 3.f.14:

Flashing Analysis

To analyze the potential for flashing, the pressure downstream of the strainer was conservatively calculated using a combination of conservative inputs that will not occur simultaneously. The calculated pressure was then compared with the water vapor pressure.

The pressure downstream of the strainer was calculated by adding the strainer submergence to and subtracting the strainer head loss from the containment pressure. The minimum strainer submergence was evaluated from the top of the strainer to the minimum sump pool water level at the start of recirculation. As shown in the Response to 3.g.1, the minimum strainer submergence is 0.03 ft for breaks greater than 6 inches. The strainer submergence for the smaller breaks was not considered since the debris quantities, strainer head losses and post-accident containment conditions for the smaller breaks are less limiting than the larger breaks. The evaluation used the total strainer head loss of 2.38 ft at the lower end of sump temperature (60°F) and maximum strainer flow rate (7,769 gpm).

$$\begin{aligned} P_{Strainer} &= P_{Containment} + H_{Submergence} - h_L = P_{Containment} + 0.03\ \text{ft} - 2.38\ \text{ft} \\ &= P_{Containment} - 2.35\ \text{ft} = P_{Containment} - 1.02\ \text{psi} \end{aligned}$$

As shown above, the pressure downstream of the strainer is lower than the containment pressure ($P_{Containment}$) by 1.02 psi at the most. Since the containment pressure was assumed to be equal to water vapor pressure, an accident pressure of 1.02 psi was credited such that the pressure downstream of the strainer would stay above water vapor pressure to prevent flashing from happening.

Note that even the air partial pressure prior to the accident is much greater than 1.02 psi accident pressure credited. The minimum TS allowable containment pressure during normal operation is –1 psig (or 13.7 psia). The maximum normal operating containment temperature is 120°F and the corresponding water vapor pressure is 1.69 psia. Assuming a 100% relative humidity, the minimum air partial pressure prior to the accident is therefore 12.0 psi (13.7 – 1.69 psi). Since this pre-accident air partial pressure is higher than the 1.02 psi required, it was concluded that flashing will not occur downstream of the strainer during the post-accident recirculation phase.

There are several conservatisms in the above flashing analysis:

- The minimum strainer submergence at the start of recirculation was used. Any increase in sump pool level over time was conservatively neglected.
- The maximum strainer head loss, which includes the clean strainer, conventional debris and chemical debris head loss, was used. As shown in the Response to 3.f.10, chemical debris would not form until the pool temperature drops to below 180°F.
- The most limiting pre-accident operating containment conditions were used to minimize the air partial pressure: highest normal operating containment temperature and minimum normal operating containment pressure.
- The increase in air partial pressure due to heat-up of the containment atmosphere following an accident was not credited.

Degasification Analysis

No containment accident pressure was credited for degasification evaluation. The void fraction of the flow through the strainer due to degasification was determined based on changes in solubilities of oxygen and nitrogen between upstream and downstream of the strainer. The evaluation was performed using a combination of conservative inputs that do not occur simultaneously.

Solubilities of oxygen and nitrogen in water were shown to vary linearly with its partial pressure for a given temperature. Since water temperature stays essentially constant as flow travels through the strainer, the rate of change in solubility of oxygen and nitrogen over pressure was estimated from the slopes of the solubility vs. partial pressure curves. For the expected range of post-LOCA sump temperatures (≤ 261°F), the curve with the largest slope (therefore the greatest change in solubility) was used to estimate the rate of change in solubility for both oxygen and nitrogen (i.e., solubility reduction per unit partial pressure drop).

The rate of change in solubility was then multiplied by the partial pressure drop for oxygen and nitrogen from the pool free surface to inside of the strainer to determine the maximum amount of oxygen and nitrogen that could come out of solution as one gram of water travels through the strainer. The overall pressure drop through the sump strainer and debris bed was calculated by subtracting the strainer submergence from the strainer head loss. The strainer submergence was conservatively calculated at the top of the strainer disks. Since the front and rear strainer sections are at different elevations, the smaller submergence of the rear disks was used for conservatism. For added conservatism, the analysis used the higher strainer head loss at 60°F. The partial pressure drop of oxygen and nitrogen was calculated from the overall pressure drop using the air composition (21% of oxygen and 79% of nitrogen).

The oxygen and nitrogen bubbles formed at the strainer were assumed to stay intact but get compressed by the increasing pressure as the bubbles travel with the flow towards the pump suction at a lower elevation. This assumption conservatively neglected redissolution of the bubbles in water during this process. The volume of bubbles at pump suction was evaluated using the Ideal Gas Law for an isothermal process since little change in temperature is expected as flow travels from the strainer to the pump suction. For conservatism, the ratio between the pressure immediately downstream of the strainer and the pressure at pump suction was maximized.

The void fraction at the pump suction was calculated by dividing the total volume of oxygen and nitrogen bubbles at pump suction formed due to degasification by the volume of one gram of water. To maximize the void fraction, the volume of water is conservatively calculated using its maximum density at 40°F. The resulting void fraction is 0.17% at the pump suction. This value is lower than the 2% limit in Attachment 4 of NEI 09-10 (Reference 24), which states that, for pumps operating at a flow rate within 40% - 120% of their best efficiency point (BEP) flow rate, the void fraction at the pump suction shall be lower than 2% to prevent mechanical damage and significant impact on the pump head.

3.g. Net Positive Suction Head

The objective of the NPSH section is to calculate the NPSH margin for the ECCS and CSS pumps that would exist during a loss-of-coolant accident (LOCA) considering a spectrum of break sizes.

1. *Provide applicable pump flow rates, the total recirculation sump flow rate, sump temperature(s), and minimum containment water level.*

Response to 3.g.1:

Pump/Strainer Flow Rates

The following pump and total recirculation sump (or strainer) flow rates, determined from hydraulic models of the post-LOCA recirculation operations, were used as basis for the GSI-191 testing and analyses.

Table 3.g.1-1: Summary of Strainer Flow Rates for GSI-191 Analysis

	RHR Pump #1 (gpm)	RHR Pump #2 (gpm)	Strainer Flow Rate (gpm)
Both RHR Pumps in Operation	3911.9	3857.1	7769
One RHR Pump in Operation during Cold Leg Recirculation	4921	N/A	4921
One RHR Pump in Operation during Hot Leg Recirculation	4900	N/A	4900

When both RHR pumps are operating with CS, a strainer flow rate of 7769 gpm was conservatively used (see Table 3.g.1-1). This represents a momentary strainer flow rate and is much higher than the maximum flow rate of 4,427 gpm through the strainer after the RHR pump flow to the cold legs is throttled per the emergency operating procedure.

During cold leg recirculation with one RHR pump in operation, the maximum flow rate through the strainer is 4,921 gpm. This flow rate occurs when one RHR pump fails after both pumps have been switched to the recirculation mode. Using this flow rate is conservative because it represents a momentary flow rate before the operator action to throttle down the RHR pump flow.

During hot leg recirculation with one RHR pump in operation, the maximum flow rate through the strainer is 4,900 gpm.

Sump Temperatures

Higher pool temperatures are more conservative for chemical effects evaluations. A sump temperature profile was therefore derived to bound the maximum sump temperature profiles from the latest containment analysis. With this profile, the maximum sump water temperature during recirculation is 261°F (see the Response to 3.o.2.3). As justified in the Response to 3.g.2, the pump NPSH margin analysis used conservative strainer head losses at assumed sump temperatures with no containment accident pressure credited.

Minimum Containment Water Level

DCPP performed minimum containment water level analysis for various break sizes: 1.5, 2, 3, 4, 6 and greater than 6 inches. For breaks larger than 6 inches, the minimum sump pool water level is at Elevation 93.7 ft at the start of recirculation when the first RHR pump switchover is initiated. This results in a minimum strainer submergence of 0.26 ft for the front strainer disks and 0.03 ft for the rear strainer disks. The water level increases to its final elevation of at least 94.97 ft when the switchover to recirculation is complete with all CS pumps no longer taking suction from the RWST and the usable water inventory has been transported into containment. This water level corresponds to a minimum strainer submergence of 1.53 ft for the front strainer disks and 1.30 ft for the rear strainer disks.

For breaks of 6 inches and smaller, the minimum sump pool water level corresponds to an elevation of 93.17 ft at the start the recirculation. This water level leaves the top 0.27 ft of the front disks and 0.5 ft of the rear disks unsubmerged.

2. *Describe the assumptions used in the calculations for the above parameters and the sources/bases of the assumptions.*

Response to 3.g.2:

Pump/Strainer Flow Rates

The following assumptions were used to maximize the RHR pump flow rates, which are conservative for the NPSH margin evaluation.

1. The analysis considered equipment lineups of both the cold leg and hot leg recirculation phases. The maximum RHR pump flow rate resulted from a cold leg recirculation case. For this case, to maximize the RHR pump flow rate, a single RHR pump failure was assumed after both RHR pumps have been aligned, resulting in one operating RHR pump supplying flow to 2 centrifugal charging pumps (CCPs), 2 safety injection pumps (SIPs) and CS headers. As noted in the Response to 3.g.1, the maximum flow rate in this configuration is only a momentary condition until the operator manually throttles the RHR flow rates.

2. To minimize the RHR system resistance, the throttling valve of the RHR system was assumed at its failed open position with a larger C_v.

3. The sump pool water level used in the hydraulic model (96.4 ft) that determined the RHR pump flow rates was higher than the actual minimum water levels shown in the Response to 3.g.1. This higher pool water level resulted in conservatively higher pump flow rates.

Sump Temperatures

As stated in the Response to 3.g.1, the maximum sump temperature during recirculation is 261°F. This temperature did not impact pump NPSH evaluation because the DCPP analysis assumed the containment pressure to be always equal to water vapor pressure, without crediting any accident containment pressure.

As shown in the Response to 3.g.16, DCPP NPSH margin analysis was performed for the two most limiting conditions. The first condition was at the start of recirculation switchover (i.e., when the first RHR pump switchover to sump recirculation is initiated) when the sump pool level is the lowest. For this case, the total strainer head loss at a sump temperature of 212°F was used. This is conservative because this head loss includes contribution from the largest conventional debris load while, in reality, the strainer is free of debris at the start of recirculation switchover.

The RHR pump NPSH margin was also evaluated at a sump temperature of 60°F when the strainer head loss is the highest. For this evaluation, the total strainer head loss at 60°F (see the Response to 3.f.10) was used, along with the minimum sump pool level when the switchover to recirculation is complete. Note that, even at this low sump temperature, the containment pressure was assumed to be equal to water vapor pressure (0.256 psia at 60°F).

Minimum Containment Water Level

The significant assumptions used in calculating the minimum water volume are listed as follows:

1. The contribution to the sump water volume due to pre-LOCA water inside the reactor vessel spilling out of the break was credited for breaks greater than 6 in only. This is reasonable because LBLOCAs have blowdown rates that far exceed the ECCS injection rate and result in a large fraction of the RCS water volume entering the containment sump.

2. The evaluation only credited accumulator injection when RCS pressure drops below the accumulator cover gas pressure up to the time of recirculation switchover.

3. The mass of water vapor in the containment atmosphere was maximized as the initial mass of air in the containment is minimized. This occurs at the maximum containment temperature allowed by the TS, 120°F, the minimum expected pressure, 1 atmosphere, and 100% relative humidity.

4. When the CSS is actuated, 487.5 ft^3 of water was assumed to be needed to fill the empty CS headers and piping. This assumed value bounds the calculated volumes.

5. Credit was taken for the additional spill volume out of the break (minimum ECCS flow rate) and CS (if actuated) during the time after the RHR pumps are tripped by the RWST low-level alarm until the earliest time they could be restarted to begin ECCS recirculation.

6. When each of the two RHR pumps restart in the recirculation mode, the RCS pressure was assumed to remain above the RHR pump shutoff head for breaks up to 6 inches. This is conservative for water level evaluation because it does not credit any RHR flow contribution to the sump after the RWST low level has been reached.

7. All of the net contributions and losses of water to the sump were initially calculated based on the nominal RWST conditions of 100°F and 14.7 psia. A temperature correction factor was used to account for the thermal expansion of the RWST water as it equilibrates to the containment sump conditions. The sump water condition was assumed to be at a temperature of 200°F and the particular post-LOCA containment pressure for each break case. Assuming a more realistic maximum RWST temperature of 90°F and a sump temperature of 220°F could increase the net sump level by approximately 0.5 inches.

8. The water in transit on the containment floor was assumed to be 250 ft^3 or approximately 1,800 gallons for each case. This is considered reasonable based on a typical small break blowdown rate (at the time of switchover) of 500 to 1,000 gpm and a corresponding estimated transport time of 2 minutes. A two-minute transport time is conservative based on the minimum expected liquid flow velocities of 0.5 - 1 ft/s, along with an average transport distance to the recirculation sump of 60 - 120 ft.

9. For breaks of 6 inch and smaller, no net RCS spill-out was credited (i.e., the injection rate is equivalent to the spill rate). For these breaks, the post-LOCA RCS volume was assumed equal to the normal full power liquid volume of 11,273.1 ft^3. This is reasonable because the ECCS injection rate usually exceeds the blowdown rates for these smaller breaks, allowing more time for the operators to initiate recovery steps and restore RCS level.

10. The water level analysis assumed the operator will maintain the RCS at a subcooled condition when possible (at least 20°F subcooling). This assumption is conservative because it results in a greater RCS shrinkage. In the analysis, a 30°F subcooling was assumed.

11. The contribution from the spray additive tank (SAT) was evaluated by crediting 90% of the nominal eductor flow of 35 gpm from CS actuation to RHR pump restart.

12. The accumulator water temperature was assumed to be 100°F. This assumption was necessary to convert the accumulator inventory from volume to mass. The normal operating temperatures in the general open area inside containment are between 50°F and 120°F. The assumed temperature for the accumulators is reasonable because the annulus area around the accumulators at the 91 ft elevation is cooler than the general open areas at the higher elevations.

13. Accumulator pressure was assumed to be 14.7 psia. The maximum nitrogen cover pressure for the accumulators is 664 psig. The difference in total accumulator injected volume between water at 100°F and 664 psig versus water at 100°F and 14.7 psia is approximately 50 gallons, which is a negligible amount. Therefore, it is reasonable to use an accumulator pressure of 14.7 psia.

3. *Provide the basis for the required NPSH values, e.g., three percent head drop or other criterion.*

Response to 3.g.3:

The pump vendor curves showed NPSH required (NPSHr) values for pump flow rates up to approximately 4750 gpm. For higher flow rate, the NPSHr value was derived based on the design condition from the vendor curve (NPSHr of 16 ft at 4000 gpm) assuming that NPSHr varies with the square of flow rate ratio. The RHR pump NPSH margin was evaluated at a conservatively high pump flow rate of 4921 gpm (see the Response to 3.g.16). The corresponding NPSHr was determined to be 24.3 ft. Note that the result was rounded up for conservatism.

$$\text{NPSHr} = \left(\frac{4921\text{ gpm}}{4000\text{ gpm}}\right)^2 \times 16\text{ ft} = 24.3\text{ ft}$$

The pump curves were obtained by the pump manufacturer through testing in accordance with the Hydraulic Institute guidelines. The 3% head drop criterion was used in pump testing for the NPSHr curve.

4. *Describe how friction and other flow losses are accounted for.*

Response to 3.g.4:

The head loss of the suction piping between the strainer exit and the pump suction was accounted for by modeling the piping and components in a hydraulic model using the Fathom software. The piping frictional loss was calculated using the standard Darcy formula with the friction factor determined using the Darcy-Weisbach method. The flow losses for the components (e.g., valves, elbows, reducers, and tee junctions) on the pump suction piping were calculated using the loss coefficients from standard industry handbooks in the modeling software (e.g., Crane Technical Paper No. 410 and the Handbook of Hydraulic Resistances by Idelchik). The total strainer head loss was separately calculated by combining the CSHL and debris bed head losses (see the Response to 3.f.10).

5. *Describe the system response scenarios for LBLOCA and SBLOCAs.*

Response to 3.g.5:

The DCPP engineered safety feature systems include two trains of ECCS pumps and two trains of CS pumps. Each ECCS train consists of one high-pressure injection pump (CCP), one intermediate-pressure injection pump (SIP), and one low-pressure injection pump (an RHR pump). The SIPs, RHR pumps, and the CS pumps are normally aligned to the RWST. The CCPs are aligned to the RWST on an SI signal. System response is determined by break size and resulting RCS and containment pressure characteristics. The discussion below is applicable for both LBLOCAs and SBLOCAs, unless noted otherwise.

During the injection phase, the ECCS pumps automatically start upon receipt of an SI signal, taking suction from the RWST. Due to the relatively low shutoff head of the RHR pumps, RHR flow to the RCS will not begin until the RCS depressurizes to approximately 170 psig. The CS pumps are actuated to take suction from the RWST by coincidence of an SI signal and a “high-high” containment pressure signal. Note that, for an SBLOCA, the CS pumps may not be actuated.

An automatic RHR pump trip is triggered by the RWST low-level alarm. Transfer to ECCS recirculation is then accomplished by manually opening the containment recirculation sump suction valves of the RHR pumps and closing the RWST suction valves. Both RHR pumps take suction from the common containment recirculation sump. The CCPs and SIPs are then aligned to take suction from the RHR pump discharge (piggyback operation). Because RHR pump discharge pressure is higher than the static pressure from the RWST, CCPs and SIPs are hydraulically isolated from the RWST by their suction check valves. All ECCS pumps discharge into the cold legs of the RCS.

If the CS pumps are actuated during injection phase, they continue taking suction from the RWST while the ECCS pumps are being switched over to recirculation mode. The CS pumps are secured before the RWST level drops to 4%. During the recirculation model, a portion of the RHR flow is supplied to the CS headers but the CS pumps are not operated.

Approximately 7.0 hours after LOCA inception, the operators will manually initiate hot leg recirculation. The ECCS pumps continue taking suction from the containment sump. The RHR and SI pumps discharge into the hot legs of the RCS while the CCPs continue discharging into the cold legs.

6. *Describe the operational status for each ECCS and CSS pump before and after the initiation of recirculation.*

Response to 3.g.6:

Operating sequence of the ECCS and CS pumps have been discussed in the Response to 3.g.5. Brief summaries are presented in this section.

Residual Heat Removal Pumps

In the event of a LOCA, the RHR pumps start automatically on receipt of an SI signal. During the injection phase, the RHR pumps take suction from the RWST and supply flow to the RCS cold legs. The RHR pumps are automatically tripped by the RWST low-level alarm. Afterwards, the RHR pumps take suction from the containment sump, supply flow to the CCPs and SIPs and discharge directly to the cold legs. Approximately 7 hours after LOCA inception, hot leg recirculation is initiated. The RHR pumps continue taking suction from the containment sump and supply flow to the CCPs and SIPs but discharge to the hot legs of the RCS. During the recirculation phase, the RHR pumps also supply water to the CS spray nozzles.

Centrifugal Charging Pumps

In the event of a LOCA, both CCPs start automatically on receipt of an SI signal and take suction directly from the RWST during the injection phase, supplying flow to the RCS cold legs. After switching to the sump recirculation mode, flow to the CCPs is provided by the RHR pump discharge. The CCPs continue supplying flow to the RCS cold legs during both cold leg and hot leg recirculation.

Safety Injection Pumps

In the event of a LOCA, both SIPs start automatically on receipt of an SI signal. During the injection phase, these pumps take suction from the RWST and deliver water to the RCS cold legs. Similar to the CCPs, flow to the SI pumps is supplied from the containment recirculation sump via the RHR pumps during the recirculation phase. The SIPs discharge to the RCS cold legs during cold leg recirculation and to the RCS hot legs during hot leg recirculation.

Containment Spray System Pumps

Following a LOCA, the CS pumps are automatically actuated by coincidence of an SI signal and a “high-high” containment pressure signal to take suction from the RWST and supply flow to the spray nozzles. The CS pumps are secured before the RWST level reaches the low-low level (4%) and are no longer required. As stated above, during the recirculation phase, the RHR pumps supply flow to the spray headers.

7. *Describe the single failure assumptions relevant to pump operation and sump performance.*

   Response to 3.g.7:

   The single failure scenario considered for the sump performance evaluation is the failure of one RHR pump after both pumps are switched to the recirculation model. As mentioned in the Response to 3.g.2, this results in one RHR pump supplying flow to RCS, both CCPs and SIPs, and the CS headers. This scenario is conservative for NPSH evaluation because the hydraulic evaluation showed that the single-pump operation resulted in higher pump flow rates and therefore higher NPSHr values. This higher pump flow rate also increases the head losses of the suction lines between strainer exit and pump inlet, which reduces pump NPSH available. Additionally, as shown in the Response to 3.f.10, the single train case had a slightly higher strainer head loss, which also reduces pump NPSH available.

8. *Describe how the containment sump water level is determined.*

   Response to 3.g.8:

   The methodology described below was used to calculate the minimum containment sump water level:

   1. Potential contribution to the sump pool volume from various water sources inside the containment were accounted for: RWST, RCS, accumulators and SAT.

   2. The quantity of water that is diverted from the containment sump by the following effects was evaluated:

      - Remaining liquid volume inside the RCS
      - Water volume required to fill the RCS to account for the shrinkage of the remaining RCS liquid as it cools from the initial operating conditions to the post-LOCA containment conditions
      - Partial to zero accumulator discharge when the RCS pressure is above 600 psig
      - Water vapor retained in the containment atmosphere
      - Spray water droplets in transit from spray nozzles to pool surface (this was determined to be negligibly small due to the short travel time of the spray droplets (8-10 sec) and the conservatisms in the evaluation of steam holdup in the containment atmosphere)
      - Water holdup on containment surfaces due to steam condensation
      - Water in transit from the break to the sump
      - Water volume required to fill the CS piping
      - RWST sample line leakage
      - RWST level instrument uncertainties

3. Subtracting the water holdups in Bullet 2 above from the water sources of Bullet 1 resulted in the net water volume for the containment recirculation sump. The post-LOCA containment water level was then calculated using a function which correlates flood elevation and free volume within containment.

4. The sump pool volume determined in the previous step was then converted to a pool level using a correlation between containment open volume and elevation.

The calculation determined minimum containment water levels for breaks of various sizes using break size-specific injection volumes and hold-up volumes (see the Response to 3.g.12).

9. *Provide assumptions that are included in the analysis to ensure a minimum (conservative) water level in determining NPSH margin.*

Response to 3.g.9:

The assumptions provided in the Response to 3.g.2 ensure that minimum (conservative) containment water levels are determined. When evaluating the RHR pump NPSH margin, two cases were considered: one at the start of recirculation and the other after the switchover to recirculation is completed with the CS pumps no longer taking suction from the RWST. For either case, the minimum sump water level for the breaks larger than 6 in was used (see the Response to 3.g.1). This is reasonable, because the strainer head losses used in the NPSH evaluation correspond to the bounding debris loads at DCPP (see the Response to 3.f), which result from the largest breaks at the plant. Additionally, the pump flow rates (and therefore pump NPSHr) for the smaller breaks are expected to be lower than those used for the large breaks.

10. *Describe whether and how the following volumes have been accounted for in pool level calculations: empty spray pipe, water droplets, condensation, and holdup on horizontal and vertical surfaces. If any are not accounted for, explain why.*

Response to 3.g.10:

The Response to 3.g.8 lists the hold-up volumes that remove water from the containment pool considered in the minimum water level analysis. These included water filling the initially empty CS piping), holdup due to condensation on containment surfaces, and steam held up in the containment atmosphere. DCPP analyzed the potential holdup due to spray water droplets in transit from the spray nozzles to the pool surface and determined that this holdup is negligibly small due to the short travel time of the spray droplets (8-10 sec) and the conservatisms in the evaluation of steam holdup in the containment atmosphere.

11. *Provide assumptions (and their bases) as to what equipment will displace water resulting in higher pool level.*

Response to 3.g.11:

The water level calculation assumes that some major permanent components will displace water, resulting in a higher pool level. These components include the following:

- Reactor vessel and piping below Elevation 91 ft
- Reactor coolant drain tank and pumps
- Crane wall
- Primary shield wall
- Permanent obstructions in the annulus
- Pressurizer relief tank stands
- RCP and SG pedestals

12. *Provide assumptions (and their bases) as to what water sources provide pool volume and how much volume is from each source.*

Response to 3.g.12:

Table 3.g.12-1 provides the volumes of water sources used to determine the minimum containment water levels for break sizes > 6 inches and ≤ 6 inches. Applicable assumptions (and their bases) are in the Response to 3.g.2.

Table 3.g.12-1: Water Source Volumes

LOCA Size	Source	Credited Volume (gal)	Credited Volume Basis
For Breaks of 6 in and Smaller	RWST	283,388	Injection from TS min RWST level to low-level setpoint plus additional CS flow from RWST during switchover to recirculation
	Accumulators	6,927	Amount of injection up to the time of recirculation switchover
	RCS	2,164	Difference between available RCS liquid volume (including injection) and retained RCS volume
	SAT	2,279	Based upon SAT eductor flow rate and amount of time prior to recirculation switchover
For Breaks Larger than 6 in	RWST	282,701	Injection from TS min RWST level to low-level setpoint plus additional CS flow from RWST during switchover to recirculation
	Accumulators	24,358	Injection of all four accumulators
	RCS	40,482	Difference between available RCS liquid volume (including injection) and retained RCS volume
	SAT	1,209	Based upon SAT eductor flow rate and amount of time prior to recirculation switchover

13. *If credit is taken for containment accident pressure in determining available NPSH, provide description of the calculation of containment accident pressure used in determining the available NPSH.*

Response to 3.g.13:

Containment accident pressure was not credited when determining pump NPSH margin. The containment pressure was assumed to be equal to water vapor pressure.

14. *Provide assumptions made which minimize the containment accident pressure and maximize the sump water temperature.*

Response to 3.g.14:

Containment Pressure

As stated in the Response to 3.g.13, when evaluating pump NPSH margin, the containment pressure was assumed to be equal to the vapor pressure at corresponding sump liquid temperature, without crediting any containment accident pressure.

Sump Temperature

As discussed in the Response to 3.g.2, maximizing sump temperature does not impact the DCPP pump NPSH analysis because the containment pressure was assumed to be always equal to water vapor pressure. The DCPP NPSH analysis was performed for two most limiting conditions to ensure the minimum pump NPSH margin was obtained (see more details in the Responses to 3.g.2 and 3.g.16).

15. *Specify whether the containment accident pressure is set at the vapor pressure corresponding to the sump liquid temperature.*

Response to 3.g.15:

The containment pressure was set equal to the vapor pressure at corresponding sump temperature. See the Response to 3.g.13.

16. *Provide the NPSH margin results for pumps taking suction from the sump in recirculation mode.*

Response to 3.g.16:

RHR pump NPSH margin was calculated for two most limiting conditions using conservative combinations of inputs.

When the first RHR pump switchover is initiated, the RHR pump NPSH margin was determined to be 3.28 ft. As stated in the Response to 3.g.2, the evaluation used the minimum sump pool water level at the start of recirculation and maximum total strainer head loss at 212°F and 4921 gpm. This head loss included contributions from the largest DCPP conventional debris loads.

The RHR NPSH margin was determined to be 4.26 ft at a sump temperature of 60°F when the total strainer head loss is the highest. The analysis for this condition used the minimum sump pool water level at the end of recirculation switchover and the maximum total strainer head loss at 60°F and 4921 gpm. This head loss included contributions from the largest DCPP conventional and chemical debris loads.

For both cases, the pump flow rate of 4921 gpm is conservatively high and represents a momentary flow rate after both RHR pumps have switched to the recirculation mode and one RHR pump failed but before the operator throttles down the RHR pump flow (see the Response to 3.g.1). Additionally, the evaluation assumed containment pressure to be equal to vapor pressure at the corresponding sump liquid temperature for both cases, without crediting any containment accident pressure.

3.h. Coatings Evaluation

The objective of the coatings evaluation section is to determine the plant-specific ZOI and debris characteristics for coatings for use in determining the eventual contribution of coatings to overall head loss at the sump screen.

1. *Provide a summary of type(s) of coating systems used in containment, e.g., Carboline CZ 11 Inorganic Zinc primer, Ameron 90 epoxy finish coat.*

Response to 3.h.1:

Several different qualified coating systems were used at DCPP. The systems that maximize qualified coatings debris loads were selected for each surface type and used in the debris generation analysis, as shown in Table 3.h.1-1. The quantities of qualified coatings debris depend on break size and location, as summarized in the Response to 3.e.5 for the bounding breaks. The characteristic size of qualified coatings debris is discussed in the Response to 3.e.6.

Table 3.h.1-1: Qualified Coatings Systems Used in Debris Generation Analyses

Substrate	Coating Systems
Steel Surfaces	Carbozinc 11
	Carboguard 890N
Concrete Floors	K&L 6129
	K&L 5000
	K&L 5000
Concrete Walls	Carboguard 890N
	Carboguard 890N

The unqualified coatings and coating systems are summarized below. The quantities of unqualified coatings debris are not break-specific and are summarized in the Response to 3.e.5. The characteristic sizes of unqualified coatings debris are shown in the Response to 3.e.6.

- T-50 unqualified coating system including the following:
  - Carboline Phenoline 305F Epoxy Finish Coat
  - Carboline Phenoline 305P Epoxy Prime Coat
  - Triangle H-197 primer
  - Triangle T-50 alkyd coating
  - Mobil 13R50 alkyd primer
- IOZ primer only coatings
- OEM coatings
- Miscellaneous modifications and defective qualified coatings
- High-heat aluminum coatings

2. *Describe and provide bases for assumptions made in post-LOCA paint debris transport analysis.*

   Response to 3.h.2:

   The following assumptions related to coatings were made in the debris transport analysis:

   1. It was assumed that unqualified coatings would enter the recirculation pool in the vicinity of the locations where they were originally applied. This is reasonable as these coatings would fail gradually following the accident.
   2. It was assumed that the unqualified coatings for which the location is unknown (including coating margins) were divided equally between upper containment and lower containment. Further, the portion of those coatings in lower containment was assumed to be located outside the missile barrier. This is conservative because debris located outside the missile barrier does not pass through any debris interceptors along its route to the strainer and would therefore have a higher transport fraction.
   3. It was assumed that fine particulate debris is generally spherical and the settling velocity can be calculated using Stokes' Law. This is reasonable since the debris would settle slowly (within the applicability of Stokes' Law). This assumption was addressed in the San Onofre (Reference 25) and Indian Point (Reference 26) Audit Reports, and was not a significant factor with respect to debris transport since no credit was taken for debris settling using this approach.

3. *Discuss suction strainer head loss testing performed as it relates to both qualified and unqualified coatings. Identify surrogate material and what surrogate material was used to simulate coatings debris.*

   Response to 3.h.3:

   Head loss testing was performed as described in the Response to 3.f.4. Both qualified and unqualified coatings were represented in head loss testing.

   Sil-Co-Sil (silica flour) was used as a surrogate for qualified and unqualified coatings that fail as 10 micron particulate on an equal volume basis. Refer to the Response to 3.f.4 for the properties of Sil-Co-Sil used in head loss testing.

   Acrylic paint chips were used as a surrogate for coatings that fail as chips on an equal volume basis. Refer to the Response to 3.f.4 for the properties of acrylic paint chips used in head loss testing.

   The Response to 3.f.4 has more details about preparation and introduction of coating surrogate materials during testing.

4. *Provide bases for the choice of surrogates.*

Response to 3.h.4:

As discussed in the Response to 3.f.4, Sil-Co-Sil was used as surrogate for coatings particulate debris on an equal volume basis. This is reasonable because the particulate debris impacts debris bed head loss by filling the voids within the debris bed and reducing its porosity. Therefore, matching the volume between the surrogate and actual debris properly accounts for this effect. Additionally, Sil-Co-Sil had a mean size distribution of approximately 10 μm, which is consistent with the characteristic size of the coatings particulate debris (see the Response to 3.h.6).

As discussed in the Response to 3.f.4, acrylic paint chips were used as surrogate for coating chips debris on an equal volume basis. The approach of matching the volume between the surrogate and actual debris is reasonable for the same reason as discussed above. The acrylic paint chips had characteristic sizes ranging from 0.05 to 0.15 inches and are finer than the coating chips debris at the plant (with characteristic sizes of 1/8 x 1/8 inches to ½ x 1 inches and a thickness of 9 mil). This results in conservatively high head loss in testing because finer debris is more likely to fill the voids in the debris bed.

5. *Describe and provide bases for coatings debris generation assumptions. For example, describe how the quantity of paint debris was determined based on ZOI size for qualified and unqualified coatings.*

Response to 3.h.5:

The following assumptions related to coatings were made in the debris generation calculation:

<u>*Qualified Coatings*</u>

1. Qualified coatings were analyzed within a 4.0D ZOI. This ZOI has been previously accepted by the NRC (Reference 27 p. 2).
2. It was assumed that the epoxy ZOI could be used for all qualified coated surfaces at DCPP. The ZOI for IOZ coatings is larger than the ZOI for epoxy coatings; however, since all the IOZ coatings at DCPP have a topcoat of epoxy, the IOZ coatings would logically not fail unless the epoxy fails.
3. Since several coated items were not modeled in CAD (including pipe hangers, non-insulated piping, access platforms, etc.), adding 20% to the steel coatings term for each break was assumed to account for these items. This is conservative based on experience with other PWR plants.
4. The quantity of qualified coatings generated from a Unit 1 reactor cavity break was assumed to be applicable for the Unit 2 break at the same weld location.

This is reasonable since the concrete and structural steel of the containment buildings for the two units are mirror images as depicted in the CAD models.

Unqualified Coatings

1. Unqualified coatings systems using Triangle T-50 were assumed to have a thickness of 3 mils for the primer coat, 3 mils for the intermediate coat (where applicable), and 6 mils for the Phenoline 305F topcoat. Triangle T-50 is used either as an intermediate coat over another primer, or as a prime coat, without an intermediate coat for touch-up work. The assumed thicknesses are consistent with the average specified application thicknesses for these or similar products based on an inspection of the containment coatings logs. Additionally, the assumed total thickness of 12 mils for a three-coat system (3 mils + 3 mils + 6 mils) is generally consistent with the average thickness tested as documented in the unqualified coatings testing.
2. The iodine removal units were coated by the manufacturer with Garlock 510 in a primer-only application. In the absence of specific data, single-coat paint systems were assumed to have a thickness of 6 mils. This is consistent with the thickness assumed for the top-coat of two-coat and three-coat paint systems. The Garlock 510 coating was assumed to fail as 10 micron particulate.
3. It was assumed that the Triangle H-197 zinc-rich epoxy primer would fail as particulate. This is a conservative assumption since this is the most easily transportable size for coatings.
4. The failure characteristics of several unqualified coatings were unknown and were therefore treated as particulate. This is conservative, as coating chips would be spaced out in the debris bed but coating particulate would fill the interstitial gaps in the bed.
5. The location of several items with unqualified coatings (instrument panels and large bore uninsulated piping) was assumed to be in lower containment. This is justified based on composite piping and general arrangement drawings.
6. The thickness of the coatings applied to the architectural and electrical components is assumed to be 2 mils, the same as the coating applied to the mechanical equipment. This is reasonable since most of these coatings are for the mechanical equipment with a known thickness.

The generated quantity of qualified coatings shown in Table 3.h.5-1 and Table 3.h.5-2 are for the respective worst-case insulation breaks (see the Response to 3.b.4 and 3.e.6). All qualified coatings were assumed to fail as particulate.

Table 3.h.5-1: Generated Qualified Coatings Debris Quantities DCPP Unit 1

Weld	WIB-RC-2-1 (SE)	WIB-RC-2-10	WIB-RC-3-7	WIB-RC-1-12
Location	Loop 2 HL @ RPV	Loop 2 Crossover	Loop 3 Crossover	Loop 1 Crossover
Break Size (in)	Nozzle	31	31	31
Epoxy (ft^3)	0.56	3.26	0.65	1.68
IOZ (ft^3)	0.00	0.28	0.40	0.31

Table 3.h.5-2: Generated Qualified Coatings Debris Quantities DCPP Unit 2

Weld	WIB-RC-2-6SE	WIB-RC-2-16 (SE)	WIB-RC-4-7	WIB-RC-1-11
Location	Loop 2 Crossover	Loop 2 CL @ RPV	Loop 4 Crossover	Loop 1 Crossover
Break Size (in)	31	Nozzle	31	31
Epoxy (ft^3)	0.80	0.51	0.65	1.68
IOZ (ft^3)	0.50	0.00	0.40	0.31

The generated quantities of unqualified coatings shown in Table 3.h.5-3 are applicable to all breaks of each unit, unless noted otherwise.

Table 3.h.5-3: Generated Unqualified Coatings Debris Loads

<table>
<tr><th rowspan="2">Coating Type</th><th colspan="2">Volume (ft^3)</th><th rowspan="2">Characteristic Size</th></tr>
<tr><th>Unit 1</th><th>Unit 2</th></tr>
<tr><td rowspan="2">Triangle T-50 Coating Systems and IOZ Primer Only</td><td>28.0</td><td>29.1</td><td>1/8”x1/8” to ½”x1” chips, 9 mil thick</td></tr>
<tr><td>7.4</td><td>0.6</td><td>10 μm particulate</td></tr>
<tr><td>OEM Coatings & Miscellaneous Modifications and Defective Qualified Coatings</td><td>5.7</td><td>6.0</td><td>10 μm particulate</td></tr>
<tr><td>High-Heat Aluminum Coatings</td><td>0.1</td><td>0.1</td><td rowspan="2">10 μm particulate</td></tr>
<tr><td>High-Heat Aluminum Coatings on Reactor Vessel (for reactor cavity breaks only)</td><td>0.4</td><td>0.6</td></tr>
<tr><td>Sub-Total for Chips</td><td>28.0</td><td>29.1</td><td>1/8”x1/8” to ½”x1” chips, 9 mil thick</td></tr>
<tr><td>Sub-Total for Particulate (non-reactor cavity breaks)</td><td>13.2</td><td>6.7</td><td>10 μm particulate</td></tr>
<tr><td>Sub-Total for Particulate (reactor cavity breaks)</td><td>13.6</td><td>7.3</td><td>10 μm particulate</td></tr>
</table>

6. *Describe what debris characteristics were assumed, i.e., chips, particulate, size, distribution and provide bases for the assumptions.*

Response to 3.h.6:

In accordance with the guidance provided in NEI 04-07 Volume 1 (Reference 12 pp. 34, 35) and the associated NRC SE on NEI 04-07 (Reference 13 p. 22), all qualified coating debris was treated as 10-micron particulate, as summarized in Table 3.h.6-1.

Table 3.h.6-1: Characteristics of Qualified Coatings

<table>
<tr><th>Substrate</th><th>Type</th><th>Dry Film Thickness (mils)</th><th>Characteristic Size</th></tr>
<tr><td rowspan="3">Steel Surfaces</td><td>Carbozinc 11</td><td>5</td><td rowspan="10">10 µm particulate</td></tr>
<tr><td>Carboguard 890N</td><td>8</td></tr>
<tr><td>Total</td><td>13</td></tr>
<tr><td rowspan="4">Concrete Floors</td><td>K&L 6129</td><td>2</td></tr>
<tr><td>K&L 5000</td><td>38</td></tr>
<tr><td>K&L 5000</td><td>40</td></tr>
<tr><td>Total</td><td>80</td></tr>
<tr><td rowspan="3">Concrete Walls</td><td>Carboguard 890N</td><td>10</td></tr>
<tr><td>Carboguard 890N</td><td>6</td></tr>
<tr><td>Total</td><td>16</td></tr>
</table>

Table 3.h.6-2 summarizes the characteristic sizes for the unqualified coatings. The failure mechanisms for the Triangle T-50 coatings systems were tested by KTA-Tator, Inc. The testing showed that delamination and blistering are the failure mechanisms (with delamination of 95-100% for much of the Triangle T-50 systems). Based on the test data, the Triangle T-50 coatings could delaminate from the substrate or primer and fail as chips. The Triangle H-197 primer was assumed to fail as particulate. All other unqualified coatings were treated as particulate based on the recommendation in the NRC SE on NEI 04-07 (Reference 13 p. 39).

Table 3.h.6-2: Unqualified Coatings Debris Characteristics

<table>
<tr><th colspan="2">Coating Type</th><th>Characteristic Size</th></tr>
<tr><td rowspan="4">Triangle T-50 Coating Systems</td><td>Triangle H-197 primer</td><td>10 µm particulate</td></tr>
<tr><td>Mobil 13R50 alkyd primer</td><td rowspan="3">1/8”x1/8” to ½”x1” chips, 9 mil thick</td></tr>
<tr><td>Triangle T-50 alkyd coatings</td></tr>
<tr><td>Carboline Phenoline 305F Epoxy finish coat</td></tr>
<tr><td colspan="2">IOZ Primer Only Coatings</td><td>10 µm particulate</td></tr>
<tr><td colspan="2">OEM Coatings & Miscellaneous Modifications & Defective Qualified Coatings</td><td>10 µm particulate</td></tr>
</table>

Coating Type	Characteristic Size
High-Heat Aluminum Coatings	10 µm particulate
High-Heat Aluminum Coatings on RPV	

7. *Describe any ongoing containment coating conditions assessment program.*

Response to 3.h.7:

The current program for controlling the quantity of unqualified/degraded coatings is performed in accordance with two DCPP procedures. The first procedure is the Containment Field Coatings procedure which provides the methods, requirements, and responsibilities for Service Level 1 coatings work inside containment and for items designated for installation inside containment. The second procedure is the Coating Quality Monitoring Program procedure which describes the coating quality monitoring program and its implementation in order to provide assurance of continued acceptable performance of coatings inside containment. This procedure describes the qualifications and training requirements for coating inspectors and applicators. Both procedures refer to the Containment Coating Specification, which incorporates the ANSI N 101.2 as a basis for comparison and selection of coating systems for Service Level 1 coating.

During each refueling outage, a thorough visual inspection is performed by a Level III inspector. These inspections are performed in accordance with recurring task work orders. At the beginning of every outage, this visual inspection is conducted on all accessible coated surfaces of the containment. This should be performed as soon as practical in the beginning of the outage and again prior to Mode 4. Included areas for inspection are components to be inspected internally, like the iodine removal unit housing, containment fan cooler unit (CFCU) fan housing, and CFCU coil housing.

During the inspection, if any degraded conditions are found, they are documented in the corrective action program. The condition is evaluated and a determination is made whether or not the repair work will be performed during the outage in which the condition was found. If the work is not completed during the current outage, then the degradation is documented as unqualified coating, to be repaired at a later date. After each outage the unqualified coatings are tracked in the Containment Coatings Tracking calculations for each unit.

3.i. Debris Source Term

This section is omitted from the submittal because no changes have been made since the previous DCPP GL 2004-02 submittal and there are no outstanding RAIs against this section.

3.j. Screen Modification Package

This section is omitted from the submittal because no changes have been made since the previous DCPP GL 2004-02 submittal and there are no outstanding RAIs against this section.

3.k. Sump Structural Analysis

This section is omitted from the submittal because no changes have been made since the previous DCPP GL 2004-02 submittal and there are no outstanding RAIs against this section.

3.I. Upstream Effects

This section is omitted from the submittal because no changes have been made since the previous DCPP GL 2004-02 submittal and there are no outstanding RAIs against this section.

3.m. Downstream Effects – Components and Systems

The objective of the downstream effects, components and systems section is to evaluate the effect of debris carried downstream of the containment sump screen on the function of the ECCS and CSS in terms of potential wear of components and blockage of flow streams.

Provide the information requested in GL 2004-02 Requested Information Item 2(d)(v) and 2(d)(vi) regarding blockage, plugging, and wear at restrictions and close tolerance locations in the ECCS and CSS downstream of the sump.

> *GL 2004-02 Requested Information Item 2(d)(v)*
> *The basis for concluding that inadequate core or containment cooling would not result due to debris blockage at flow restrictions in the ECCS and CSS flowpaths downstream of the sump screen (e.g., a HPSI throttle valve, pump bearings and seals, fuel assembly inlet debris screen, or containment spray nozzles). The discussion should consider the adequacy of the sump screen's mesh spacing and state the basis for concluding that adverse gaps or breaches are not present on the screen surface.*
>
> *GL 2004-02 Requested Information Item 2(d)(vi)*
> *Verification that the close-tolerance subcomponents in pumps, valves and other ECCS and CSS components are not susceptible to plugging or excessive wear due to extended post-accident operation with debris-laden fluids.*

1. *If NRC-approved methods were used (e.g., WCAP-16406-P-A with accompanying NRC SE), briefly summarize the application of the methods. Indicate where the approved methods were not used or where exceptions were taken, and summarize the evaluation of those areas.*

   Response to 3.m.1:

   DCPP developed a series of calculations to address effects of debris carried downstream of the containment sump strainer on the function of the ECCS and CSS in terms of potential wear of components and blockage of flow streams. Close-tolerance subcomponents in pumps, valves and other ECCS and CSS components were evaluated for potential plugging or excessive wear due to post-accident recirculation with debris-laden fluids. The calculations were developed in accordance with WCAP-16406-P-A, Revision 1 (Reference 28) and the NRC SE on this WCAP. The evaluation did not take any exceptions to NRC-approved methods. The overall approach is summarized below.

   Maximum Debris Ingestion Determination

   The strainer has stainless-steel perforated plates with 3/32-inch diameter holes. A post installation inspection was performed on the replacement strainer to verify that there were no gaps between the joints of any two adjacent surfaces greater than the nominal hole or gap size.

The debris that could transport to and pass through the strainer (therefore reaching the components downstream of the strainer) was first quantified conservatively. For particulate debris with quantities varying with break locations and sizes (e.g., Cal-Sil, qualified epoxy and inorganic zinc coatings), the maximum loads from the worst break were used with additional margins added. For latent debris, the common quantities that were applicable for all breaks were used. For unqualified coatings with quantities varying slightly with break locations, the maximum quantity was used. Additionally, these types of particulate debris were assumed to have high transport fractions (85% for latent particulate, 97% for Cal-Sil and qualified coatings, and 100% for unqualified coatings) and all transportable particulate debris passes through the strainer.

For fibrous debris, the evaluation used the maximum total fiber bypass quantity measured during fiber bypass testing (see the Response to 3.n.1) and scaled to the plant strainer surface area. This measured bypass quantity was based on a test using a transportable fiber debris load that bounded all of the postulated breaks at DCPP. Additionally, as stated in the Response to 3.n.1, the quantity of Temp-Mat fines used for fiber bypass testing is greater than the plant debris load when a 11.7D ZOI is applied for all Temp-Mat insulation, including encapsulated Temp-Mat.

Certain types of debris (e.g., tags/labels, RMI, vapor barrier material, silicone rubber, light bulbs and paint chips) were excluded from the ex-vessel downstream evaluation. This is acceptable because these debris types will not pass through the strainer perforation openings per Section 5.5 of WCAP-16406-P-A (Reference 28).

- The deformable debris types (e.g., vapor barrier, silicone rubber and paint chips) have characteristic sizes of at least 0.125 inches, larger than the nominal diameter of sump strainer perforation opening (3/32 inches, see the Response to 3.j.1) plus 10%.
- The characteristic sizes of the non-deformable debris types (e.g., tags/labels, RMI and light bulbs) are also greater than 0.125 inches, which is larger than the nominal diameter of sump strainer perforation opening (3/32 inches, see the Response to 3.j.1).

Initial Debris Concentrations

Initial debris concentrations, defined as the ratio between the solid mass of debris and the mass of water in the sump pool, were developed based on the assumptions and methodology in Chapter 5 of WCAP-16406-P-A (Reference 28). The evaluation used conservatively large debris loads (as described above) and the minimum sump pool water volume at the start of the recirculation. This approach conservatively neglected the sump pool water level increase as the RHR pumps switch over to recirculation. The total maximum initial debris concentration was determined to be 1,409.3 ppm, with fiber debris contributing 6.4 ppm, and particulate and coating debris contributing 1,402.9 ppm (1,409.3 ppm – 6.4 ppm).

Methodology for Evaluating Component Blockage and Wear

The evaluation of component blockage and wear was based on the methodology in WCAP-16406-P-A (Reference 28). Both trains of the ECCS and CSS were reviewed to ensure that all of the flow paths and components impacted by the debris-laden recirculation fluids were considered using system piping and instrumentation diagrams (P&IDs) and other plant design documents as applicable. ECCS and CSS components addressed in the evaluations included pumps, heat exchangers, orifices, spray nozzles, instrumentation tubing, system piping, and valves required for the post-LOCA recirculation mode of operation. The evaluations included the following steps:

- Identifying all components in the ECCS and CSS flow paths that could be impacted by the debris-laden recirculation fluid.
- Evaluating the potential for plugging of heat exchanger tubes, orifices, spray nozzles, system piping, and valves by comparing the maximum debris size expected to be ingested through the sump strainer to the clearances within the components.
- Evaluating the potential for debris sedimentation inside system piping, heat exchanger tubes, and valves by comparing flow velocities inside these piping and components to the minimum velocity required to avoid sedimentation, as given in WCAP-16406-P-A.
- Evaluating erosive wear for ECCS and CSS valves using the methodology in Section 8.2.2 of WCAP-16406-P-A (Reference 28). The valves were first analyzed using a conservative constant debris concentration model. If this was shown to be overly conservative, the valves were reanalyzed by crediting depletion of large particles.
- Evaluating erosive wear for heat exchangers, orifices and spray nozzles using the wear rate model from Section 7.3 and Appendix F of WCAP-16406-P (Reference 28).
- Evaluating impact on pump hydraulic performance (e.g., pump head and flow rate) and mechanical performance (e.g., vibration) due to exposure to debris-laden recirculation fluids. Both erosive and abrasive wear was considered. The abrasive wear models developed in Appendix F.4 of WCAP-16406-P-A (Reference 28) were applied as appropriate in the evaluations.
- Evaluating wear and leakage of pump disaster bushing after a postulated single passive failure of the primary seal. The abrasive wear model from WCAP-16406-P was refined to account for the differences in pressure drop and debris characterization between DCPP and the tests, from which the WCAP-16406-P wear model was derived.
- Evaluating the potential for debris collection in the instrument sensing lines per the methodology in Section 8.6 of WCAP-16406-P (Reference 28).

2. *Provide a summary and conclusions of downstream evaluations.*

Response to 3.m.2:

The following is the summary of results and conclusions of the downstream effects evaluations:

ECCS/CSS Pumps

The evaluation for pumps addressed the effects of debris ingestion through the sump strainer on three aspects of operability: hydraulic performance, mechanical performance, and mechanical-shaft seal assembly performance. The hydraulic and mechanical performances of the ECCS and CSS pumps were shown not to be adversely affected by the recirculating sump debris for the 30-day mission time of the pumps.

The DCPP RHR pumps, SIPs and CCPs all have carbon/graphite disaster bushings. The wear in the mechanical seal disaster bushings due to exposure to the debris-laden fluids was analyzed. The evaluation estimated the increase in disaster bushing diametrical clearance as a result of debris ingestion, and the resulting maximum leakage increase as a result of enlarged clearances. The analysis showed a negligible increase in diametrical clearance of the disaster bushings, resulting in less than 0.3% increase of the seal leakage rate. An existing procedure was enhanced to address the potential of post-LOCA external recirculation loop leakage, and to provide the process to detect and isolate the leak. In support of this procedure, a new Operations procedure was created to provide the direction necessary to isolate one train of ECCS in the event a leak is detected during post-LOCA recirculation, and an existing annunciator response procedure was revised.

ECCS/CSS Valves

The DCPP analysis showed that all valves that are required for the post-accident recirculation operation passed the acceptance criteria for the blockage evaluation. Also, the flow velocities through all valves were higher than the minimum velocity required to avoid sedimentation. Therefore, debris sedimentation was not an issue.

The valves were also evaluated for erosive wear by the debris-laden recirculation fluids. The screening criteria from WCAP-16406-P-A were applied to the DCPP valves and determined that 12 ECCS throttle valves require detailed erosive wear evaluation. The analysis credited depletion of large particles using the depletion coefficient recommended in Appendix K of WCAP-16406-P-A (Reference 28). The wear rate was calculated each hour for a total of 720 hours. The erosive wear analysis established the minimum valve opening required in order for the increase in valve flow area due to erosive wear to meet the WCAP-16406-P-A acceptance criterion. Site operation ensured these requirements were met in the field.

ECCS/CSS Heat Exchangers, Orifices, Spray Nozzles, and System Piping

Evaluation showed no blockage/plugging issues for the heat exchanger tubes, orifices, CS nozzles and system piping on the ECCS and CSS recirculation flow paths. For all piping, the minimum flow velocity was found to be greater than the minimum velocity required to prevent debris sedimentation.

Heat exchanger tubes, orifices, and spray nozzles were evaluated for the effects of erosive wear and were shown not to be adversely impacted. No credit was taken for depletion of large particles when evaluating erosive wear for the heat exchanger tubes and CS nozzles.

ECCS/CSS Instrumentation Tubing

Instrumentation tubing (or sensing lines) was evaluated for debris settling per Section 8.6.6 of WCAP-16406-P (Reference 28). Note that the fluid in the instrument tubing is stagnant, and the instrument tubing is designed to remain water solid without taking flow from the process stream. This prevents direct introduction of debris laden fluid into the instrument tubing. Settling of the debris is the only process by which the debris could be introduced into the instrument tubing. The analysis showed that the instrument lines for the RHR and SI systems, as well as chemical volume control system (CVCS), are installed at horizontal locations and above the piping centerlines. Additionally, the terminal settling velocities of the debris particles in the process streams are small, compared with the process fluid velocities. Therefore, blockage or wear of ECCS or CSS instrument tubing due to debris laden fluids are not expected.

3. *Provide a summary of design or operational changes made because of downstream evaluations.*

Response to 3.m.3:

There have been no design changes made because of downstream evaluations. As noted in the Response to 3.m.2, there was a revision to existing procedures and the creation of a new procedure to provide instructions for detecting and isolating a post-LOCA external recirculation loop leakage.

3.n. Downstream Effects – Fuel and Vessel

The objective of the downstream effects, fuel and vessel section is to evaluate the effects that debris carried downstream of the containment sump screens and into the reactor vessel has on core cooling.

1. *Show that the in-vessel effects evaluation is consistent with, or bounded by, the industry generic guidance (WCAP-16793-NP), as modified by NRC staff comments on that document. Briefly summarize the application of the methods. Indicate where the WCAP methods were not used or where exceptions were taken, and summarize the evaluation of those areas.*

Response to 3.n.1:

In-vessel downstream effects for DCPP were evaluated per the methodology in WCAP-16793-NP (Reference 7) and the associated NRC SE (Reference 29), WCAP-17788 (Reference 8; 9; 10) and the NRC review guidance on in-vessel effects (Reference 30). The evaluation included the following:

1. Peak cladding temperature (PCT) due to deposition of debris on fuel rods (WCAP-16793-NP).
2. Deposition thickness (DT) due to collection of debris on fuel rods (WCAP-16793-NP).
3. Amount of fiber accumulation at reactor core inlet and inside reactor vessel (WCAP-17788).

These analyses concluded that post-accident long-term core cooling (LTCC) will not be challenged by deposition of fiber, particulate, and chemical debris on the fuel rods; accumulation of fiber debris at the core inlet; or accumulation of fiber debris in the heated region of the core for all postulated LOCAs inside containment.

Provided below is a brief summary of the relevant testing and analyses used to inform the in-vessel effects evaluations, consistent with the WCAP methodologies mentioned above.

<u>DCPP Fiber Bypass Testing</u>

DCPP conducted fiber bypass testing in 2016. The purpose of the testing was to collect time-dependent fiber bypass data of a prototypical DCPP strainer. One test was conducted with testing parameters selected to be representative of the most conservative plant operating conditions (e.g., flow rate and flow split, water chemistry). The test results were used to derive a model that can be used to quantify fiber bypass for the DCPP strainer at plant conditions.

Test Loop Design

The closed test loop for fiber bypass testing included a metal test tank with acrylic windows that housed a test strainer. The test tank used for fiber bypass test is the same as that for head loss testing, as described in the Response to 3.f.4. Test water was circulated by a pump through the test strainer, a fiber filtering system, and various piping components. The piping layout for the test loop is shown in Figure 3.n.1-1. Note that, different from head loss testing, at least one of the two in-line filter housings (with filter bags installed inside) was always online during the bypass test to ensure the debris-laden water downstream of the test strainer traveled through the filter bags before being returned to the test tank.

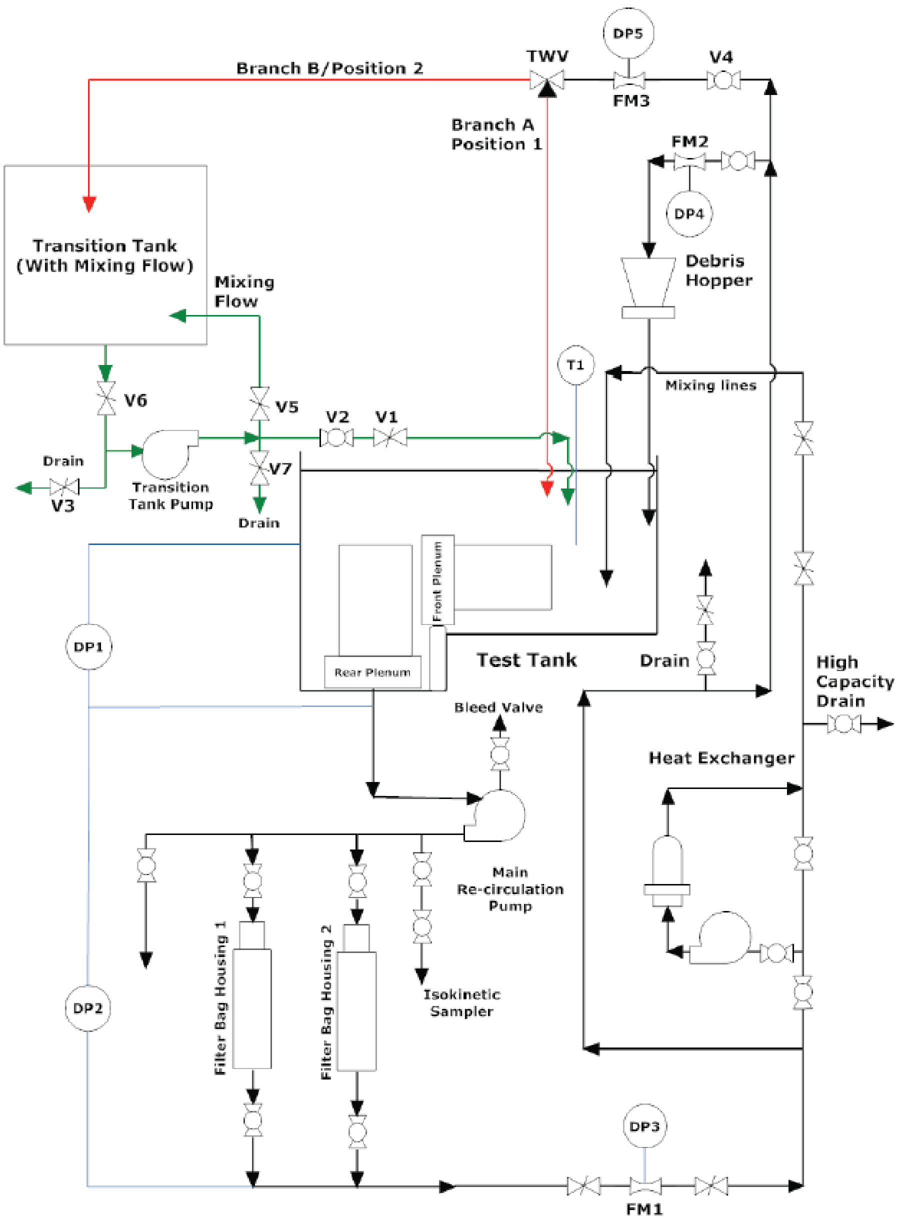

Figure 3.n.1-1: DCPP Bypass Testing Piping and Instrumentation Diagram

Test Strainer

The test strainer used for fiber bypass test is the same as that for head loss testing. Refer to the Response to 3.f.4 for details.

Test Parameters

The fiber bypass test was performed with prototypical water chemistry and strainer approach velocity. The test water used for fiber bypass testing had a boron concentration of 1,776 ppm and a pH of 9.5. Test water was prepared by adding pre-weighed boric acid into deionized water to achieve the prescribed boron concentration. Afterwards, small batches of sodium hydroxide (NaOH) were added to achieve the prescribed pH. During this process, the solution was continuously mixed while the pH was monitored.

To match the test strainer approach velocity to plant conditions, the test flow rate for bypass testing was determined by scaling the maximum plant strainer flow rate of 8,000 gpm with the ratio in surface area between the test strainer (340.2 ft^2) and plant strainer (3,278.7 ft^2). Note that different from head loss testing, the scaling here used the total strainer surface area, instead of the net surface area (3,073.5 ft^2). This approach is reasonable and ensures consistency because, when quantifying fiber bypass for the plant strainer, the larger total strainer surface area was used to maximize fiber bypass. This scaling resulted in a target test flow rate of 830.1 gpm (8000 gpm × 340.2 ft^2/ 3278.7 ft^2) for bypass testing. The actual test flow rate was maintained between -0/+5% of 830.1 gpm. The nominal test temperature was 120°F.

Debris Types and Preparation

For fiber bypass testing, Nukon, Temp-Mat, and Kaowool were used in the fiber bypass test. Similar to head loss testing, all fiber fines were prepared according to the NEI protocol (Reference 6). Refer to the Response to 3.f.4 for details in fiber preparation. Figure 3.n.1-2 shows the prepared fines for all three debris types after pressure washing. After each debris type was separately pressure-washed, the Nukon, Temp-Mat, and Kaowool prepared for each batch were combined in a barrel and stirred to form a homogeneous mixture before introduction.

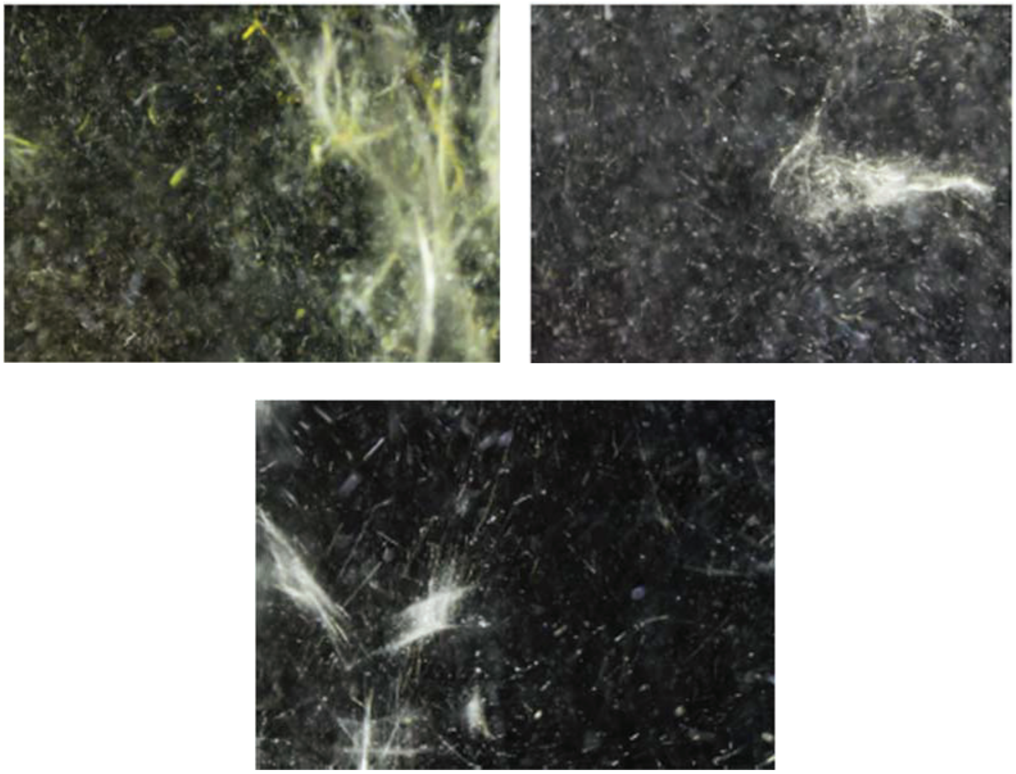

Figure 3.n.1-2: Nukon Fines (left) Kaowool Fines (right), and Temp-Mat Fines (Bottom) Prepared for DCPP Bypass Test

Debris Introduction

Debris was introduced in four separate batches of increasing batch size, as shown in Table 3.n.1-1. All batches consisted only of fiber fines. The theoretical LDFG-equivalent uniform bed thicknesses of batch one through batch four are 0.049, 0.049, 0.086, and 0.102 inches. The first two batches, which contained Nukon, Kaowool, and Temp-Mat, had nearly identical batch size and composition. During testing, 100% of the tested Kaowool fines were added in the first two batches, because Kaowool penetrates more readily than Nukon or Temp-Mat. This was conservative, since Kaowool was introduced at the minimal strainer fiber loading, when bypass is the highest. In the third batch, only Nukon and Temp-Mat were added. Finally, for the last batch, only Temp-Mat was added into the test tank.

Table 3.n.1-1: Fiber Batches for Bypass Testing at Test Scale

Batch No.	Kaowool (g)	Nukon (g)	Temp-Mat (g)
1	185.41	181.40	1148.7
2	185.40	181.41	1148.7
3	0	362.90	2297.5
4	0	0	3137.7

Debris slurry was added to the debris hopper before being transferred to the test tank. During this process, the debris slurry was stirred to maintain a homogeneous mixture in the barrel. Additionally, the debris added to the hopper and transported into the tank was stirred, as necessary to break up any agglomeration of fibers that formed.

For each batch, the debris introduction was timed so that the debris addition rate was controlled to maintain a prototypical debris concentration in the test tank. The sump pool debris concentration at the plant ranges between 0.00031 lbm/ft^3, which is the latent fiber divided by the sump water volume, and 0.00340 lbm/ft^3, which is the maximum fiber load divided by the sump water volume. During testing, the target debris introduction time was varied with batch size in order to maintain the debris concentration in the test tank within the above range.

The fiber debris loads presented in Table 3.n.1-1 are at the test scale. These correspond to total debris loads of 7.9 lbm, 15.4 lbm and 163.9 lbm for Kaowool, Nukon and Temp-Mat fines, respectively at the plant scale. Note that the tested Temp-Mat quantity is greater than the plant debris load when a 11.7D ZOI is applied for all Temp-Mat insulation, including encapsulated Temp-Mat.

Debris Capture

Fiber can pass through the strainer by two different mechanisms: prompt bypass and shedding. Prompt bypass occurs when fiber reaching the strainer travels through the strainer immediately. Shedding occurs when fiber that already accumulated on the strainer migrates through the bed and ultimately travels through the strainer. Both mechanisms were considered during fiber bypass testing.

Fibers that passed through the strainer were collected by in-line filter bags downstream of the test strainer and the pump. All of the flow downstream of the strainer travelled through a set of 5-micron filter bags inside a filter housing before returning to the test tank. The capture efficiency of the filter bags was verified to be above 97%. The filtering system allowed the installation of two sets of filter bags, with each set consisting of five bags, in parallel lines such that one set of filter bags could be left online at all times, even during periods in which filter bag sets were swapped.

Before the test, all of the filter bags required were uniquely marked and dried, and their weights were recorded. The filter bags were placed in an oven for at least an hour before being cooled and weighed inside a humidity-controlled chamber. This process was repeated for each set of bags until two consecutive bag weights (taken at least 30 minutes apart) were within 0.10 g of each other.

A clean filter bag set was placed online before a debris batch was introduced to the test tank and was left online for a minimum of three pool turnovers (PTOs) to capture the prompt fiber bypass. For each batch, at least two additional filter bags were used to capture the fiber bypass due to shedding. For Batches 3 and 4, a third shedding filter bag was used to capture long-term shedding data. Before each debris addition, the test tank and debris hoppers were visually checked to verify that all introduced debris had transported to the strainer. The overall approach allowed the testing to capture time-dependent fiber bypass data, which was used to develop a model for the rate of fiber bypass as a function of time or fiber quantity on the strainer.

After testing, the debris-laden filter bags were rinsed with deionized water to remove residual chemicals before being dried and weighed. The processing of the debris-laden filter bags followed the same procedure as that discussed above for the clean bags. The weight gain of the filter bags was used to quantify fiber bypass.

Test Results

Table 3.n.1-2 summarizes the total amount of fiber added to the test tank and the total amount of bypass fiber measured for each batch. The quantities are given at the test scale. As expected, the bypass fraction decreased as a debris bed forms on the strainer.

Table 3.n.1-2: Summary of Bypass Test Results

Batch	Amount of Fiber Added per Batch (g)	Total Bypass Quantity Measured per Batch (g)
1	1515.5	171.30
2	1515.5	165.29
3	2660.4	215.47
4	3137.7	178.75

Strainer Bypass Model Development

Data gathered from the DCPP fiber bypass test was used to develop a model for quantifying the strainer fiber bypass under plant conditions. The model was developed per the following steps:

- General governing equations were developed to describe both the prompt fiber bypass and shedding through the strainer as a function of time and fiber quantity on the strainer. The equations contain coefficients whose values were determined based on the test results.
- The bypass test results were curve-fit to the governing equations using various optimization techniques to refine the coefficient values.

The derived model was applied to the test conditions (e.g., flow rate, strainer surface area, fiber batching timing and schedule). Figure 3.n.1-3 compares the model results (solid blue line) with the measured bypass quantities (data points). As can be seen in the figure, the model adequately represented the test data.

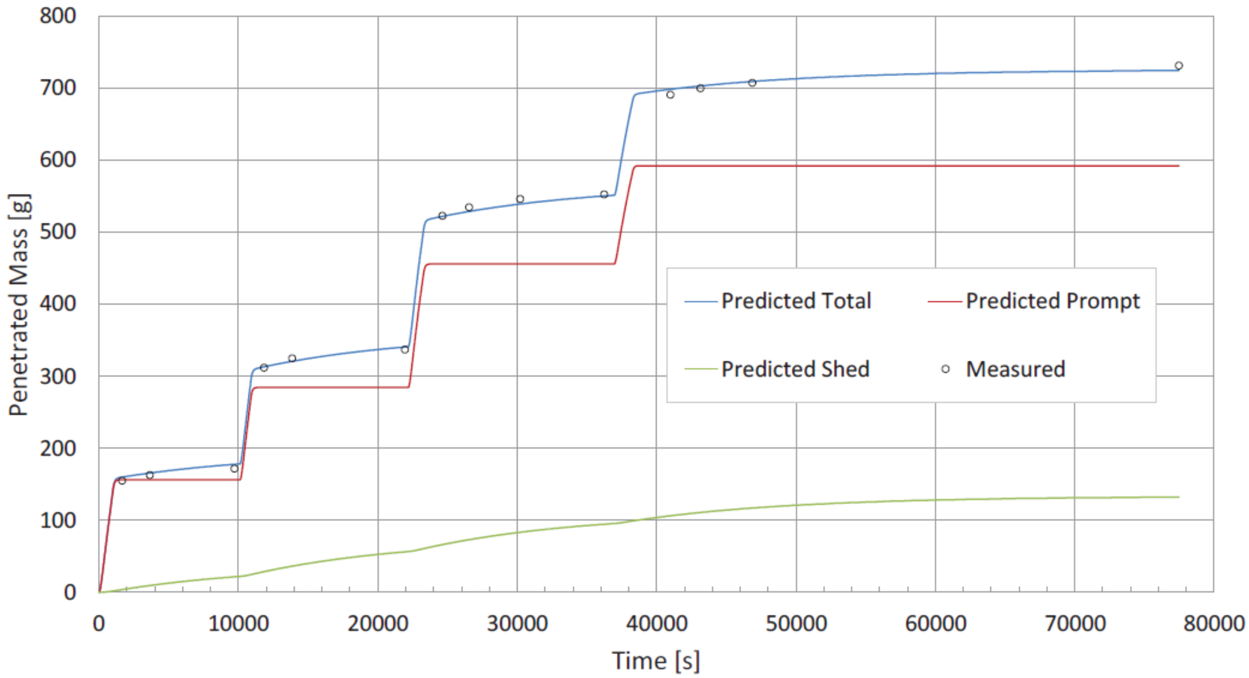

Figure 3.n.1-3: Comparison of Fiber Bypass Model and Test Results

The bypass models can be used to determine the prompt fiber bypass fraction and shedding fraction for a given time and amount of fiber accumulated on the strainer. Coupled with a fiber transport model, a time-dependent evaluation of fiber bypass of the plant strainer can be performed. An example application of the model on the plant strainer is shown below. The fiber debris was assumed to be uniformly distributed in the sump pool at the start of the recirculation phase. For the time-dependent analysis, the recirculation duration was divided into smaller time steps. For each time step, the amount of fiber that arrived at the strainer was first calculated based on the strainer flow rate and fiber concentration in the pool. The fiber bypass rates and quantities were then calculated using the bypass model. The cumulative bypass can be calculated by summing up the results from individual time steps. Figure 3.n.1-4 shows the resulting cumulative fiber bypass quantities over time at plant conditions.

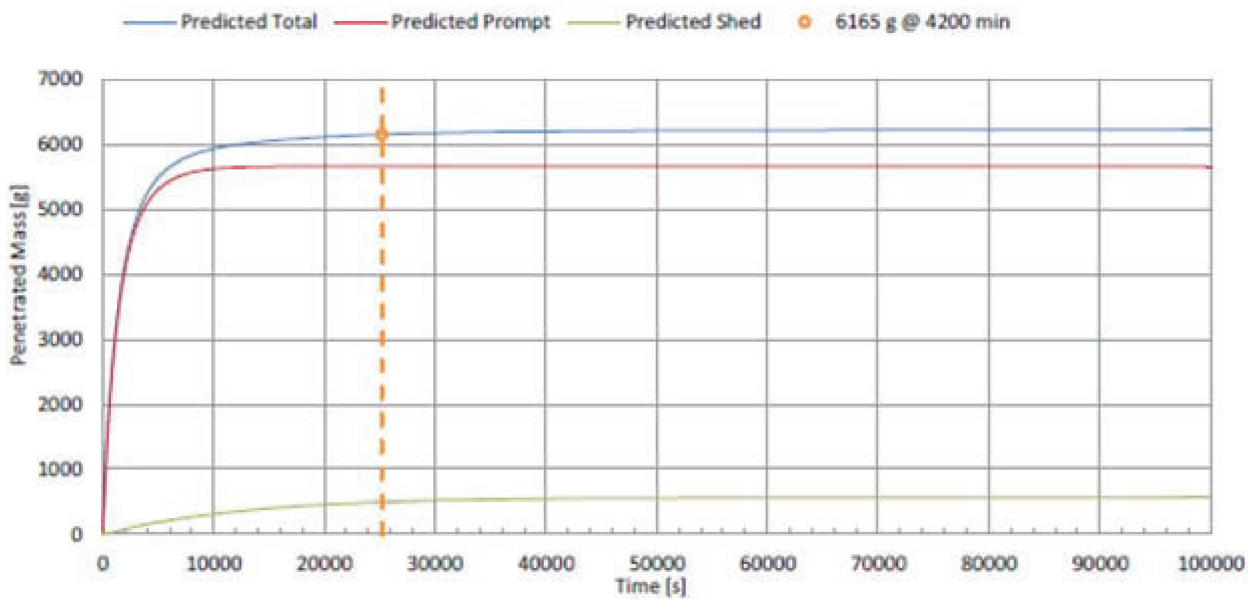

Figure 3.n.1-4: DCPP Bypass Model Applied to Plant Conditions

Figure 3.n.1-5 shows the prompt fiber bypass fraction as a function of fiber quantity on the strainer derived using the fiber bypass model. As expected, the prompt bypass fraction decreases as a fiber debris bed forms on the strainer.

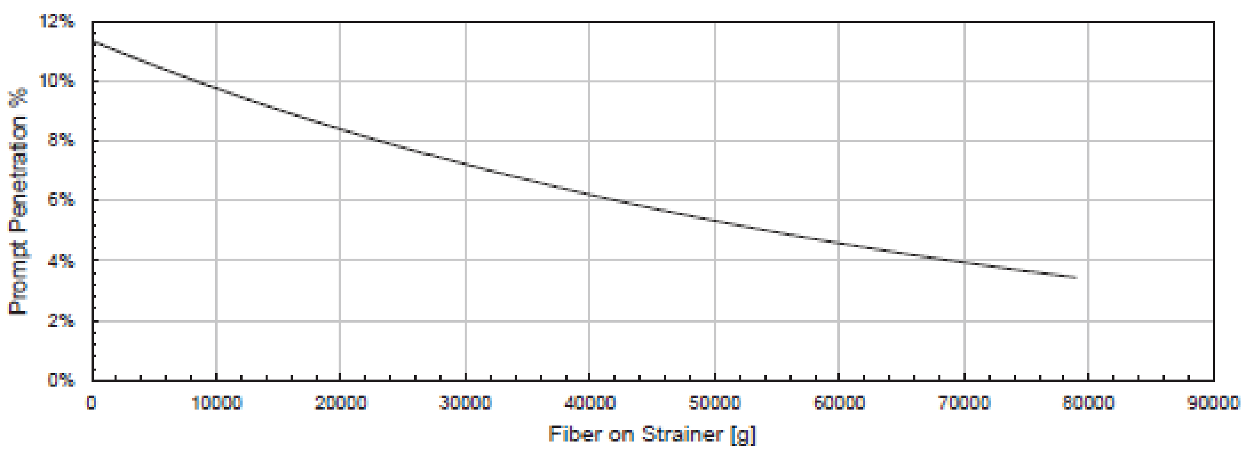

Figure 3.n.1-5: Prompt Bypass Fraction from Bypass Model

Figure 3.n.1-6 shows the shedding rate calculated from the model as a function of time. Note that shedding bypass depends on the fiber quantity on the strainer and time. As shown in the figure, the shedding rate decreases over time for a given amount of fiber on the strainer.

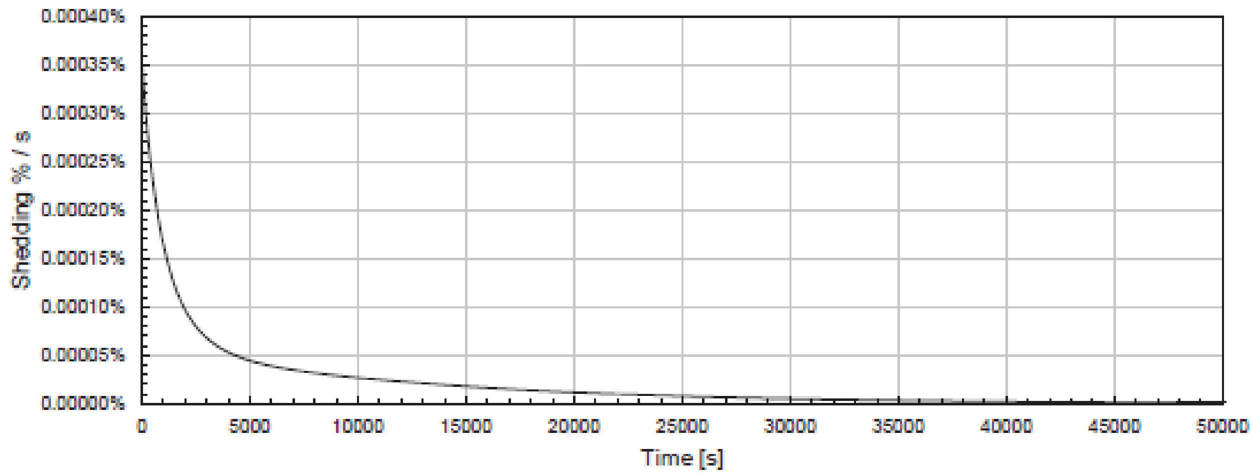

Figure 3.n.1-6: Shedding Rate from Bypass Model

Accumulation of Fiber Inside Reactor Vessel

During the post-LOCA sump recirculation phase, debris that passes through the strainer could accumulate at the reactor core inlet or inside the reactor vessel, and challenge LTCC. DCPP elected to use Option 4 from the NRC review guidance on in-vessel effects (Reference 30) to address this impact. The following table summarizes the key parameters for DCPP that are required by this resolution option.

Table 3.n.1-3: Summary of In-Vessel Effects Parameters

Parameters	WCAP-17788 Values	DCPP Values	
		Unit 1	Unit 2
Nuclear Steam Supply System (NSSS) Design	Various	Westinghouse 4-loop	
Fuel Type	Various	Westinghouse 17 x 17 VANTAGE+ fuel	
Barrel/Baffle Configuration	Various	Downflow	Upflow
Maximum Core Inlet Fiber Load for Hot Leg Break (HLB)	WCAP-17788, Volume 1 (Reference 8) Table 6-3	27.35 g/FA[(1)]	
Minimum Sump Switchover (SSO) Time	20 minutes (Reference 30)	24.9 minutes	
Minimum Chemical Precipitation Time	t_{block} from WCAP 2.38 hours - Upflow 4.33 hours - Downflow	>24 hours	
Maximum HLSO Time	N/A	7 hours	
Maximum Rated Thermal Power	3658 MWt - Upflow 2951 MWt - Downflow	3411 MWt	
Maximum Alternate Flow Path (AFP) Resistance	WCAP-17788, Volume 4 (Reference 9) Table 6-1 (Unit 2) and Table 6-2 (Unit 1)	WCAP-17788, Volume 4 (Reference 9) Table RAI-4.2-24	
ECCS Flow per FA	8 – 40 gpm/FA	7.7 gpm/FA[(2)] 26.9 gpm/FA	

(1) This is the maximum core inlet fiber load. DCPP used bounding inputs (e.g., minimum flow to spray header, maximum transported fiber load, shortest spray duration and earliest SSO time) and various combinations of other input parameters (e.g., strainer flow rates and sump pool volume) to ensure the maximum core inlet fiber load is captured. No flow diversion to the AFPs was credited.

(2) The 7.7 gpm/FA ECCS flow rate was for the single train failure case, which resulted in the maximum in-vessel fiber load. The 26.9 gpm/FA flow rate was for the two-train operating case, which represents the most likely equipment lineup during post-LOCA recirculation.

As shown in Table 3.n.1-3, all of the parameters for DCPP Unit 2 are bounded by those used in the WCAP-17788 analyses, as detailed below.

1. Chemical effects are shown not to occur earlier than the latest HLSO time or prior to t_{block} for Unit 2.
2. Maximum amount fiber that reaches the RCS for an HLB is below the WCAP-17788 fiber limit.
3. The earlier SSO time is greater than 20 minutes.
4. The rated thermal power for Unit 2 is lower than that analyzed for Westinghouse 4-loop plant with a upflow barrel/baffle configuration.
5. Plant AFP resistance is lower than that analyzed in WCAP-17788.
6. ECCS flow rate per FA is either comparable or within the analyzed range. Note that this parameter is not relevant for DCPP because DCPP did not credit any flow diversion from the core inlet to the AFPs. Additionally, the DCPP in-vessel fiber load is lower than the limit identified in WCAP-17788. As a result, the flow resistance at the core inlet will not be high enough to initiate any flow diversion.

For Unit 1, all parameters are bounded except for the thermal power, which is approximately 16% higher than that analyzed in WCAP-17788. However, the overall conservatism in the parameters used for the DCPP in-vessel analysis is adequate to offset the higher thermal power for Unit 1. It is concluded that accumulation of debris at the reactor core inlet will not adversely impact LTCC for DCPP Unit 1, as summarized below.

1. For DCPP, the earliest time that one RHR pump starts to draw flow from the containment sump (and therefore for any debris to reach the reactor) is 24.9 minutes after the accident, which is later than the 20 minutes assumed in the WCAP. As stated in the NRC review guidance (Reference 30), the potential for a debris-induced core uncovery heatup is greatly reduced when the sump switchover time is increased from 20 minutes to 23 minutes. Therefore, with the later sump recirculation switchover time, the risk of such debris-induced core heatup is low for DCPP Unit 1.
2. DCPP's maximum fiber load at the core inlet is smaller than the acceptance limit developed in WCAP-17788 for complete core blockage. Testing documented in Volume 1 of this WCAP (Reference 8) showed that the smaller fiber load significantly reduces the pressure drop at the core inlet, when compared with that associated with WCAP limits. Therefore, accumulation of fiber debris at the reactor core inlet will not cause complete blockage of the core inlet. Note that the DCPP analysis for the maximum fiber load at core inlet did <u>not</u> credit any flow diversion from the core inlet to the AFPs. The bullet list below summarizes the key steps of the analysis.

    - Transportable fiber debris was assumed to be uniformly distributed in the sump pool.

- Time-dependent debris arrival at the sump strainer was calculated based on fiber concentration in the pool and strainer/pump flow rates.
- Time-dependent fiber penetration through the ECCS and CS strainers was quantified based on DCPP-specific fiber bypass testing and the fiber debris load on the strainer at the time when incremental fiber arrives.
- Fiber that passes through the strainer is split between the reactor core and spray header. The spray duration and fraction of flow diverted to the spray header are conservatively reduced in the analysis.
- Fiber that reaches the reactor was assumed to accumulate at the reactor core inlet only, without crediting any AFPs.
- The analysis conservatively used a worst-case combination of input parameters (e.g., pool volume, transport fiber load, pump flow rates, sump recirculation and hot leg switchover time, and CS duration).

3. As stated in the NRC review guidance (Reference 30), the debris bed formed at the reactor core inlet is expected to be non-uniform due to non-uniform flow distribution. Coupled with the limited amount of fiber debris reaching the core inlet (as stated above), the non-uniform debris distribution will result in part of the core inlet staying clear of a filtering debris bed without interrupting the core flow.
4. As shown in Table 3.n.1-3, for DCPP Unit 1, chemical precipitation occurs after t_{block} and switchover to hot leg recirculation. Therefore, formation of chemical precipitate will not result in complete blockage of the reactor core inlet.
5. As stated above, DCPP did not credit the AFPs when analyzing fiber load at the reactor core inlet. Additionally, blockage of the reactor core inlet is unlikely due to the small fiber load and non-uniform fiber accumulation. Table 3.n.1-3 shows that the AFPs for the DCPP reactors have lower resistance than those analyzed in WCAP-17788. This would allow flow to reach the heated core through the AFPs more easily than analyzed in the WCAP in an unlikely event with the core inlet clogged.

Peak Cladding Temperature and Deposition Thickness

The LOCA deposition model (LOCADM), which is contained as part of WCAP-16793-NP, Revision 2 (Reference 7), was used to determine the scale thickness due to deposition of fiber, particulate, and chemical debris that passes through the strainer on the fuel rod surfaces and the resulting PCT. The calculated scale thickness was then combined with the thickness of existing fuel cladding oxidation and crud build-up to determine the total DT. The calculated total DT and PCT were compared with the acceptance criteria provided in WCAP-16793-NP. The limitations and conditions identified in the NRC's SE of this WCAP (Reference 29) were also addressed.

The inputs (such as pH values, temperature profiles, debris quantities, etc.) used in the DCPP LOCADM analysis conservatively bound all postulated breaks at the plant, and thus, the results are applicable for all breaks at DCPP for both units. The bump-up factor used to account for the impact of fibrous debris that passes through the strainer was calculated based upon an assumed 100 grams of fiber bypass per fuel assembly (FA). This value conservatively bounds the in-vessel fiber load determined for DCPP using the bypass model, as shown earlier in this submittal. Table 3.n 1-4 summarizes the PCT and DT.

Table 3.n 1-4: Summary of PCT and DT

Case	PCT (°F)		DT (mils)	
	Results	Acceptance Criteria	Results	Acceptance Criteria
Minimum Pool Volume	365.47	<800	19.76	< 50
Maximum Pool Volume	365.47		19.30	

The PCT is much lower than the acceptance criterion of 800 °F, and the DT value is well within the acceptance criterion of 50 mils. Therefore, deposition of post-LOCA debris and chemical precipitate product on the fuel rods will not block the LTCC flow through the core or create unacceptable local hot spots on the fuel cladding surfaces.

The 15 g/FA fiber limit at the reactor core inlet given in WCAP-16793-NP was not used. Instead, accumulation of fiber on the reactor core inlet and inside the reactor vessel was evaluated using the WCAP-17788 methodology, as discussed previously in this section.

The NRC Safety Evaluation of WCAP-16793-NP identified 14 limitations and conditions that must be addressed when using the WCAP methodology. DCPP's responses to these limitations and conditions are summarized below.

1. Assure the plant fuel type, inlet filter configuration, and ECCS flow rate are bounded by those used in the FA testing outlined in Appendix G of the WCAP. If the 15 g/FA acceptance criterion is used, determine the available driving head for an HL break and compare it to the debris head loss measured during the FA testing. Compare the fiber bypass amounts with the acceptance criterion given in the WCAP.

   Response:

   This condition is associated with the 15 g/FA limit established in WCAP-16793-NP, and is not being used for DCPP. Therefore, this condition is not applicable.

2. Each licensee's GL 2004-02 submittal to the NRC should state the available driving head for an HL break, ECCS flow rates, LOCADM results, type of fuel and inlet filter, and amount of fiber bypass.

Response:

This condition is associated with the 15 g/FA limit established in WCAP-16793-NP, and is not being used for DCPP. Therefore, this condition is not applicable.

3. If a licensee credits alternate flow paths in the reactor vessel in their LTCC evaluations, justification is required through testing or analysis.

   Response:

   This condition is associated with the 15 g/FA limit established in WCAP-16793-NP, and is not being used for DCPP. Therefore, this condition is not applicable.

4. The numerical analyses discussed in Sections 3.2 and 3.3 of the WCAP should not be relied upon to demonstrate adequate LTCC.

   Response:

   The fuel blockage modeling concerns discussed in Sections 3.2 and 3.3 of WCAP-16793 were not credited in the DCPP LOCADM analysis. Therefore, this condition is not applicable.

5. The SE requires that a plant must maintain its debris load within the limits defined by the testing (e.g., 15 g/FA), and any debris amounts greater than those justified by generic testing in the WCAP must be justified on a plant-specific basis.

   Response:

   This condition is associated with the 15 g/FA limit established in WCAP-16793-NP, and is not being used for DCPP. Therefore, this condition is not applicable.

6. The debris acceptance criterion can only be applied to fuel types and inlet filter configurations evaluated in the WCAP FA testing.

   Response:

   This condition is associated with the 15 g/FA limit established in WCAP-16793-NP, and is not being used for DCPP. Therefore, this condition is not applicable.

7. Each licensee's GL 2004-02 submittal to the NRC should compare the PCT from LOCADM with the acceptance criterion of 800 degrees F.

   Response:

   As shown in Table 3.n 1-4 , the bounding PCT are well within the acceptance criteria of 800 °F.

8. When utilizing LOCADM to determine PCT and DT, the aluminum release rate must be doubled to predict aluminum concentrations in the sump pool in the initial days following a LOCA more accurately.

   Response:

   The rate of aluminum release was doubled, as required by the SE on WCAP-16793-NP (Reference 7).

9. If refinements specific to the plant are made to the LOCADM to reduce conservatisms, the licensee should demonstrate that the results still adequately bound chemical product generation.

   Response:

   The LOCADM runs for DCPP did not employ any conservatism-reducing refinements specific to the plant. Therefore, no additional justification is required.

10. The recommended value for scale thermal conductivity of 0.11 BTU/(h-ft-°F) should be used for LTCC evaluations.

    Response:

    The recommended thermal conductivity of 0.11 BTU/(h-ft-°F) was used in the evaluation for DCPP.

11. The licensee's submittals should include the means used to determine the amount of debris that bypasses the ECCS sump strainer and the fiber loading at the fuel inlet expected for the HL and CL break scenarios. Licensees should provide the debris loads, calculated on a fuel assembly basis, for both the HL and CL break cases in their GL 2004-02 responses.

    Response:

    As shown in Table 3.n.1-3, the amount of fiber at the reactor core inlet was determined using the WCAP-17788 methodology.

12. Plants that can qualify a higher fiber load based on the absence of chemical deposits should ensure that tests for their conditions determine limiting head losses using particulate and fiber loads that maximize the head loss with no chemical precipitates included in the tests. In this case, licensees must also evaluate the other considerations discussed in the first limitation and condition.

    Response:

    This condition is associated with the 15 g/FA limit established in WCAP-16793-NP, and is not being used for DCPP. Therefore, this condition is not applicable.

13. The size distribution of the debris used in the FA testing must represent the size distribution of fibrous debris expected to pass through the ECCS sump strainer at the plant.

Response:

This condition is associated with the 15 g/FA limit established in WCAP-16793-NP, and is not being used for DCPP. Therefore, this condition is not applicable.

14. Each licensee’s GL 2004-02 submittal to the NRC should not utilize the “Margin Calculator” as it has not been reviewed by the NRC.

Response:

The evaluation for DCPP does not use the “Margin Calculator”.

3.o. Chemical Effects

The objective of the chemical effects section is to evaluate the effect that chemical precipitates have on head loss and core cooling.

1. *Provide a summary of evaluation results that show that chemical precipitates formed in the post-LOCA containment environment, either by themselves or combined with debris, do not deposit at the sump screen to the extent that an unacceptable head loss results, or deposit downstream of the sump screen to the extent that long-term core cooling is unacceptably impeded.*

Response to 3.o.1:

The chemical effects strategy for DCPP includes:

- Quantification of chemical precipitates using the WCAP-16530-NP-A methodology.
- Introduction of those pre-prepared precipitates in prototypical array testing.
- Application of an aluminum solubility correlation to determine the maximum precipitation temperature.
- Time-based determination of acceptable head losses.
- Extrapolation of the resulting head losses to 30 days.

As discussed in the Response to 3.a.1, DCPP has determined the debris generated at all ISI welds on the primary RCS piping inside containment. The amount/mass of chemical precipitates was quantified for bounding quantities of LOCA generated debris. Other plant-specific inputs such as pH, temperature, aluminum quantity, and spray times were selected to maximize the generated amount of precipitates. These amounts were scaled by the ratio of the test strainer area to the plant-strainer surface area and are compared with the chemical debris quantities used in the prototypical strainer tests to determine the resulting head loss across the strainers.

As described in the Response to 3.f.4, the strainer head loss tests used a full scale section of the plant strainer as a test strainer, which was both geometrically and hydraulically similar to the plant strainer. Before the tests were conducted, AlOOH was prepared according to the WCAP-16530-NP-A recipe and was verified to meet the settling criteria within 24 hours of the test. During the test, a fiber and particulate debris bed was established on the strainer surfaces, the stabilization criteria was satisfied, and the pre-prepared precipitates were added to the test tank in batches. See the Response to 3.f.4 for a detailed summary of the methodology, assumptions, and results of head loss testing.

Per the Response to 3.n.1, analyses using the methodologies of WCAP-16793-NP and WCAP-17788 concluded that post-accident LTCC will not be challenged by deposition of fiber, particulate, and chemical debris on the fuel rods, accumulation of fiber debris at the core inlet, or accumulation of fiber debris in the heated region of the core for all postulated LOCAs inside containment.

2. *Content guidance for chemical effects is provided in Enclosure 3 dated March 2008 to a letter from the NRC to NEI (ADAMS Accession No. ML080380214).*

Response to 3.o.2:

The NRC identified evaluation steps in "NRC Staff Review Guidance Regarding Generic Letter 2004-02 Closure in the Area of Plant-Specific Chemical Effect Evaluations" in March of 2008 (Reference 5). DCPP's responses to the GL Supplement Content evaluation steps are summarized below. The numbering of the following subsections to the Response to 3.o.2 follow the numbering scheme provided in Section 3 and Figure 1 of the March 2008 guidance (Reference 5). Figure 3.o.2-1 highlights the DCPP chemical effects evaluation process using the flow chart in Figure 1 of the March 2008 guidance (Reference 5).

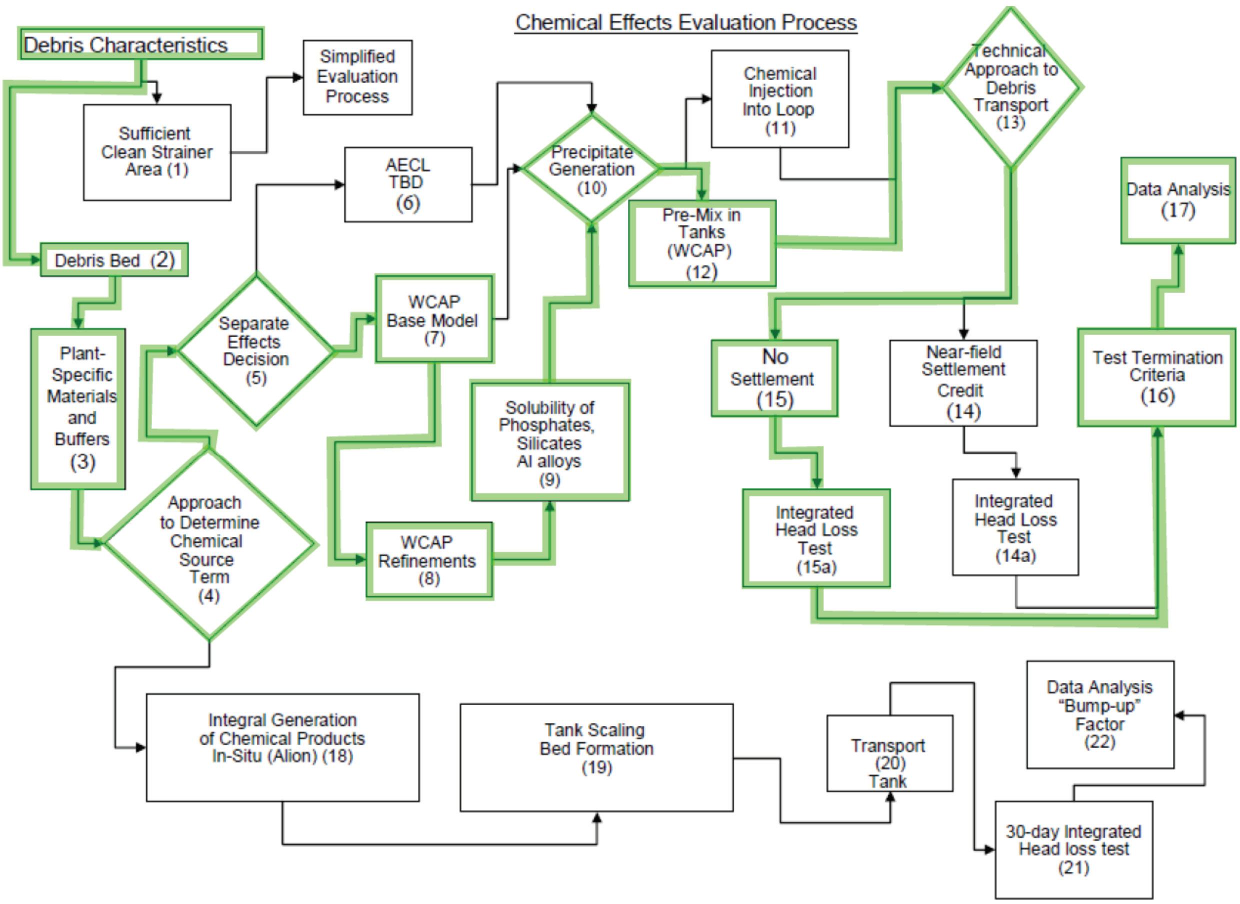

Figure 3.o.2-1: Chemical Effects Evaluation Process for DCPP (Reference 5)

1. *<u>Sufficient 'Clean' Strainer Area</u>: Those licensees performing a simplified chemical effects analysis should justify the use of this simplified approach by providing the amount of debris determined to reach the strainer, the amount of bare strainer area and how it was determined, and any additional information that is needed to show why a more detailed chemical effects analysis is not needed.*

   Response to 3.o.2.1:

   DCPP is not crediting clean strainer area to perform a simplified chemical effects analysis. See Figure 3.o.2-1.

2. *<u>Debris Bed Formation</u>: Licensees should discuss why the debris from the break location selected for plant-specific head loss testing with chemical precipitate yields the maximum head loss. For example, plant X has break location 1 that would produce maximum head loss without consideration of chemical effects. However, break location 2, with chemical effects considered, produces greater head loss than break location 1. Therefore, the debris for head loss testing with chemical effects should be based on break location 2.*

   Response to 3.o.2.2:

   DCPP performed both thin-bed and full debris load head loss tests. These tests were used to develop the head loss contributions from conventional debris and aluminum precipitates. The full debris load test was performed to bound the maximum debris loads of all postulated breaks. For the thin-bed test, a debris bed that was saturated with particulate debris was formed. Chemical precipitate was added to these tests as described in the Response to 3.f.4. The Response to 3.f.7 compares the bounding chemical debris load of DCPP with those used in the DCPP head loss tests.

3. *<u>Plant-Specific Materials and Buffers</u>: Licensees should provide their assumptions (and basis for the assumptions) used to determine chemical effects loading: pH range, temperature profile, duration of containment spray, and materials expected to contribute to chemical effects.*

   Response to 3.o.2.3:

   The chemical model requires a number of plant-specific inputs. Each input is chosen to maximize the calculated quantity and minimize the solubility (aluminum only) of the chemical precipitates.

   DCPP adds NaOH to the injection sprays, which in turn buffers the post-LOCA containment sump pool. The injection pH is between 8.5 and 10 for the spray flow (i.e., NaOH with borated water from the RWST only; this pH is not in the pool). The containment sump pool increases to a final pH between 8 and 9.5. After the start of cold leg recirculation, the spray flow is recirculated from the containment sump pool and therefore has the same pH. The pH values used for chemical release were set conservatively high, and the pH value used for aluminum solubility was set conservatively low. Different pH values for release and solubility are combined in a non-physical way (i.e. the containment sump pool is conservatively assumed to be at both a pH of 9.5 for chemical release and a pH of 7.5 for aluminum solubility), bounding the effects of all potential pH profile variations. The pH values used in the chemical model to maximize chemical release (conservatively high pH) and to minimize aluminum solubility (conservatively low pH) are summarized in Table 3.o.2.3-1:

Table 3.o.2.3-1: DCPP pH Values

Sump and Recirculation Spray pH Used to Determine Chemical Release Rates	9.5
Injection Spray pH Used to Determine Chemical Release Rates	10
Sump pH Used to Determine Aluminum Solubility	7.5

Bounding containment sump pool and containment temperature profiles were used to maximize chemical release rates. The temperature profiles are shown in Table 3.o.3-2.

Table 3.o.2.3-2: Temperature Profiles used to Determine Chemical Release Rates

Time (s)	Post-LOCA Sump Temperature (°F)	Post-LOCA Containment Temperature (°F)
6	234.24	240.00
30	255.00	265.00
60	251.09	258.00
120	240.79	258.00
180	245.00	258.00
200	246.00	258.00
400	252.00	258.00
600	255.00	258.00
800	257.00	258.00
1000	259.00	258.00
1200	260.00	253.00
1400	261.00	253.00
1600	261.00	253.00
1800	261.00	253.00
3200	252.00	250.00
4600	244.00	250.00
6000	235.83	250.00
7400	232.00	250.00
8800	228.84	250.00
10200	226.14	245.00
11600	223.79	245.00
13000	221.71	245.00
25200	214.00	240.00
46400	198.47	240.00
86400	187.12	220.00

Time (s)	Post-LOCA Sump Temperature (°F)	Post-LOCA Containment Temperature (°F)
172800	174.45	210.00
259200	167.05	198.00
345600	161.79	198.00
432000	157.72	185.00
864000	145.06	160.00
1296000	137.65	153.00
1728000	132.40	153.00
2160000	128.32	145.00
2592000	124.99	145.00

The total surface area of unsubmerged aluminum exposed to CS is 1100 ft^2 (includes contingency). The total surface area of submerged aluminum exposed to the containment sump fluid at DCPP Units 1 and 2 is 525 ft^2 (includes contingency). The mass for both unsubmerged and submerged aluminum were set to 1,000,000 lbm to avoid limiting the total release. These values do not include metallic aluminum paint, which varies in quantity from case to case. As discussed in the Response to 3.o.2.7.i, the WCAP base model spreadsheet has been modified to allow for the separate accounting of metallic aluminum paint from other types of metallic aluminum. The pressurizer and the reactor vessel are the only elements in containment with metallic aluminum paint. All metallic aluminum paint destroyed by the LOCA is assumed to be submerged in addition to intact submerged metallic aluminum paint on the reactor vessel.

The total surface area of concrete assumed to be exposed and submerged in the containment sump pool is 10,000 ft^2. The calculated quantity of chemical precipitates is negligibly increased by the assumption of a large surface area of exposed concrete. Therefore, exposed concrete is not a significant impact to chemical product generation in the DCPP post-LOCA containment sump pool and is not tracked for this purpose.

Injection sprays are assumed to begin immediately post-LOCA. Recirculation is assumed to start at 3200 seconds or 53.3 minutes after LOCA initiation, which is conservatively greater than the time calculated in the containment analysis. Because the assumed injection spray pH is greater than the sump pH, it is conservative to prolong the time until recirculation switchover in the chemical model. Containment spray is assumed to be terminated 7 hours after the accident, which is the maximum amount of time CS would run post-LOCA.

Higher concentrations of elements in the sump pool slows the release rate of elements released from insulation and concrete in the WCAP-16530-NP-A methodology. The sump pool is assumed never mixed. This is a conservative assumption since a mixed pool allows the elemental mass already released into the sump solution to impact the dissolution rate from each material containing that element while the WCAP-16530-NP-A methodology assumes that the elemental mass released from each material is dispersed throughout the sump volume but only affects the dissolution rate from that same material. In the WCAP-16530-NP-A methodology, these dissolved elements, released from insulation and concrete, are stoichiometrically proportional to the chemical debris that precipitate from solution.

Minimum and maximum water volume cases were run to determine both maximum generation of precipitates and maximum precipitation temperatures, since aluminum release rates from some materials (e.g., concrete, E-Glass, aluminum silicate, and Cal-Sil) are concentration dependent. At DCPP, the maximum containment sump pool volume that is available for chemical dissolution is 75,844 ft^3. The minimum containment sump pool volume that is available for chemical dissolution is 68,925 ft^3. The containment sump pool volume is converted to mass in the WCAP base model spreadsheet using the density of boric acid at 185°F, which is 60.957 lbm/ft^3.

Table 3.o.2.3-3 summarizes the remaining materials inputs for each case. Cases 1 through 4 are selected breaks which maximize the mass of aluminum silicate or E-Glass debris types at Unit 1 or Unit 2. As shown in Section 3.o.2.7ii, Case 3 is the bounding realistic case for precipitate generation, and Case 5 was developed to determine the maximum temperature where aluminum precipitation may occur by using the minimum water volume with the inputs from Case 3. Case 6 is an unrealistic combination of inputs from multiple breaks designed to determine a bounding quantity of precipitate.

Table 3.o.2.3-3: Case Specific Inputs

Case	Cal-Sil	E-Glass		Aluminum Silicate		Metallic Al Paint
		Latent Fiber and Foamglas	Other E-Glass**	Kaowool Blanket	Mica	
Bulk Density (lbm/ft^3)	14.5	2.4 (LDFG eq.)	2.4 (LDFG eq.)	2.4 (LDFG eq.)	74.9	---
Case 1: Unit 1 Loop 1 HLB at RPV (WIB-RC-1-1 SE), Max Sump Volume	0 ft^3	6.875 ft^3	102.52 ft^3	3.41 ft^3	0 ft^3	2414 ft^2 (40.2 lbm)*
Case 2: Unit 1 Loop 2 Crossover Leg Break (WIB-RC-2-10), Max Sump Volume	5.30 ft^3	12.925 ft^3	34.87 ft^3	3.41 ft^3	0.797 ft^3	1547 ft^2 (25.8 lbm)*
Case 3: Unit 2 Loop 4 CLB at RPV (WIB-RC-4-16 SE), Max Sump Volume	0 ft^3	6.875 ft^3	59.73 ft^3	3.388 ft^3	0 ft^3	2414 ft^2 (60.4 lbm)*
Case 4: Unit 2 Loop 2 Crossover Leg Break (WIB-RC-2-6), Max Sump Volume	7.95 ft^3	13.429 ft^3	42.57 ft^3	3.388 ft^3	1.007 ft^3	1547 ft^2 (33 lbm)*
Case 5: Unit 2 Loop 4 CLB at RPV (WIB-RC-4-16 SE), Min Sump Volume	0 ft^3	6.875 ft^3	59.73 ft^3	3.388 ft^3	0 ft^3	2414 ft^2 (60.4 lbm)*
Case 6: Unrealistic Max Chemical Break, Max Sump Volume	25.22 ft^3	13.429 ft^3	102.52 ft^{3+}	3.41 ft^3	1.007 ft^3	3104 ft^2 (71.9 lbm)

* Note that the high heat aluminum coatings on the reactor vessel are 2 mils thick at Unit 1 and are 3 mils thick at Unit 2. Although the area associated with high heat aluminum coatings on the reactor vessel are the same for both units, the mass is larger for Unit 2.
** This includes Fiberglass Overbraid and Flexicone Sleeves, Temp-Mat, and TIW.
+ The Temp-Mat debris load used to calculate this total is greater than the plant debris load when a 11.7D ZOI is applied for all Temp-Mat insulation, including encapsulated Temp-Mat.

4. *<u>Approach to Determine Chemical Source Term (Decision Point)</u>: Licensees should identify the vendor who performed plant-specific chemical effects testing.*

   Response to 3.o.2.4:

   DCPP is using the separate chemical effects approach to determine the chemical source term. Alden Research Laboratory, Inc. performed the head loss testing in their test lab in Holden, MA. See the Response to 3.f.4 for a detailed summary of the methodology, assumptions, and results of head loss testing.

5. *<u>Separate Effects Decision (Decision Point)</u>: Within this part of the process flow chart, two different methods of assessing the plant-specific chemical effects have been proposed. The WCAP-16530-NP-A study (Box 7 WCAP Base Model) uses predominantly single-variable test measurements. This provides baseline information for one material acting independently with one pH-adjusting chemical at an elevated temperature. Thus, one type of insulation is tested at each individual pH, or one metal alloy is tested at one pH. These separate effects are used to formulate a calculational model, which linearly sums all of the individual effects. A second method for determining plant-specific chemical effects that may*

rely on single-effects bench testing is currently being developed by one of the strainer vendors (Box 6, AECL).

Response to 3.o.2.5:

DCPP is using the WCAP-16530-NP-A chemical effects base model to determine the chemical source term. The application of an aluminum solubility correlation to determine a maximum precipitate formation temperature is discussed in the Response to 3.o.2.9.i.

6. *AECL Model:*

   i. *Since the NRC is not currently aware of the complete details of the testing approach, the NRC staff expects licensees using it to provide a detailed discussion of the chemical effects evaluation process along with head loss test results.*

   Response to 3.o.2.6.i:

   This question is not applicable because DCPP is not using the AECL model. See Figure 3.o.2-1.

   ii. *Licensees should provide the chemical identities and amounts of predicted plant-specific precipitates.*

   Response to 3.o.2.6.ii:

   This question is not applicable because DCPP is not using the AECL model. See Figure 3.o.2-1.

7. *WCAP Base Model:*

   i. *Licensees proceeding from block 7 to diamond 10 in the Figure 1 flow chart [in Enclosure 3 dated March 2008 to a letter from the NRC to NEI (Reference 106)] should justify any deviations from the WCAP base model spreadsheet (i.e., any plant specific refinements) and describe how any exceptions to the base model spreadsheet affected the amount of chemical precipitate predicted.*

   Response to 3.o.2.7.i:

   The chemical model quantifies chemical precipitates using the WCAP-16530-NP-A (Reference 23) methodology with the following two deviations:

   1. The application of an aluminum solubility correlation to determine a maximum precipitate formation temperature is discussed in the Response to 3.o.2.9.i.

2. The use of a modified base model spreadsheet that allows for the separate accounting of metallic aluminum paint from other types of metallic aluminum.

An aluminum solubility correlation was used to determine a maximum temperature for precipitate formation. As compared with the methodology of WCAP-16530-NP-A, which assumes precipitation immediately upon release, the calculated maximum precipitation temperature is used to effectively delay the onset of aluminum precipitation. Therefore, the aluminum release rate from aluminum metal was doubled over the initial 15 days to address the requirement in the Limitations and Conditions of the WCAP-16530-NP-A SE for applying time-based NPSH margin acceptance criteria. These calculations were performed by hand calculations using the results of the WCAP base model spreadsheet.

The base model WCAP-16530-NP-A spreadsheet was modified to allow for the input of submerged and not-submerged metallic aluminum paint separate from other types of aluminum metals due to the relatively high surface area/mass of these coatings. The equations and methodology used for metallic aluminum paint are identical to the equations and methodology used for aluminum metals and were confirmed by Westinghouse to be correctly implemented.

ii. Licensees should list the type (e.g., AlOOH) and amount of predicted plant-specific precipitates.

Response to 3.o.2.7.ii:

Table 3.o.2.7.ii-1 provides the released/precipitated aluminum mass and maximum aluminum precipitation temperatures that were calculated for multiple cases. See the Response to 3.o.2.3 for a description of the inputs for each case. Note that, per the WCAP-16530-NP-A SE, both sodium aluminum silicate (SAS, $NaAlSi_3O_8$) and AlOOH precipitates are acceptable surrogates for aluminum precipitate in head loss testing, and SAS, when predicted to form, can be converted to the stoichiometric equivalent amount of AlOOH (based on aluminum) for head loss testing. Therefore, Table 3.o.2.7.ii-1 reports aluminum precipitate in terms of the elemental aluminum mass component of the precipitated chemical debris.

Table 3.o.2.7.ii-1: Summary of Aluminum Precipitate Quantities and Precipitation Temperatures

Case	Total Al Released/Precipitated	Al Precipitation Temperature
Case 1: DCPP Unit 1 Loop 1 HLB at RPV (WIB-RC-1-1 SE), Max Sump Volume	213.43 lbm	170.09°F
Case 2: DCPP Unit 1 Loop 2 Crossover Leg Break (WIB-RC-2-10), Max Sump Volume	198.11 lbm	168.76°F
Case 3: DCPP Unit 2 Loop 4 CLB at RPV (WIB-RC-4-16 SE), Max Sump Volume	231.57 lbm	171.55°F
Case 4: DCPP Unit 2 Loop 2 Crossover Leg Break (WIB-RC-2-6), Max Sump Volume	206.46 lbm	169.50°F
Case 5: DCPP Unit 2 Loop 4 CLB at RPV (WIB-RC-4-16 SE), Min Sump Volume	231.42 lbm	173.25°F
Case 6: DCPP Unrealistic Max Chemical Break, Max Sump Volume	248.35 lbm	172.80°F

8. *<u>WCAP Refinements:</u> State whether refinements to WCAP-16530-NP-A were utilized in the chemical effects analysis.*

   Response to 3.o.2.8:

   Refinement to the model for aluminum solubility is discussed in the Response to 3.o.2.9.i. No other refinements to the WCAP-16530-NP-A methodology were used.

9. *<u>Solubility of Phosphates, Silicates and Al Alloys:</u>*

   i. *Licensees should clearly identify any refinements (plant-specific inputs) to the base WCAP-16530-NP-A model and justify why the plant-specific refinement is valid.*

      Response to 3.o.2.9.i:

      The base WCAP-16530-NP-A model assumes that aluminum precipitates form immediately upon the release of aluminum into solution. However, as justified in the Response to 3.o.2.7.i, the DCPP chemical model includes the following application of an aluminum solubility correlation to determine the maximum aluminum precipitation temperature and the timing of aluminum precipitation.

The aluminum solubility limit was determined using Equation 3.o.2.9-1, developed by Argonne National Laboratory (ANL) (Reference 31).

$$C_{Al,sol} = \begin{cases} 26980 \cdot 10^{pH-14.4+0.0243T}, \text{ if } T \leq 175\ °F \\ 26980 \cdot 10^{pH-10.41+0.00148T}, \text{ if } T > 175\ °F \end{cases} \qquad \text{(Equation 3.o.2.9-1)}$$

Where,

$C_{Al,sol}$ = Aluminum solubility limit, ppm
pH = Sump pool pH
T = Solution temperature, °F

The aluminum solubility limit equation was used to determine the temperature and timing of aluminum precipitation and to determine the aluminum concentration in solution for use in the aluminum release equations for concrete and insulation. When precipitation was predicted by this equation, the full amount of aluminum released was assumed to precipitate. The aluminum solubility limit equation was not used to reduce the predicted quantity of precipitate by crediting the amount remaining in solution.

ii. For crediting inhibition of aluminum that is not submerged, licensees should provide the substantiation for the following: (1) the threshold concentration of silica or phosphate needed to passivate aluminum, (2) the time needed to reach a phosphate or silicate level in the pool that would result in aluminum passivation, and (3) the amount of containment spray time (following the achieved threshold of chemicals) before aluminum that is sprayed is assumed to be passivated.

Response to 3.o.2.9.ii:

Silicon and phosphate inhibition of aluminum release were not credited.

iii. For any attempts to credit solubility (including performing integrated testing), licensees should provide the technical basis that supports extrapolating solubility test data to plant-specific conditions. In addition, licensees should indicate why the overall chemical effects evaluation remains conservative when crediting solubility given that small amount of chemical precipitate can produce significant increases in head loss.

Response to 3.o.2.9.iii:

Reductions in precipitate quantity due to residual solubility of aluminum after precipitation occurs was not credited. See the Response to 3.o.2.9.i.

iv. *Licensees should list the type (e.g., AlOOH) and amount of predicted plant-specific precipitates.*

Response to 3.o.2.9.iv:

The type and amount of plant-specific precipitates are provided in the Response to 3.o.2.7.ii.

10. *<u>Precipitate Generation (Decision Point):</u> State whether precipitates are formed by chemical injection into a flowing test loop or whether the precipitates are formed in a separate mixing tank.*

Response to 3.o.2.10:

As discussed in the Response to 3.o.2.12, DCPP pre-mixed surrogate chemical precipitates in a separate mixing tank for chemical head loss testing. The direct chemical injection method was not used in head loss testing.

11. *<u>Chemical Injection into the Loop:</u>*

i. *Licensees should provide the one-hour settled volume (e.g., 80 ml of 100 ml solution remained cloudy) for precipitate prepared with the same sequence as with the plant-specific, in-situ chemical injection.*

Response to 3.o.2.11.i:

The direct chemical injection method was not used in head loss testing for DCPP. See Figure 3.o.2-1.

ii. *For plant-specific testing, the licensee should provide the amount of injected chemicals (e.g., aluminum), the percentage that precipitates, and the percentage that remains dissolved during testing.*

Response to 3.o.2.11.ii:

The direct chemical injection method was not used in head loss testing for DCPP. See Figure 3.o.2-1.

iii. *Licensees should indicate the amount of precipitate that was added to the test for the head loss of record (i.e., 100 percent, 140 percent of the amount calculated for the plant).*

Response to 3.o.2.11.iii:

The direct chemical injection method was not used in head loss testing for DCPP. See Figure 3.o.2-1.

12. *Pre-Mix in Tank: Licensees should discuss any exceptions taken to the procedure recommended for surrogate precipitate formation in WCAP-16530-NP-A.*

Response to 3.o.2.12:

The WCAP-16530-NP-A precipitate formation methodology for AlOOH was followed with no exceptions.

13. *Technical Approach to Debris Transport (Decision Point): State whether near-field settlement is credited or not.*

Response to 3.o.2.13:

DCPP chemical effects testing used hydraulic and manual agitation and turbulence in the test tank to ensure that essentially all debris transported to the test strainer in head loss testing. DCPP did not credit any near field settlement in head loss testing. Refer also to the Response to 3.f.4.

14. *Integrated Head Loss Test with Near-Field Settlement Credit:*

   i. *Licensees should provide the one-hour or two-hour precipitate settlement values measured within 24 hours of head loss testing.*

   Response to 3.o.2.14.i:

   DCPP is not crediting near field settlement of chemical precipitate in chemical head loss testing. See Figure 3.o.2-1.

   ii. *Integrated Head Loss Test with Near-Field Settlement Credit: Licensees should provide a best estimate of the amount of surrogate chemical debris that settles away from the strainer during the test.*

   Response to 3.o.2.14.ii:

   DCPP is not crediting near field settlement of chemical precipitate in chemical head loss testing. See Figure 3.o.2-1.

15. *Head Loss Testing Without Near Field Settlement Credit:*

   i. *Licensees should provide an estimate of the amount of debris and precipitate that remains on the tank/flume floor at the conclusion of the test and justify why the settlement is acceptable.*

   Response to 3.o.2.15.i:

   In each head loss test, upon draining the test tank, settled particulates and small amounts of fiber were observed between the test tank walls and the outer most disks of the front strainer. Settled particulates were also observed directly upstream of the front strainer, but within 12 inches. This showed that all efforts to facilitate debris transport to the strainer were successful. See the response to Response to 3.f.12.

ii. *Licensees should provide the one-hour or two-hour precipitate settlement values measured and the timing of the measurement relative to the start of head loss testing (e.g., within 24 hours).*

Response to 3.o.2.15.ii:

The maximum allowable clear volume at the top of a 10 mL sample of AlOOH precipitates after one hour of settling was 4 mL. The precipitates were continuously mixed and used within 24 hours of the execution of a successful settling test. After 24 hours, the settling test could be re-executed to document the continued acceptability of the precipitate. All precipitates met the criteria provided in the Safety Evaluation to WCAP-16530-NP-A.

16. *Test Termination Criteria: Licensees should provide the test termination criteria.*

Response to 3.o.2.16:

The head loss test was terminated once the last chemical debris addition did not produce a new head loss peak. The debris bed in this state was characterized using a flow sweep. In the bounding head loss test, the maximum chemical debris head loss was observed after the second batch of chemical debris was introduced. As subsequent batches of debris were introduced, the measured head loss decreased over time.

17. *Data Analysis:*

i. *Licensees should provide a copy of the pressure drop curve(s) as a function of time for the testing of record.*

Response to 3.o.2.17.i:

The Response to 3.f.4 detail the head loss tests. Figure 3.f.4-5 and Figure 3.f.4-7 show the chemical head loss results for the bounding full debris load test and the thin-bed test, respectively.

ii. *Licensees should explain any extrapolation methods used for data analysis.*

Response to 3.o.2.17.ii:

In the bounding head loss test, the maximum chemical debris head loss was observed after the second batch of chemical debris was introduced. As subsequent batches of debris were introduced, the measured head loss decreased over time. Therefore, the maximum chemical debris head loss bounds all of the head losses recorded during testing and does not need to be extrapolated over time.

18. *<u>Integral Generation (Alion):</u> Licensees should explain why the test parameters (e.g., temperature, pH) provide for a conservative chemical effects test.*

Response to 3.o.2.18:

DCPP is using the separate chemical effects approach to determine the chemical source term. This section is not applicable to the DCPP chemical effects analysis. See Figure 3.o.2-1.

19. *<u>Tank Scaling / Bed Formation:</u>*

    i. *Explain how scaling factors for the test facilities are representative or conservative relative to plant-specific values.*

    Response to 3.o.2.19.i:

    DCPP is using the separate chemical effects approach to determine the chemical source term. This section is not applicable to the DCPP chemical effects analysis. See Figure 3.o.2-1.

    ii. *Explain how bed formation is representative of that expected for the size of materials and debris that is formed in the plant specific evaluation.*

    Response to 3.o.2.19.ii:

    DCPP is using the separate chemical effects approach to determine the chemical source term. This section is not applicable to the DCPP chemical effects analysis. See Figure 3.o.2-1.

20. *<u>Tank Transport:</u> Explain how the transport of chemicals and debris in the testing facility is representative or conservative with regard to the expected flow and transport in the plant-specific conditions.*

Response to 3.o.2.20:

DCPP is using the separate chemical effects approach to determine the chemical source term. This section is not applicable to the DCPP chemical effects analysis. See Figure 3.o.2-1.

21. *<u>30-Day Integrated Head Loss Test:</u> Licensees should provide the plant-specific test conditions and the basis for why these test conditions and test results provide for a conservative chemical effects evaluation.*

Response to 3.o.2.21:

DCPP is using the separate chemical effects approach to determine the chemical source term. This section is not applicable to the DCPP chemical effects analysis. See Figure 3.o.2-1.

22. *Data Analysis Bump Up Factor: Licensees should provide the details and the technical basis that show why the bump-up factor from the particular debris bed in the test is appropriate for application to other debris beds.*

Response to 3.o.2.22:

DCPP is using the separate chemical effects approach to determine the chemical source term. This section is not applicable to the DCPP chemical effects analysis. See Figure 3.o.2-1.

3.p. Licensing Basis

The objective of the licensing basis is to provide information regarding any changes to the plant licensing basis due to the sump evaluation or plant modifications.

1. *Provide the information requested in GL 2004-02 Requested Information Item 2(e) regarding changes to the plant-licensing basis. The effective date for changes to the licensing basis should be specified. This date should correspond to that specified in the 10 CFR 50.59 evaluation for the change to the licensing basis.*

   GL 2004-02 Requested Information Item 2(e)
   A general description of and planned schedule for any changes to the plant licensing bases resulting from any analysis or plant modifications made to ensure compliance with the regulatory requirements listed in the Applicable Regulatory Requirements section of this GL. Any licensing actions or exemption requests needed to support changes to the plant licensing basis should be included.

   Response to 3.p:

   As summarized in Section 2 of this submittal, various plant modifications and procedural changes have been implemented by DCPP Unit 1 and Unit 2 to resolve GL 2004-02 and GSI-191 concerns. The earlier sub-sections in Section 3 of this submittal summarized the testing and analyses performed using a deterministic methodology to demonstrate that the sump recirculation strainer meets its safety function requirements.

   The DCPP Unit 1 and Unit 2 UFSAR was updated to summarize the modifications, testing and evaluations performed to resolve GL 2004-02 and demonstrate that the sump recirculation strainer will serve its safety function during the post-LOCA recirculation phase. A markup to the UFSAR is attached in this submittal.

4. NRC Requests for Additional Information

DCPP received two rounds of RAIs from the NRC by letters dated August 1, 2008 (Reference 32) and October 15, 2009 (Reference 33). The first round of RAIs contained 13 questions based on the review of DCPP Supplemental Responses to GL 2004-02: Letters dated February 1, 2008 (Reference 34) and July 10, 2008 (Reference 35). DCPP responded to these RAIs by a letter dated November 3, 2008 (Reference 36). Afterwards, the second round of RAIs, dated October 15, 2009 (Reference 33), was issued after the NRC reviewed the responses to the first round of RAIs (Reference 36). The second set of RAIs added RAI #24, replaced RAI #2 with RAIs #14 - #23, and raised additional questions on RAIs #5, #7, and #12. The final PG&E responses to RAIs #1 through #24 are summarized in the table below.

RAI No.	**RAIs in Letters Dated August 1, 2008** (Reference 32) **and October 15, 2009** (Reference 33)	**Response**
1	Please verify that debris generation values were maximized, in light of the reduced zones of influence (ZOIs) for certain debris sources and the fact that the licensee's break selection methodology does not follow the incremental location guidance provided by the Nuclear Energy Institute (NEI) and the NRC staff. Please explain whether the originally applied break selection methodology was reconsidered once the ZOIs were reduced.	RAI response accepted by the NRC with no further questions raised in the NRC Letter dated October 15, 2009 (Reference 33)
2	Please provide the basis for comparability/use of the jet impingement testing resulting ZOIs with a 3.5 inch jet when much larger jets could be experienced in a loss-of-coolant accident (LOCA). <u>Additional Request (October 15, 2009)</u> This RAI questioned the basis for comparability/use of jet impingement testing resulting in zones of influence (ZOIs) with a 3.5 inch jet when much larger jets could be experienced in a loss-of-coolant accident (LOCA). The NRC staff had noted that the licensee had deviated from the Nuclear Energy Institute 04-07 Guidance Report (GR) by assuming plant-specific ZOI radii based on jet impingement testing conducted by Westinghouse at a Wyle Laboratories facility, as documented in WCAP-16720-P. In its review of the licensee's RAI response, the NRC staff noted that the licensee provided additional information on the testing conducted by Westinghouse as reported in WCAP-16720-P. This additional information on the testing conducted to define the ZOIs for the site-specific insulation system installations did not address the intent of the question. Also, since the original RAI No.2 was developed for DCPP, the NRC staff has performed additional evaluations of the methodology utilized by Westinghouse during the debris generation testing for licensees. This evaluation resulted in a more detailed set of questions regarding the debris generation testing listed below. The licensee's RAI 2 response indicates that similar methodology was used for the DCPP testing.	No longer applicable. Replaced by RAIs 14-23 in the NRC Letter dated October 15, 2009 (Reference 33)

RAI No.	**RAIs in Letters Dated August 1, 2008** (Reference 32) **and October 15, 2009** (Reference 33)	**Response**
	Although, the list of questions was based on, and specifically references, different WCAPs than were used by DCPP in its evaluation, it is expected that similar concerns exist with WCAP-16720-P since the NRC staff understands the methods were similar.	
3	Please provide the volumes of the inactive and sump pools to substantiate the 15% entrapment fraction of all debris in the inactive pools (i.e., is the volume of inactive pools greater or equal to 15% of total pool volume), and provide the justification for assuming all of the latent debris, instead of being distributed throughout containment, would be located in the sump pool during the pool fill phase, thereby maximizing the credit for latent debris to be captured in inactive pool volumes.	RAI response accepted by the NRC with no further questions raised in the NRC Letter dated October 15, 2009 (Reference 33)
4	Please provide the basis for crediting reflective metal insulation (RMI) debris with filtering out paint chips at the debris interceptors in light of the facts that (1) an insufficient amount of RMI for paint chip filtering may be destroyed for some break scenarios for which coating debris is generated, (2) the size distribution of actual destroyed RMI may be biased toward less transportable pieces than assumed by the NEI and NRC staff guidance for debris transport to the sump strainer, and (3) the flow velocity in the pool may not in actuality transport RMI to the interceptors for some of the breaks for which coating debris is generated (i.e., the transport metrics are biased towards maximizing RMI transport to the sump strainers).	RAI response accepted by the NRC with no further questions raised in the NRC Letter dated October 15, 2009 (Reference 33)
5	Please state whether the fire stops and unjacketed debris in containment outside the crane wall would be exposed to the runoff of spray drainage streams, and state whether this effect was accounted for in the erosion testing that was performed on these materials (as opposed to assuming that all spray flow was in the form of fine droplets). <u>Additional Request (October 15, 2009)</u> The NRC staff requested that the licensee state whether unjacketed debris and fire stops would be exposed to runoff from spray drainage and describe whether this effect was accounted for in the spray erosion testing. The licensee's response, dated November 3, 2008, described erosion testing performed for both unjacketed insulation and for fire stops in cable trays. Regarding the unjacketed insulation tests, the runoff flow was modeled as impacting the insulation with a velocity of 0.4 ft/s, while the spray nozzle exit velocity was modeled as being greater than or equal to 15.75 ft/s. Although a basis was provided for the spray nozzle exit velocity, the response did not adequately demonstrate that 0.4 ft/s is a conservative or prototypical velocity for drainage runoff to impact unjacketed insulation. Furthermore, since the test results of the unjacketed insulation subjected to runoff were used as a justification not to conduct testing of vertical cable tray fire stops	See the Response to 3.b.1 regarding the evaluation of firestops inside the annulus that are subject to erosion from containment sprays.

RAI No.	**RAIs in Letters Dated August 1, 2008** (Reference 32) **and October 15, 2009** (Reference 33)	**Response**
	exposed to runoff drainage, the choice of 0.4 ft/s as a velocity for runoff drainage also affects the vertical cable tray fire stop testing. Therefore, please provide a technical basis to demonstrate that 0.4 ft/s is a conservative or prototypical velocity for drainage runoff that could impact unjacketed insulation and vertical cable tray fire stops in order to show that the erosion testing and assumptions made for these materials are justified.	
6	Please provide the amount of each size category of fiber added to each head loss test (e.g., fine, small, large, and intact). Provide a comparison between the amount of each fiber size category added to each test versus the amount of each fiber size category predicted to reach the strainer in the transport calculation. Verify that the fine fibers added to the test flume had not agglomerated during preparation and entered the test flume as suspended fiber.	RAI response accepted by the NRC with no further questions raised in the NRC Letter dated October 15, 2009 (Reference 33)
7	Please provide an evaluation that shows that the stirring in the tank to prevent debris settling did not affect the formation of the strainer debris bed in a non-prototypical or nonconservative manner (prevention or wash away of debris beds, or disturbance of the debris bed by non-prototypical intrusion of paint chips or large pieces of fiber). <u>Additional Request (October 15, 2009)</u> The NRC staff requested additional information regarding how stirring affected the results of the head loss test. The licensee provided information that justified that excessive debris settlement did not occur. However, it is also possible that the stirring affected the debris bed non-prototypically such that debris did not accumulate uniformly over the strainer surface as would occur if added turbulence was not present. Post-test photographs and inspection of the strainer showed that an unexpected non-uniform distribution of debris on the strainer occurred. It was particularly unusual that photographs showed less debris accumulation near the bottom of the strainer than elsewhere. Additionally, the test resulted in a significantly increased deposition of paint chips on the strainer compared to what would be expected in the plant. The licensee should provide information that justifies that the debris bed formed during testing is a realistic or conservative representation of what would occur in the plant.	DCPP performed new head loss testing in 2016. As stated in the Response to 3.f.4, “the placement of the mixing lines was adjusted such that the turbulence from the flow exiting the mixing lines promoted a homogeneous mixture of debris in the tank water but did not affect the debris bed on the test strainer.”
8	Please provide a basis for not performing a time-based extrapolation of the test data out to the emergency core cooling system (ECCS) mission time. [The staff understands that the integrated chemical head loss test was run for the number of fluid turnovers that would occur in the plant. However, there are potential time-based debris bed change mechanisms that could result in additional head loss (e.g., compaction). It has been observed in testing, after many test rig fluid volume turnovers, that	RAI response accepted by the NRC with no further questions raised in the NRC Letter dated October 15, 2009 (Reference 33)

RAI No.	RAIs in Letters Dated August 1, 2008 (Reference 32) and October 15, 2009 (Reference 33)	Response
	after particulate debris has been filtered from the water the strainer head loss continues to increase with time.]	
9	The supplemental response states that the strainer is completely submerged for a large break LOCA at the onset of recirculation. However, the supplemental response also states that the top of the strainers are at 93.6 ft and the water level is at 93.4 ft at the onset of recirculation. This implies that the strainer is not fully submerged at the onset of recirculation. Please provide clarification as to whether the strainer is submerged at the onset of recirculation. If it is not, provide an evaluation of the acceptability of the strainer performance under partially submerged conditions.	RAI response accepted by the NRC with no further questions raised in the NRC Letter dated October 15, 2009 (Reference 33)
10	The supplemental response states that for a small-break LOCA (SBLOCA) the strainer is not submerged completely. The response describes how the strainers were modified to reduce the potential for vortexing under partially submerged conditions and tested to verify the modifications were effective. However, it was not stated whether strainer testing was completed for partial submergence conditions with the expected debris loading on the strainer. Please provide an evaluation of strainer performance under partially submerged and debris laden conditions. Additionally, provide information that verifies that the clean strainer head loss calculation includes losses associated with the flow straighteners added to prevent vortex formation during SBLOCAs. [Regulatory Guide 1.82, Revision 3 discusses criteria that the strainer should meet under various conditions, including a criterion for allowable head loss for partially submerged strainers.]	RAI response accepted by the NRC with no further questions raised in the NRC Letter dated October 15, 2009 (Reference 33)
11	Please provide justification for the computed limiting ECCS flow rate being "worst case flow conditions." Please include a description of the methodology used to determine the maximum flow rate (e.g., runout flow from the vendor pump curve, a calculation using a standard hydraulics code, etc.), as well as a description of the assumptions and the assumed system and component configuration that provides the conservative maximum flow rate (e.g., for single pump operation, can flow cross over to downstream piping in the non-operating train?).	RAI response accepted by the NRC with no further questions raised in the NRC Letter dated October 15, 2009 (Reference 33)
12	Please provide a revised table of net positive suction head (NPSH) available and NPSH margin calculation results which does not include clean strainer head loss and head loss from accumulated debris. <u>Additional Request (October 15, 2009)</u> The NRC staff requested that the licensee provide a revised table showing the results of the net positive suction head margin calculation without including the head loss from accumulated debris. The table provided by the licensee on page 29 of the November 3, 2008, supplemental response showed the individual contributions from the increased containment water level	The NPSH margin evaluation has been updated, along with the minimum post-LOCA pool water level evaluation. Refer to the Responses to 3.g.1 and 3.g.16 for updated information.

RAI No.	**RAIs in Letters Dated August 1, 2008** (Reference 32) **and October 15, 2009** (Reference 33)	**Response**
	assumed by the licensee, as well as the impact of the strainer and debris bed head losses. The licensee indicated that the previous net positive suction head calculations conservatively did not take credit for minimum sump water levels. The NRC staff questions this response because a 5-ft level increase was credited for cold-leg recirculation, whereas only a 2-ft level increase was credited for hot-leg recirculation. The NRC staff expected that the minimum water level available for hot-leg recirculation would be greater than or equal to the minimum cold-leg recirculation water level. Furthermore, the licensee's response, dated July 10, 2008, indicates that the minimum pool depth is 1.8 ft for a small-break LOCA and 2.6 ft for a large-break LOCA. Even at the point when the containment spray pumps are secured, this supplemental response states that the calculated minimum pool level could be a minimum of 3.5 ft. Therefore, the basis for crediting a 5 ft increase in water level for the cold-leg recirculation case to account for the minimum containment water level was not clear to the NRC staff, since it appeared that a minimum level of 5 ft could not be assured post-LOCA. In light of the discussion above, please provide a technical basis to demonstrate that the increased water levels credited for cold-leg and hot-leg recirculation are justified in light of the minimum containment water levels for Diablo Canyon, or provide a different level with justification.	
13	Please verify that the 9.7 g/l AlOOH concentration for the Diablo Canyon settling test shown in the Figure 6 note is correct. The staff notes that the AlOOH precipitate settlement data provided in WCAP-16530-NP was obtained after diluting the various mixing tank concentrations to a 2.2 g/l concentration and that a higher concentration would favor more rapid settling.	RAI response accepted by the NRC with no further questions raised in the NRC Letter dated October 15, 2009 (Reference 33)
14	Although the American National Standards Institute/American Nuclear Society (ANSI/ANS) standard predicts higher jet centerline stagnation pressures associated with higher levels of subcooling, it is not apparent that this would necessarily correspond to a generally conservative debris generation result. Please justify the initial debris generation test temperature and pressure with respect to the plant-specific reactor coolant system (RCS) conditions, specifically the plant hot and cold leg operating conditions. If ZOI reductions are also being applied to lines connecting to the pressurizer, then please also discuss the temperature and pressure conditions in these lines. Please discuss whether any tests were conducted at alternate temperatures and pressures to assess the variance in the destructiveness of the test jet to the initial test condition specifications, and if so, provide that assessment.	As stated in the Response to 3.b.1, only the ZOI for encapsulated Temp-Mat was based on WCAP-17561-P. This WCAP was previously submitted to the NRC for information (Reference 18).
15	Please describe the jacketing/insulation systems used in the plant for which the testing was conducted and compare those systems	

RAI No.	**RAIs in Letters Dated August 1, 2008** (Reference 32) **and October 15, 2009** (Reference 33)	**Response**
	to the jacketing/insulation systems tested. Demonstrate that the tested jacketing/insulation system is adequately representative of the plant jacketing/insulation system. The description should include differences in the jacketing and banding systems used for piping and other components for which the test results are applied, potentially including steam generators, pressurizers, reactor coolant pumps, valves, etc. At a minimum, the following areas should be addressed: • How did the characteristic failure dimensions of the tested jacketing/insulation compare with the effective diameter of the jet at the axial placement of the target? The characteristic failure dimensions are based on the primary failure mechanisms of the jacketing system, e.g., for a stainless steel jacket held in place by three latches where all three latches must fail for the jacket to fail, then all three latches must be effectively impacted by the pressure for which the ZOI is calculated. Applying test results to a ZOI based on a centerline pressure for relatively low length to diameter (L/D) nozzle to target spacing would be nonconservative with respect to impacting the entire target with the calculated pressure. • Was the insulation and jacketing system used in the testing of the same general manufacture and manufacturing process as the insulation used in the plant? If not, what steps were taken to ensure that the general strength of the insulation system tested was conservative with respect to the plant insulation? For example, it is known that there were generally two very different processes used to manufacture calcium silicate whereby one type readily dissolved in water but the other type dissolves much more slowly. Such manufacturing differences could also become apparent in debris generation testing, as well. The information provided should also include an evaluation of scaling the strength of the jacketing or encapsulation systems to the tests. For example, a latching system on a 30-inch pipe within a ZOI could be stressed much more than a latching system on a 10-inch pipe in a scaled ZOI test. If the latches used in the testing and the plants are the same, the latches in the testing could be significantly under-stressed. If a prototypically sized target were impacted by an undersized jet it would similarly be under-stressed. Evaluations of banding, jacketing, rivets, screws, etc., should be made. For example, scaling the strength of the jacketing was discussed in the Ontario Power Generation report on calcium silicate debris generation testing.	This response is applicable for RAIs #14 through #23.

RAI No.	RAIs in Letters Dated August 1, 2008 (Reference 32) and October 15, 2009 (Reference 33)	Response
16	There are relatively large uncertainties associated with calculating jet stagnation pressures and ZOIs for both the test and the plant conditions based on the models used in the WCAP reports. Please describe what steps were taken to ensure that the calculations resulted in conservative estimates of these values. Please provide the inputs for these calculations and the sources of the inputs.	
17	Please describe the procedure and assumptions for using the ANSI/ANS-58-2-1988 standard to calculate the test jet stagnation pressures at specific locations downrange from the test nozzle. • Please discuss why the analysis was based on the initial condition of 530 °F whereas the initial test temperature was specified as 550 °F (if applicable to WCAP-16720-P). • Describe whether the water subcooling used in the analysis was that of the initial tank temperature or was it the temperature of the water in the pipe next to the rupture disk. Test data indicated that the water in the piping had cooled below that of the test tank. • The break mass flow rate is a key input to the ANSI/ANS-58-2-1988 standard. Describe how the associated debris generation test mass flow rate was determined. If the experimental volumetric flow was used, then explain how the mass flow was calculated from the volumetric flow given the considerations of potential two-phase flow and temperature dependent water and vapor densities. If the mass flow was analytically determined, then describe the analytical method used to calculate the mass flow rate. • Noting the extremely rapid decrease in nozzle pressure and flow rate illustrated in the test plots in the first tenths of a second; discuss how the transient behavior was considered in the application of the ANSI/ANS-58-2-1988 standard. Specifically, address whether the inputs to the standard represent the initial conditions or the conditions after the first extremely rapid transient, e.g., say at one tenth of a second. Given the extreme initial transient behavior of the jet, justify the use of the steady state ANSI/ANS-58-2-1988 standard jet expansion model to determine the jet centerline stagnation pressures rather than experimentally measuring the pressures.	
18	Please describe the procedure used to calculate the isobar volumes used in determining the equivalent spherical ZOI radii using the ANSI/ANS-58-2-1988 standard by addressing the following questions. ○ What were the assumed plant-specific RCS temperatures and pressures and break sizes used in the calculation? Note that the isobar volumes would be different for a hot leg break than for a cold leg break since the degrees of subcooling is a direct input to the ANSI/ANS-58-2-1988 standard and which affects	

RAI No.	**RAIs in Letters Dated August 1, 2008** (Reference 32) **and October 15, 2009** (Reference 33)	**Response**
	the diameter of the jet. Note that an under calculated isobar volume would result in an under calculated ZOI radius. o What was the calculational method used to estimate the plant-specific and break-specific mass flow rate for the postulated plant LOCA, which was used as input to the standard for calculating isobar volumes? Given the extreme initial transient behavior of the jet, justify the use of the steady state ANSI/ANS-58-2-1988 standard jet expansion model to determine the jet centerline stagnation pressures rather than experimentally measuring the pressures. o Given that the degree of subcooling is an input parameter to the ANSI/ANS-58-2-1988 standard and that this parameter affects the pressure isobar volumes, what steps were taken to ensure that the isobar volumes conservatively match the plant-specific postulated LOCA degree of subcooling for the plant debris generation break selections? Were multiple break conditions calculated to ensure a conservative specification of the ZOI radii?	
19	Please provide a detailed description of the test apparatus specifically including the piping from the pressurized test tank to the exit nozzle including the rupture disk system. a. Based on the temperature traces in the test reports it is apparent that the fluid near the nozzle was colder than the bulk test temperature. How was the fact that the fluid near the nozzle was colder than the bulk fluid accounted for in the evaluations? b. How was the hydraulic resistance of the test piping which affected the test flow characteristics evaluated with respect to a postulated plant-specific LOCA break flow where such piping flow resistance would not be present? c. What was the specified rupture differential pressure of the rupture disks?	
20	Please address the following questions relating to the testing: a. Was any analysis or parametric testing conducted to get an idea of the sensitivity of the potential to form a shock wave at different thermal-hydraulic conditions? Were temperatures and pressures prototypical of pressurized-water reactor hot legs considered? b. Was the initial lower temperature of the fluid near the test nozzle taken into consideration in the evaluation? Specifically, was the damage potential assessed as a function of the degree of subcooling in the test initial conditions? c. What is the basis for scaling a shock wave from the reduced-scale nozzle opening area tested to the break opening area for a limiting rupture in the actual plant piping? d. How is the effect of a shock wave scaled with distance for both the test nozzle and plant condition?	

RAI No.	RAIs in Letters Dated August 1, 2008 (Reference 32) and October 15, 2009 (Reference 33)	Response
21	Please provide the basis for concluding that a jet impact on piping insulation with a 45° seam orientation is a limiting condition for the destruction of insulation installed on steam generators, pressurizers, reactor coolant pumps, and other non-piping components in the containment, if the testing was applied to these components. For instance, considering a break near the steam generator nozzle, once insulation panels on the steam generator directly adjacent to the break are destroyed, the LOCA jet could impact additional insulation panels on the generator from an exposed end, potentially causing damage at significantly larger distances than for the insulation configuration on piping that was tested. Furthermore, it is not clear that the banding and latching mechanisms of the insulation panels on a steam generator or other RCS components provide the same measure of protection against a LOCA jet as those of the piping insulation that was tested. Although WCAP-16710-P asserts that a jet at Wolf Creek or Callaway cannot directly impact the steam generator. but will flow parallel to it, it seems that some damage to the steam generator insulation could occur near the break, with the parallel flow then jetting under the surviving insulation, perhaps to a much greater extent than predicted by the testing. Similar damage could occur to other component insulation. Please provide a technical basis to demonstrate that the test results for piping insulation are prototypical or conservative of the degree of damage that would occur to insulation on steam generators and other non-piping components in the containment. If the testing was not applied to other components or addressed other components in some manner, please provide these details.	
22	Some piping oriented axially with respect to the break location (including the ruptured pipe itself) could have insulation stripped off near the break. Once this insulation is stripped away, succeeding segments of insulation will have one open end exposed directly to the LOCA jet, which appears to be a more vulnerable configuration than the configuration tested by Westinghouse. As a result, damage would seemingly be capable of propagating along an axially oriented pipe significantly beyond the distances calculated by Westinghouse. Please provide a technical basis to demonstrate that the reduced ZOIs calculated for the piping configuration tested are prototypical or conservative of the degree of damage that would occur to insulation on piping lines oriented axially with respect to the break location.	
23	WCAP-16710-P noted damage to the cloth blankets that cover the fiberglass insulation in some cases resulting in the release of fiberglass. The tears in the cloth covering were attributed to the steel jacket or the test fixture and not the steam jet. It seems that any damage that occurs to the target during the test would be likely to occur in the plant. Discuss whether the potential for damage to plant insulation from similar conditions was	

RAI No.	**RAIs in Letters Dated August 1, 2008** (Reference 32) **and October 15, 2009** (Reference 33)	**Response**
	considered. For example, the test fixture could represent a piping component or support, or other nearby structural member. The insulation jacketing is obviously representative of itself. Describe the basis for the statement in the WCAP that damage similar to that which occurred to the end pieces in not expected to occur in the plant. It is likely that a break in the plant will result in a much more chaotic condition than that which occurred in testing. Therefore, it would be more likely for the insulation to be damaged by either the jacketing or other objects nearby. If the testing referenced by the plant noted similar damage mechanisms and did not account for debris created by such, please provide a basis for the determination that the debris generation would not occur in the plant.	
24	The potential for deaeration of the coolant as it passes through the debris bed should be considered. Please provide an evaluation of the potential for deaeration of the fluid as it passes through the debris bed and strainer and whether any entrained gasses could reach the pump suction. If detrained gasses can reach the pump suction, please evaluate whether pump performance could be affected as described in Appendix A of Regulatory Guide 1.82, Revision 3.	See a summary of the deaeration/ degasification evaluation in the Response to 3.f.14.

5. References

1. **NRC Generic Letter 2004-02 (ML042360586).** Potential Impact of Debris Blockage on Emergency Recirculation During Design Basis Accidents at Pressurized Water Reactors. September 2004.
2. **NRC (ML073110278).** Revised Content Guide for Generic Letter 2004-02 Supplemental Responses. November 2007.
3. **NRC (ML080230038).** NRC Staff Review Guidance Regarding Generic Letter 2004-02 Closure in the Area of Strainer Head Loss and Vortexing. March 2008.
4. **NRC (ML080230462).** NRC Staff Review Guidance Regarding Generic Letter 2004-02 Closure in the Area of Coatings Evaluation. March 2008.
5. **NRC (ML080380214).** NRC Staff Review Guidance Regarding Generic Letter 2004-02 Closure in the Area of Plant-Specific Chemical Effects Evaluation. March 2008.
6. **NEI (ML120481057).** ZOI Fibrous Debris Preparation: Processing, Storage, and Handling, Revision 1. January 2012.
7. **Westinghouse WCAP-16793-NP.** Evaluation of Long-Term Cooling Considering Particulate, Fibrous and Chemical Debris in the Recirculating Fluid. October 2011.
8. **Westinghouse WCAP-17788-P, Volume 1.** Comprehensive Analysis and Test Program for GSI-191 Closure (PA-SEE-1090). Revision 1, December 2019.
9. **Westinghouse WCAP-17788-P, Volume 4.** Comprehensive Analysis and Test Program for GSI-191 Closure (PA-SEE-1090) - Thermal-Hydraulic Analysis of Large Hot Leg Break with Simulation of Core Inlet Blockage. Revision 1, December 2019.
10. **Westinghouse WCAP-17788-P, Volume 5.** Comprehensive Analysis and Test Program for GSI-191 Closure (PA-SEE-1090) - Autoclave Chemical Effects Testing for GSI-191 Long-Term Cooling. Revision 1, December 2019.
11. **NRC (ML080810015).** Diablo Canyon Power Plant, Unit Nos. 1 and 2 - Issuance of Amendments RE: Technical Specification 3.5.4, “Refueling Water Storage Tank (RWST)" (TAC Nos. MD6895 and MD6896). March 2008.
12. **NEI 04-07 Volume 1.** Pressurized Water Reactor Sump Performance Evaluation Methodology 'Volume 1 - Pressurized Water Reactor Sump Performance Evaluation Methodology'. December 2004.
13. **NEI 04-07 Volume 2.** Pressurized Water Reactor Sump Performance Evaluation Methodology 'Volume 2 - Safety Evaluation by the Office of Nuclear Reactor Regulation Related to NRC Generic Letter 2004-02'. December 2004.
14. **NUREG-1829.** Estimating Loss-of-Coolant Accident (LOCA) Frequencies Through the Elicitation Process. April 2008.
15. **PG&E Letter DCL 98-045 (ML17083C688).** License Amendment Request 98-03 Containment Spray During the Recirculation Phase of a LOCA. March 1998.
16. **NRC.** Safety Evaluation by the Office of Nuclear Reactor Regulation Related to Amendment No. 139 to Facility Operating License No. DPR-80 and Amendment No.

139 to Facility Operating License No. DPR-82 PG&E Co. DCPP, Units 1 and 2 Docket Nos. 50-275 and 50-323. February 2000.

17. **Westinghouse WCAP-17561-P.** Testing and Analysis to Reduce Debris Generation Zones of Influence for GSI-191 (PA-SEE-0778, Revision 1), Revision 0. April 2012.
18. **PWROG Letter OG-12-196.** PWR Owners Group For Information Only - WCAP-17561-P, Volume 1, Revision 0, "Testing and Analysis to Reduce Debris Generation Zones of Influence for GSI-191," (PA-SEE-0778, Revision 3). May 2012.
19. **NUREG/CR-6772.** GSI-191: Separate Effects Characterization of Debris Transport in Water. August 2002.
20. **NUREG/CR-6808.** Knowledge Base for the Effect of Debris on Pressurized Water Reactor Emergency Core Cooling Sump Performance. February 2003.
21. **NUREG/CR-6916.** Hydraulic Transport of Coating Debris, A Subtask of GSI-191. December 2006.
22. **NUREG/CR-6224.** Parametric Study of the Potential for BWR ECCS Strainer Blockage due to LOCA Generated Debris. October 1995.
23. **Westinghouse WCAP-16530-NP-A.** Evaluation of Post-Accident Chemical Effects in Containment Sump Fluids to Support GSI-191. March 2008.
24. **NEI 09-10.** Guidelines for Effective Prevention and Management of System Gas, Revision 1. December 2010.
25. **NRC (ML070950240).** San Onofre Nuclear Generating Station Unit 2 and Unit 3 GSI-191 Generic Letter 2004-02 Corrective Actions Audit Report. May 2007.
26. **NRC Audit Report (ML082050433).** Indian Point Energy Center Corrective Actions for Generic Letter 2004-02. July 2008.
27. **NRC (ML100960495).** NRC Revised Guidance Regarding Coatings Zone of Influence for Review of Final Licensee Responses to Generic Letter 2004-02, "Potential Impact of Debris Blockage on Emergency Recirculation During Design Basis Accidents at Pressurized-Water Reactors". April 2010.
28. **Westinghouse WCAP-16406-P.** Evaluation of Downstream Sump Debris Effects in Support of GSI-191, Revision 1. August 2007.
29. **NRC.** Final Safety Evaluation by the Office of Nuclear Reactor Regulation – Topical Report WCAP-16793-NP, Revision 2 – “Evaluation of Long-Term Cooling Considering Particulate, Fibrous and Chemical Debris in the Recirculating Fluid"-PWROG-Project No. 694. April 2013.
30. **NRC (ML19228A011).** U.S. Nuclear Regulatory Commission Staff Review Guidance for In-Vessel Downstream Effects Supporting Review of Generic Letter 2004-02 Responses. September 2019.
31. **C.B. Bahn, K.E. Kasza, W.J. Shack and K. Natesan (ML091610696).** Aluminum Solubility in Boron Containing Solutions as a Function of pH and Temperature. September 2008.

32. **NRC Letter to PG&E (ML082050608).** DCPP Units Nos. 1 and 2 Request for Additional Information Regarding Supplemental Response to Generic Letter 2004-02, "Potential Impact of Debris Blockage on Emergency Recirculation During Design Basis Accidents at Pressurized-Water Reactors". TAC No. MD4682 and MD4683. August 2008.

33. **NRC Letter to PG&E (ML092310763).** DCPP Unit Nos. 1 and 2 - Request for Additional Information (RAI) Regarding Supplemental Response to Generic Letter 2004-02, "Potential Impact of Debris Blockage on Emergency Recirculation During Design Basis Accidents at Pressurized Water Reactors". TAC Nos. MD4682 and MD4683. October 2009.

34. **PG&E Letter DCL-08-002 (ML080420438).** Diablo Canyon Units 1 and 2 Supplemental Response to Generic Letter 2004-02, "Potential Impact of Debris Blockage on Emergency Recirculation During Design Basis Accidents at Pressurized Water Reactors". February 2008.

35. **PG&E Letter DCL-08-059 (ML081980104).** Diablo Canyon Units 1 and 2 Supplemental Response to Generic Letter 2004-02, "Potential Impact of Debris Blockage on Emergency Recirculation During Design Basis Accidents at Pressurized Water Reactors", Revision 1. July 2008.

36. **PG&E Letter DCL-08-094 (ML083190020).** DCPP Units 1 and 2 Response to Request for Additional Information Regarding Supplemental Response to Generic Letter 2004-02, "Potential Impact of Debris Blockage on Emergency Recirculation During Design Basis Accidents at Pressurized Water Reactors". November 2008.

Updated Final Safety Analysis Report Changes

(Changes to Section 6.3.3.35, 2 pages)

6.3.3.35

Generic Letter 2004-02, September 2004 – Potential Impact of Debris Blockage on Emergency Recirculation During Design Basis Accidents at Pressurized-Water Reactors

The evaluation of insulation, coatings, and other debris affecting containment recirculation sump availability during the post-LOCA sump recirculation phase was completed to address the requirements of Generic Letter 2004-02. Various testing and analyses have been performed by DCPP in accordance with the methodology and acceptance criteria specified in NEI 04-07 and its associated Safety Evaluation, and NRC review guidance.

The analysis confirmed that the ECCS and CSS recirculation functions supported by the sump strainer under debris loading conditions comply with 10 CFR 50.46; 10 CFR 50.67; 10 CFR 100; and 10 CFR 50, Appendix A, GDC 35, 38, and 41. This confirmation provides assurance of long-term core cooling capability during recirculation following a LOCA, thereby ensuring that the design basis containment heat removal capabilities are maintained and that the containment atmosphere cleanup capability is preserved.

The analysis is performed by first quantifying the debris that is generated from pipe break locations throughout containment. The break size, location, and orientation determine the type, size distribution, and quantity of generated debris. The fractions of generated debris that could transport to the sump strainer were determined and used to quantify the debris at the sump strainer. Products of chemical reactions inside the sump pool could precipitate out of solution as the sump temperature drops and could then transport to the sump strainer. The debris bed that forms on the sump strainer, consisting of fibrous, particulate, and chemical debris, increases the head loss across the sump strainer, thereby affecting the NPSH margin of the RHR pumps. The debris could also challenge the structural integrity of the sump strainer; therefore, testing was performed to determine the debris bed head loss. A portion of the debris passes through the perforations of the sump strainer and could impact the ECCS and CSS piping and components downstream of the sump strainer by wear and clogging. Some debris could also reach the reactor and impact the long-term core cooling by accumulating at the core inlet, or accumulating inside the heater region, or depositing on the fuel rods. All of the debris effects stated above have been analyzed, and the evaluation provides assurance of long-term cooling capability during recirculation.

6.3.3.35 (continued)

The pumps, valves and other ECCS and CSS components were evaluated for potential plugging or excessive wear during the post LOCA sump recirculation phase using the methodology in WCAP-16406-P-A Revision 1. The evaluation of peak cladding temperature and deposition thickness due to deposition of debris on fuel rods was performed using the methodology in WCAP-16793-NP-A Revision 2, and the evaluation of the amount of fiber accumulation at reactor core inlet and inside reactor vessel was performed using the methodology in WCAP-17788 Revision 1.

OUTGOING CORRESPONDENCE SCREEN
(Remove prior to NRC submittal)

Document: PG&E Letter DCL-20-031
Subject: Final Supplemental Response to Generic Letter 2004-02

File Location: S:\RS\CLERICAL\DCLs - Draft\DCL-20-031, Final Supplemental Response to GL 2004-02\DCL 20-031.docx

FSAR Update Review
Utilizing the guidance in XI3.ID2, does the FSAR Update need to be revised? Yes ☒ No ☐ If "Yes", submit an FSAR Update Change Request in accordance with XI3.ID2 (or if this is an LAR, process in accordance with WG-9)

Commitment:
Statement of Commitment: None

Clarification: None

When will commitment be implemented?	*BEFORE OR AFTER LICENSE AMENDMENT RECEIPT* N/A	
Tracking Document:	*Notification/Order #* N/A	*Task/Operation #* N/A
Assigned To:	*NAME* N/A	*ORGANIZATION CODE* N/A
Commitment Code:	*FIRM or TARGET* N/A	*DUE DATE:* N/A
Outage Commitment?	*YES or NO* N/A	*IF YES, WHICH? (E.G., 2R9, 1R10, ETC.)* N/A
New PCD Commitment?	*YES (Specify #) or NO* N/A	*IF YES, LIST THE IMPLEMENTING DOCUMENTS (IF KNOWN)*
Modifies Existing Commitment in PCD?	*YES (Specify #) or NO* N/A	*IF YES, CLARIFY HOW COMMITMENT IS TO BE REVISED*